UNIVERSITÀ DEGLI STUDI DI UDINE
hic sunt futura
www.uniud.it

Corso di dottorato di ricerca in:

Scienze Biomediche e Biotecnologiche

Ciclo XXXV

Titolo della tesi:

# *In vitro* modelling and characterization of cells involved in Gaucher Disease-related bone defects

**Dottoranda**
Eleonora Pavan

**Supervisore**
Prof. Claudio Brancolini

**Co-supervisore**
Dott.ssa Andrea Dardis

Anno 2023

# ABSTRACT

Gaucher disease (GD) is an autosomal recessive lysosomal storage disorder caused by mutations in the acid β-glucosidase encoding gene (*GBA1*), resulting in a deficient activity of acid β-glucosidase (GCase). The enzymatic defect leads to progressive accumulation of glucosylceramide (GlcCer) and glucosylsphingosine (GlcSph) within lysosomes, mainly in cells of the reticuloendothelial lineage. Up to 90% of GD patients report bone symptoms (including osteopenia, osteoporosis, osteonecrosis, and bone pain) which, along with neurological impairment that occurs only in the most severe forms of GD (approximately 5% of patients), represent the most debilitating aspect of the disease, severely reducing patients' quality of life. The molecular basis of bone involvement in GD is not clear. However, several lines of evidence suggest that both osteoblasts and osteoclasts play a role in the pathogenic process, whereas almost no information is available about cartilage cells.

For these reasons, the general objective of this project was to explore the role played by different cells in GD bone pathology. Specifically, we aimed to (1) develop GD models of osteoclasts, osteoblasts, and chondrocytes (GBA KO cells) by using CRISPR/Cas9 editing technology to knock out (KO) the *GBA1* gene in continuous cell lines relevant to the study of bone pathophysiology, (2) characterize the different features and behaviour of wild-type (wt) and GBA KO cells, and (3) examine cell-to-cell interactions.

Firstly, we modelled GD monocytes using the THP-1 cell line. We observed increased osteoclastogenesis of THP-1 GBA KO monocytes compared with THP-1 wt. As the number of differentiated osteoclasts was reduced by providing THP-1 GBA KO with (I) the recombinant human GCase, (II) an inhibitor of GlcCer synthesis, or (III) an anti-inflammatory compound, we demonstrated that glycosphingolipid accumulation and inflammation play a central role in this process.

Secondly, we modelled GD osteoblasts using the osteosarcoma cell line SaOS and characterized these cells in terms of type I collagen, which is produced by osteoblasts and is the most abundant constituent of the organic component of bone extracellular matrix (ECM), and alkaline phosphatase (ALP), an enzyme required for the formation of hydroxyapatite crystals, which represent the inorganic component of bone ECM. Compared with SaOS wt, SaOS GBA KO showed a slight decrease in ALP mRNA expression and calcium deposition, no differences in ALP activity, and a significant decrease in type I collagen mRNA expression and deposition. Moreover, we performed the miRNA profile of these cells using NGS technology. More than 700 miRNAs were analysed in cell lysates and exosomal preparations. Among the significantly up- and down-regulated candidates, we focused on miR-488-3p, which was strongly overexpressed by GBA KO cells.

We further validated the overexpression of miR-488-3p in primary osteoblasts treated with the GCase inhibitor conduritol B epoxide to mimic GD. Furthermore, to characterize the functional impact of miR-488-3p overexpression, we transfected this miRNA into SaOS wt and we showed that it downregulates the expression of ALP- and collagen type I (*COL1A1*)-encoding genes, probably by downregulating their transcription factor RUNX2. Taken together, these data suggest an impairment of matrix deposition by GD osteoblasts that can be explained, at least in part, by the action of the overexpressed miR-488-3p.

Thirdly, we modelled GD chondrocytes using the C28I2 cell line. As we found decreased expression of collagen type II (*COL2A1*)- and increased expression of collagen type X (*COL10A1*)- encoding genes in GBA KO cells, we hypothesize changes in matrix composition and a different fate of GD chondrocytes compared with normal cells. In addition, these cells release more interleukin-8 and attract more neutrophils than wt: these observations may explain the pain experienced by GD patients.

Finally, we examined the role of GD osteoblasts and chondrocytes in osteoclastogenesis. We found increased osteoclastogenesis when the conditioned medium of SaOS GBA KO cells was used to differentiate THP-1 wt, likely due to increased release of the receptor activator of NF-kB ligand (RANKL). Furthermore, in a preliminary experiment, we found a similar trend in osteoclasts formation when C28I2 GBA KO-conditioned medium was used, suggesting a possible role of also GD chondrocytes in enhancing osteoclastogenesis.

In conclusion, we provide evidence for the role of osteoclasts, osteoblasts, and chondrocytes in bone involvement in GD.

# 1 INTRODUCTION

# 1.1 GAUCHER DISEASE

Gaucher disease (GD) is an autosomal recessive lysosomal storage disorder caused by the deficient activity of the acid β-glucosidase (GCase) enzyme. As GCase catalyses the breakdown of the glycosphingolipid glucosylceramide (GlcCer) to ceramide and glucose, its deficiency causes a progressive accumulation of GlcCer and other glycolipids within the lysosomes, mainly in cells of the reticuloendothelial lineage [1,2]. GD is pan-ethnic, with cases described worldwide; even though it can reach 1/800 births in the Ashkenazi Jewish population, the estimated prevalence in the general population is between 1/40'000 and 1/100'000 individuals: for this reason, it is classified as a rare disease [3–5]. In Italy, a retrospective analysis of the pediatric population in the 1993 to 1997 period indicates an incidence of 1:40'247, whereas, in accordance with the outcomes of a pilot study on neonatal screening carried out since 2015 in North-eastern Italy, the GD prevalence is 1 in 16'063 [6,7].

## 1.1.a Genetics and biochemistry of GD

GCase is encoded by the *GBA1* gene, which is located on chromosome 1q21 and contains 11 exons spread out in approximately 7,6 kb of genomic sequence. Two different transcript variants arise because of alternate polyadenylation sites. Two in-frame ATGs located in exons 1 and 2 are efficiently translated, resulting in two different protein isoforms [8,9]. The existence of a pseudogene (*GBAP1*) with a homology of 96% and in physical proximity with *GBA1* allows recombination events, resulting in complex gene-pseudogene rearrangements [9–11]. Moreover, a specific PCR known as Long-template PCR has been developed to specifically amplify the gene [12].

GCase is synthesized as a typical protein of the secretory pathway and undergoes co-translational glycosylation during transit through the Golgi which is essential for its catalytic activity *in vivo* [13–15]. The lysosomal delivery of GCase occurs by the mediation of the lysosomal integral membrane protein type 2 (LIMP-2): the two proteins interact in the pH-neutral environment of the ER to form a complex that passes through the Golgi and eventually reaches the lysosome, where acidic pH causes dissociation and subsequent release of active GCase [16].

As already mentioned, GCase hydrolyses GlcCer into ceramide and glucose (**figure I1**). To reach maximal activity, it requires an acidic pH (between 4,2 and 5,9, which is consistent with the lysosomal environment) and the coordinated action of an activator protein (Saposin C) and negatively charged lipids [17–19].

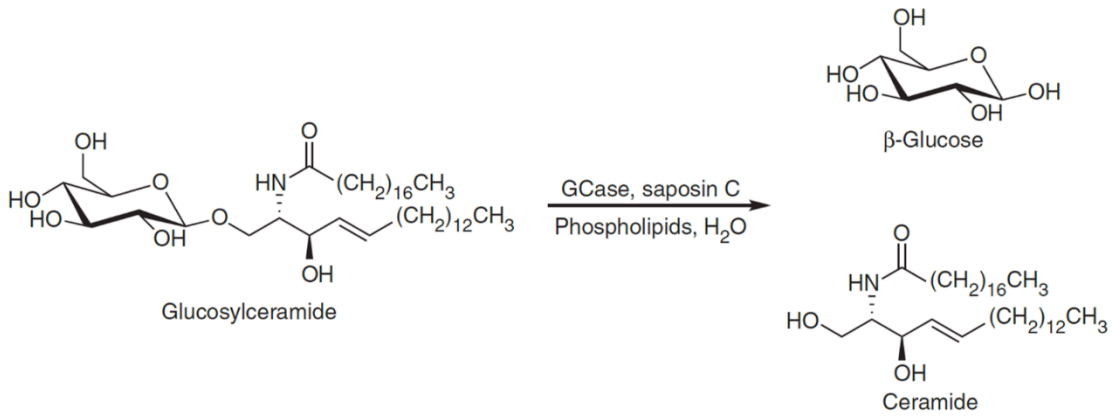


**Figure I1** | Schematic representation of GCase activity [20].

The main cause of the deficient activity of GCase is the presence of mutations in the *GBA1* gene. To date, 501 damaging mutations have been described in the *GBA1* gene [21]: the wide majority are missense or nonsense variants, even though also splice junction variants, deletions, and insertions of one or more nucleotides, and complex alleles resulting from gene conversion or gene fusion with *GBAP1* have been reported. Although the spectrum of mutations is very heterogeneous, two mutations, the c.1226A>G (p.Asn409Ser, commonly known as N370S), and c.1448T>C (p.Leu483Pro, commonly known as L444P) account for 50-75% of the GD alleles worldwide, while N370S, c.84dup, L444P and c.115+1G>A account for approximately 90% of alleles among Ashkenazi Jewish patients. The N370S mutation is rarely seen in Asian and Arab populations. About 10% of patients present large deletions or recombinant alleles [5,12,22,23].

A deficient activity of GCase may also occur when its activator protein Saposin C or its transporter LIMP-2 are missing (i.e., without *GBA1* mutations), resulting in two different diseases referred to as Saposin C deficiency and Action myoclonus – renal failure (AMRF), respectively [24–29].

As GCase activity is deficient, GCase substrate GlcCer accumulates within lysosomes. The cells of the reticuloendothelial lineage are the most affected ones, as they play an important role in eliminating the erythroid cells and leukocytes, which contain large amounts of glycosphingolipids, a source of GlcCer. The GlcCer engorged macrophages (known as Gaucher cells) are found in the bone marrow, the liver, the spleen, the lymph nodes, and the lungs, and are considered the hallmark of GD. They have a specific morphology, are metabolically active and alternatively activated: this activation results in the release of two peculiar cytokines known as chitotriosidase and CCL18/PARC, which are widely used as biomarkers assisting disease diagnosis and for monitoring GD progression and response to therapy [30–34].

As regards lipid storage, even though the primary effect of GCase deficiency is GlcCer accumulation, other metabolites derived from GlcCer accumulate as well. These include increased anabolism to gangliosides and an excessive transglycosylation with the subsequent formation of glycosyl-β-cholesterol (GlcChol) by the cytosol-faced retaining β-glucosidase GBA2, whose levels are increased when GCase is missing. Finally, the accumulating GlcCer in lysosomes is actively converted by lysosomal acid ceramidase to its sphingoid base, known as glucosylsphingosine (GlcSph); for this reason, GlcSph is considered an excellent biomarker for GD [23,31,35–39].

## 1.1.b Disease symptoms and classification

GD is defined as a multi-organ, chronic, heterogeneous disorder. Gaucher cells, as well as the accumulation of glycosphingolipids that interfere with multiple cellular processes and cause inflammatory and immunological responses, can be considered responsible for GD symptoms. The most common symptoms include enlargement of the spleen and liver, infiltration of the bone marrow by storage cells, thrombocytopenia, coagulation abnormalities, anemia, and bone disease, but in some cases also lung, renal and cardiac involvement, pulmonary hypertension, and neurological impairments have been reported [4,5].

The presence and severity/rate of progression of neurological involvement have been historically used as discriminating factors for GD classification into three different clinical phenotypes, although the clinical picture presents as a phenotypic continuum: type 1 GD is the non-neuronopathic form of GD, whereas type 2 GD and type 3 GD are collectively referred as neuronopathic GD (nGD), representing the acute and chronic neuronopathic phenotypes, respectively [40,41].

Type 1 GD is mostly present in Caucasians (90-95%) and may present clinically anytime between infancy and late adulthood. Common manifestations include minimal to marked splenomegaly (90% of patients) and hepatomegaly (60-80%), anemia (20-50%), thrombocytopenia (60-90%), and potentially disabling skeletal pathology (70-100% of patients). Although it is historically referred to as non-neuropathic, evidence of peripheral neuropathy and symptomatic Lewy body-associated parkinsonism when middle-aged or elderly has emerged [5,42–44].

Type 2 GD (<5% in most countries) usually occurs at an early age (neonate to 6 months) eventually leading to death usually at 2 to 3 years of age. Besides neurological symptoms which are severe and always present, visceral ones include splenomegaly (almost always present), thrombocytopenia (60% of cases), and rarely lung lesions; no bone symptoms have been reported [4,5].

Type 3 GD accounts for 5 % of all GD cases, but it is proportionately more prevalent in the Middle East, India, China, and Japan. It is more heterogeneous than type 2: some individuals have an aggressive neurodegenerative disease and markedly decreased life expectancy (6–20 years) whereas others, although usually manifesting severe systemic signs and symptoms, may have minimal and non-progressive neurological findings, normal cognitive function, and, with available specific treatments for the haematological and visceral symptoms, survival with good quality of life until late middle age. Moreover, a peculiar form characterized by cardiovascular disease with calcification of the mitral and aortic valves is referred to as type 3c. A particular subtype of type 3 GD known as Norrbottnian has probably arisen in the 17$^{th}$ century in Northern Sweden due to a founder effect; these patients display a specific genotype and course of clinical manifestations [4,5,41,45–48].

Genotype-phenotype correlations in GD are imperfect. However, some observations apply: individuals with at least one N370S allele do not develop the primary neurologic disease, whereas individuals who are homozygous for the L444P usually develop severe disease, often with neurologic complications. The cardiovascular form has been only associated with homozygosity for p.Asp448His (commonly known as D409H). Moreover, even though no live-born homozygote for either c.155+1G>A or c.84dup variant has been identified, suggesting that these genotypes are lethal, children who are compound heterozygotes for these mutations develop a subacute disease course with progressive pulmonary involvement and death in the first to the second decade of life [41].

## 1.1.c Diagnosis and treatment

The gold standard for GD diagnosis is the demonstration of deficient GCase activity measured in peripheral blood leukocytes and/or cultured skin fibroblasts homogenates: an enzyme activity below 15% of normal activity is diagnostic of GD. The residual enzyme activity does not correlate with disease severity, and thus, cannot be used for GD carriers' identification. The diagnosis should always be accompanied by the detection of pathogenic biallelic variants on the *GBA1* gene. The use of plasma disease biomarkers (GlcSph, chitotriosidase, CCL18) may support the clinical suspicion of GD, but the measurement of the GCase activity is required for an appropriate diagnosis [23].

All the therapeutic approaches for GD treatment aim to reduce glycosphingolipid storage: this goal can be achieved in two ways: (1) by the recovery of GCase activity, and (2) by reducing the GCase substrate synthesis.

Enzyme replacement therapy (ERT) exploits the first of these two mechanisms and consists of intravenous infusions of the recombinant human GCase. Three ERT formulations were approved by Food and Drug

Administration (FDA): imiglucerase, a recombinant GCase (Cerezyme, Sanofi-Genzyme), velaglucerase alfa (Vpriv, Shire), and taliglucerase alfa (Elelyso, Pfizer). ERT has shown efficacy and safety; however, many issues remain unresolved, including the lifelong intravenous injections and the limited effect on neuropathic features, as these recombinant enzymes due to their high molecular weight are not able to cross the blood brain barrier (BBB) [49,50].

Substrate reduction therapy (SRT) uses small molecules to reduce the biosynthesis of GlcCer. Two SRTs were approved by FDA: miglustat (N-butyldeoxynojirimycin; Zavesca, Actelion) and eliglustat tartrate (Cerdelga, Sanofi/Genzyme). They all demonstrated good efficacy and safety, but neither miglustat (despite crossing the BBB) nor eliglustat (unable to cross BBB), are a good option for neuronopathic GD; furthermore, they have an inhibitory effect on unwanted metabolic pathways, causing adverse events and eventually leading to discontinuation [49,50].

Recovery of GCase activity can be achieved also by introducing or replacing the disease-causing gene with a wild-type copy of it, by directly delivering it to the patient (*in vivo* gene therapy), or by administering it to cultured hematopoietic stem cells derived from the patient and subsequently transplanting the modified cells back to the host (*in vitro* gene therapy). Three formulations to be used as either *in vitro* or *in vivo* gene therapy were developed, and five clinical trials (NCT05324943, NCT04411654, NCT05487599, NCT04836377, NCT04145037) are currently being carried out to evaluate their outcomes in GD treatment [4,50,51].

Finally, in the last decade, increased interest in GCase chaperons has emerged. Indeed, many *GBA1* mutations cause the synthesis of misfolded proteins that are retained in the endoplasmic reticulum (ER) and subjected to ER-associated degradation (ERAD), which involves their translocation to the cytosol and the elimination by the ubiquitin-proteasomal pathway [52]. Thus, the use of molecules that help the proper folding may help in restoring the GCase activity. One of the most promising molecules is ambroxol, an FDA approved drug that showed amelioration of neurological symptoms in GD [53–58]. However, a precise mechanistic description of its beneficial effect is still pending, as the sole chaperone activity cannot explain all the observations [59].

# 1.2 BONE TISSUE

Bone is a specialized connective tissue that provides mechanical support for locomotion and protects the internal organs by forming the skeleton. In addition, it acts as a reservoir for several minerals including calcium, phosphate, magnesium, and organic molecules such as collagen fibers and amorphous matrix. It consists of an extracellular matrix (ECM) and cells [60].

## 1.2.a Extracellular matrix (ECM)

Two phases can be identified in the ECM, referred to as organic and inorganic matrixes. The first one provides the tensile properties to the tissue and is mainly composed of type I collagen (90-95%), which is organised in a three-dimensional network serving as a scaffold for mineral deposition; the final ~5% of the organic matrix is represented by noncollagenous proteins and proteoglycans. The inorganic part of the ECM consists of calcium phosphate in the form of hydroxyapatite nanocrystallites ($Ca_{10}(PO_4)_6(OH)_2$), with small amounts of carbonate, magnesium, and acid phosphate which are deposited onto the collagen fibers to provide mechanical rigidity and strength of bone [61].

## 1.2.b Bone cells

Three main cell types can be found in bone: osteoblasts, capable of bone deposition, osteoclasts, involved in bone resorption, and osteocytes, orchestrators of these processes. Within the microenvironment niche, osteoblasts, osteocytes, and osteoclasts synthesize and secrete paracrine signalling molecules, including growth factors, cytokines, and chemokines to maintain the remodelling and architecture of bone.

### *Osteoblasts*

Accounting for 5% of all bone cells, osteoblasts are the bone-forming cells. Indeed, they are responsible for the deposition of an ECM rich in type I collagen but not yet mineralized, known as osteoid, and its subsequent mineralization through the accumulation of calcium phosphate in the form of hydroxyapatite nanocrystallites [62].

Osteoblasts differentiate from mesenchymal stem cells (MSCs). Since these precursors have the potential of differentiating into adipocytes, chondrocytes, fibroblasts, or myoblasts, specific signals are required to drive MSCs to the osteoblastic lineage [63].

Among the many transcription factors (TFs) which have been reported to play a role in this process, the runt-related related transcription factor 2 (RUNX2) and its downstream target osterix (OX) act as the master TFs conferring the differentiation of MSCs into osteoblasts in response to external stimuli [64].

Key stimuli for osteoblast differentiation include insulin-like growth factor (IGF)-1, parathyroid hormone (PTH), bone morphogenic proteins (BMPs), fibroblast growth factor (FGF), hedgehog (Hh), and Wingless and Int-1 (Wnt) proteins. The latter is involved in one of the most well-characterized pathways for osteoblast differentiation: Wnt proteins bind to surface receptors on MSCs (including low-density lipoprotein receptor-related protein (LRP)-5/6 and Frizzle), triggering the phosphorylation and inactivation of GSK3β eventually resulting in the nuclear translocation of β-catenin, which induces the transcription of genes involved in osteoblast differentiation [64,65].

Osteoblasts maturation process occurs in three differentiation phases [66,67]:

1. cell proliferation: pre-osteoblasts undergo active proliferation and express collagen, fibronectin, osteopontin (OPN), and transforming growth factor-β (TGF-β) receptor 1;
2. ECM secretion and matrix maturation: immature osteoblasts turn into mature osteoblasts, capable of secreting type I collagen and expressing alkaline phosphatase (ALP). The main role of ALP is to hydrolyse inorganic pyrophosphate (PPi) to generate phosphate (Pi) which is used in the formation of calcium hydroxyapatite nanocrystallites: for this reason, it is considered a biomarker of mature osteoblasts;
3. matrix mineralization: mature osteoblasts continue to express various osteoblastogenic markers such as OPN, type I collagen, ALP, but they also produce osteocalcin (OCN) and bone sialoprotein (BSP). Finally, mature osteoblasts undergo apoptosis, become inactive bone-lining cells, or progressively incorporate into the bone matrix as terminally differentiated osteocytes.

Differentiation steps and TFs involved in osteoblastogenesis are schematized in **figure I2**.

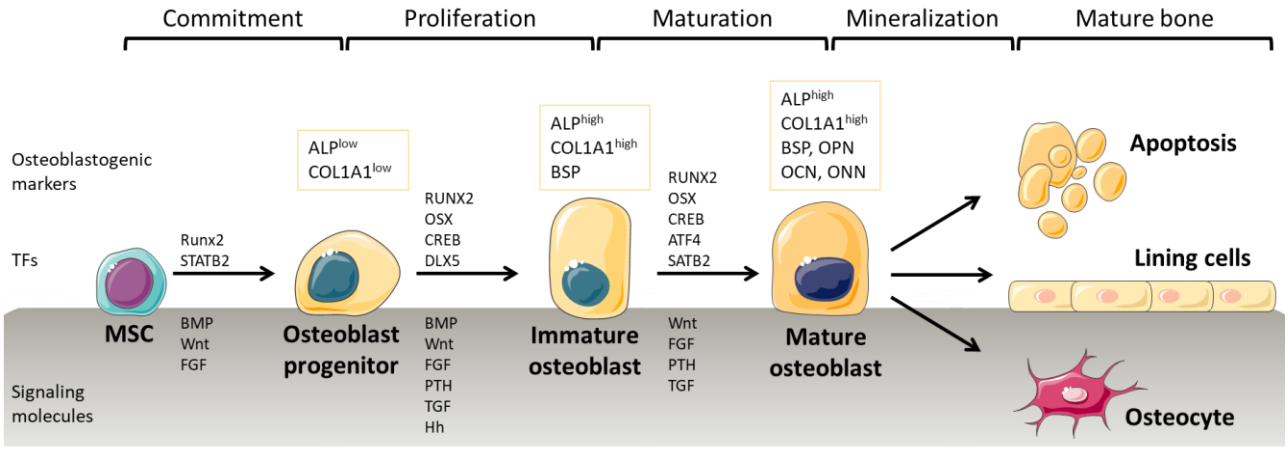


**Figure I2** | Osteoblastogenesis (adapted from Amarasekara *et al*. [67]).

Other than playing a crucial role in bone formation, osteoblasts are also involved in osteoclasts differentiation and activity. Indeed, during bone remodelling, these two cell types interact in both direct and indirect ways.

The two cell types have direct contacts through the interactions between EFNB2-EPHB4, FAS-FASL, and NRP1-SEMA3A to regulate cell proliferation, differentiation, and survival.
Ephrin B2 (EFNB2), expressed on the cell surface of osteoclasts, binds to osteoblast surface molecule EPHB4. This interaction suppresses osteoclast differentiation and promotes osteoblast differentiation. FAS is expressed on the surface of osteoclasts and binds its ligand FASL on osteoblast surface, inducing osteoclast apoptosis. Finally, SEMA3A, produced by osteoblast lineage cells, inhibits bone resorption, and promotes bone formation by binding to its receptor neuropilin-1 (NRP1) on the osteoclasts surface.

Moreover, osteoblasts release the receptor activator of nuclear factor kβ ligand (RANKL), which binds its receptor RANK, expressed by osteoclast precursors, promoting their differentiation into mature osteoclasts. In addition, osteoblasts produce also osteoprotegerin (OPG), a soluble receptor of RANKL which, through its binding with RANKL, avoids RANKL/RANK interaction inhibiting osteoclastogenesis and osteoclastic activity. Thus, osteoblasts regulate osteoclastogenesis and osteoclasts activity by modulating RANKL/OPG ratio [68]. In addition, osteoblasts produce other osteoclastogenic factors including macrophage-colony stimulating factor (M-CSF), tumour necrosis factor alpha (TNF-α), interleukin-1β (IL-1β), WNT5A. Osteoblasts produce also WNT16, a negative regulator of osteoclastogenesis (**figure I3**) [69–71].

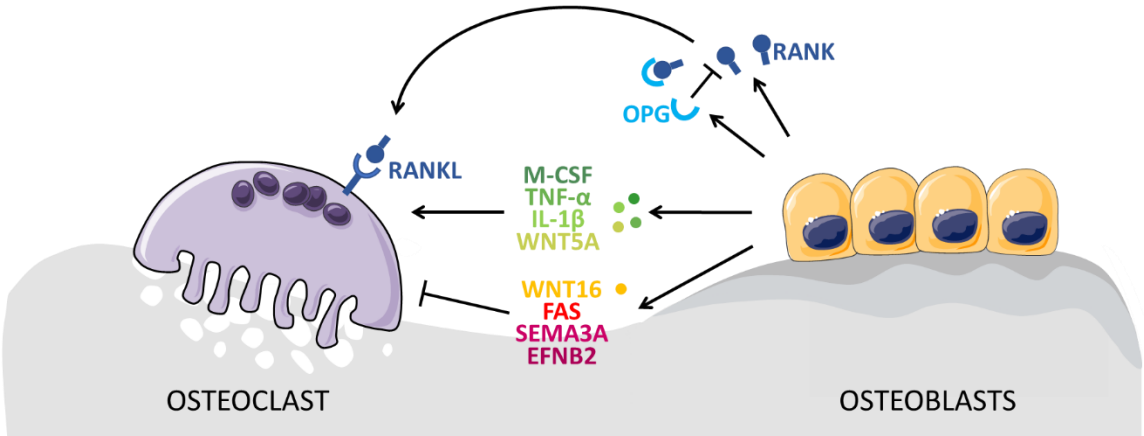


**Figure I3** | Osteoblasts-derived main factors that influence the other bone cells (adapted from Han *et al*. [71]).

### *Osteocytes*

Accounting for 90-95% of bone cells, osteocytes are terminally differentiated osteoblasts that have become embedded in the bone matrix; they occupy small chambers (lacunae) and present ramification of the cell body forming the *so-called* dendritic processes, which serve for mechanosensing and intercellular communication, as they connect them to other osteocytes, osteoblasts, and osteoclasts via tiny tunnels (canaliculi). A fluid called canalicular or bone fluid travels through the lacunar-canalicular space and bathes the osteocyte, providing oxygen and nutrients to maintain the viability of the cell in this environment [72].

Osteocytes display several functions [71,73–77]:

1. regulation of mechanosensation and mechanotransduction: they sense local mechanical cues and respond to these cues, mediating mechanically induced bone formation and adaptation, disuse-induced bone loss, and skeletal fragility;
2. perilacunar matrix remodelling: under calcium-demanding conditions (i.e., lactation and hibernation) osteocytes can remove their perilacunar matrix (mimicking the osteoclast) and also can replace that matrix (mimicking the osteoblast);
3. communication with and regulation of distant organs: osteocytes release FGF23 which regulates phosphate homeostasis in the kidney, osteocalcin which affects male fertility, cognition, energy metabolism, and muscle formation; osteocytes can regulate plasma calcium by releasing minerals from their surrounding matrix, especially in response to PTH and PTHrP;
4. bone remodelling via regulation of osteoclast activity (**figure I4**): osteocytes produce pro-osteoclastogenic factors (RANKL, M-CSF, interleukin-6 (IL-6), TNF-α, sclerostin (SOST) and HMGB1), but also the anti-osteoclastogenic factor OPG;
5. bone remodelling via regulation of osteoblasts activity (**figure I4**): pro-osteoblastogenesis and matrix formation stimulatory factors released by osteocytes include lipids (e.g., PGE2), growth factors (e.g., IGF-1), glycoproteins (e.g., Wnts), free radicals (e.g., NO), nucleotides (e.g., ATP). Negative regulators of osteoblastogenesis include the LRP 5/6 antagonists sclerostin (SOST) and DKK1, and neuropeptide Y (NPY); finally, MEPE acts as an inhibitor of matrix mineralization by promoting renal phosphate excretion.

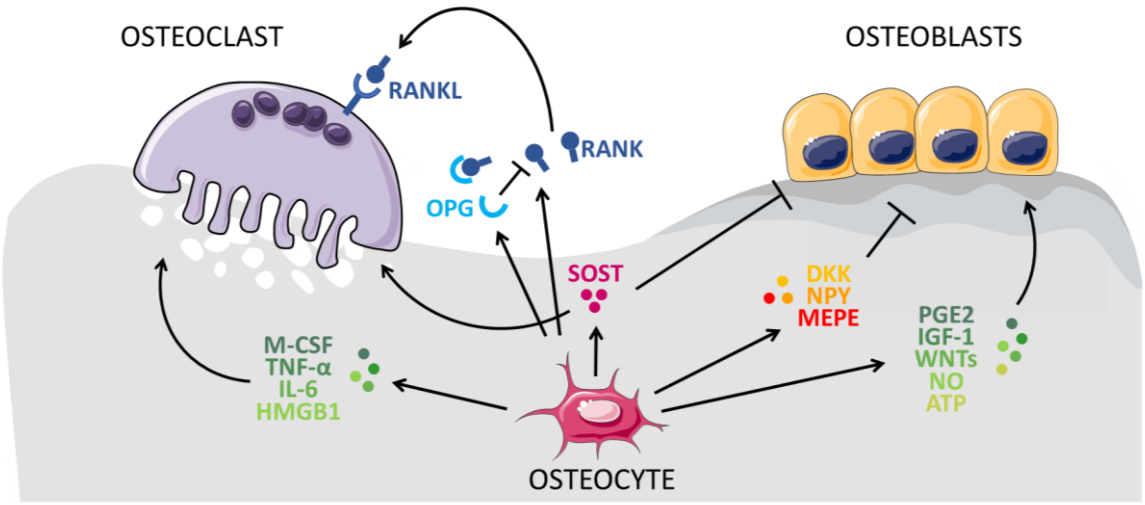


**Figure I4** | Osteocytes-derived main factors that influence the other bone cells (adapted from Han *et al*. [71]).

### *Osteoclasts*

Osteoclasts are giant, multi-nucleated cells, directly attached to the bone surface building resorption lacunae; they account for 1-2% of bone cells and their main role is bone resorption. They display a highly folded portion of plasma membrane facing the bone matrix referred to as the ruffled border, which is designed to secrete and resorb proteins and ions. The space between the ruffled border and bone surface known as the clear zone is sealed by a contractible ring of proteins (an F-actin-rich core that is surrounded by a "rosette" of integrins) and tight junctions and represents the location in which bone resorption takes place (**figure I5**). The degradation process occurs in two steps: (1) firstly, the inorganic component of the matrix is degraded by the acidification of the clear zone by the release of $Cl^-$ and $H^+$ through proton pumps coupled with ATPases; (2) secondly, the organic bone matrix is degraded by enzymes including tartrate-resistant acid phosphatase (TRAP), lysosomal cathepsin K, and matrix metalloproteinases 1 and 9 (MMP1, MMP9) [62,78,79].

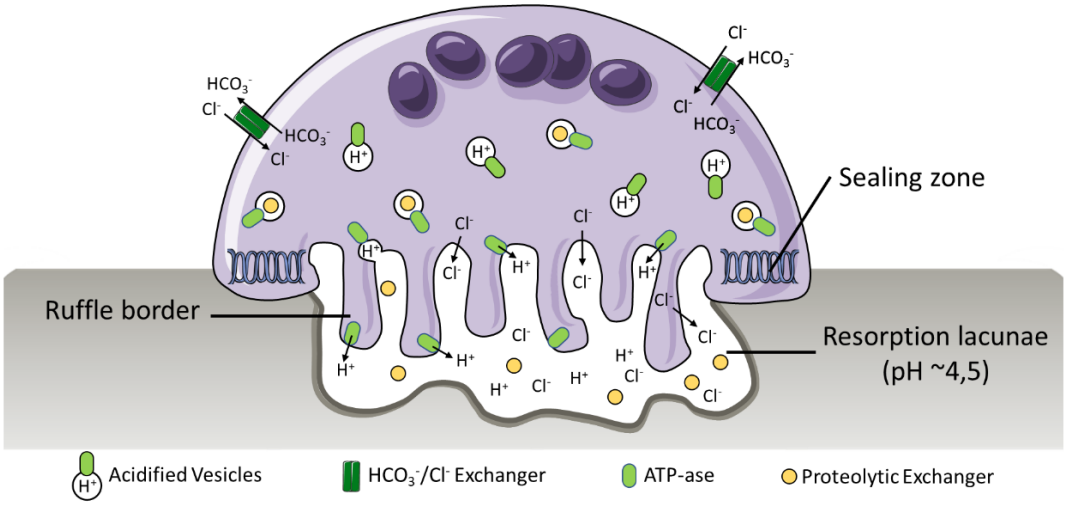


**Figure I5** | Overview of osteoclastic bone resorption (adapted from Qin *et al*. [79]).

Osteoclasts originate from mononuclear cells of the hematopoietic stem cell (HSC) lineage, under the influence of several factors. Osteoclastogenic progenitors are firstly differentiated into TRAP-positive mononuclear cells, before becoming TRAP-positive and calcitonin receptor (CTR) positive mononucleate cells that eventually fuse to form multinucleate, functional mature osteoclasts (**figure I6**) [80].

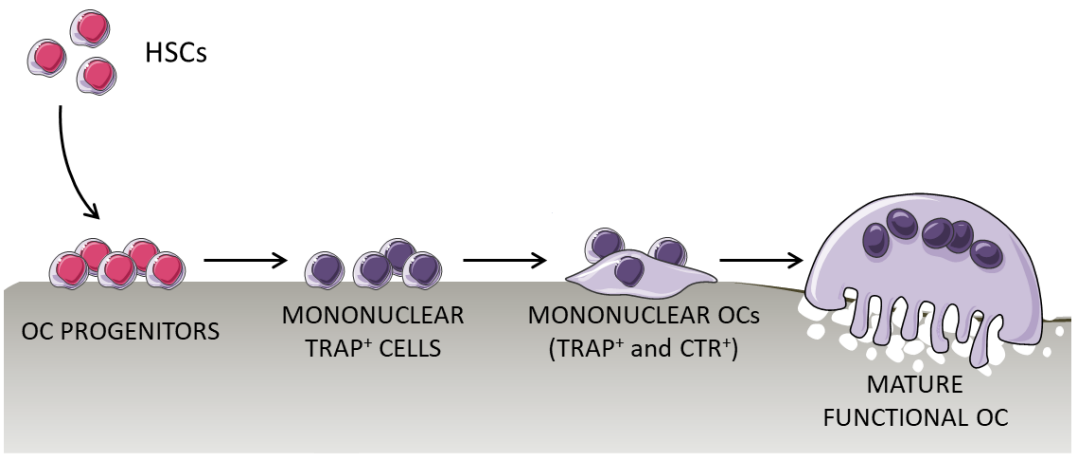


**Figure I6** | Osteoclasts differentiation steps (adapted from Kartsogiannis *et al*. [80]).

Crucial factors for the differentiation process are M-CSF and RANK ligand (RANKL), which promote the activation of transcription factors and gene expression in osteoclasts. M-CSF binds to its receptor (cFMS) present in osteoclast precursors, which stimulates their proliferation and inhibits their apoptosis, whereas the binding of RANKL to its receptor RANK allows the differentiation of precursors, the fusion, and the further differentiation to become functional osteoclasts. As previously mentioned, the secreted glycoprotein OPG acts as a receptor for RANKL, avoiding its binding to RANK. For this reason, OPG can be defined as a negative regulator for osteoclastogenesis [81,82]. Moreover, several cytokines have been reported to play a role in the process, including TNF-α, IL-1β, IL-6, as osteoclastogenic factors. These compounds can be released not only by bone cells, but also produced by monocytes, macrophages, dendritic cells, and innate and adaptive immune cells [83,84].

Other than the direct interaction between osteoblasts and osteoclasts involving EFNB2-EPHB4, FAS-FASL and NRP1-SEMA3A already mentioned in the chapter "*Osteoblasts*", osteoclasts release many factors influencing osteoblasts: positive regulators of bone deposition and osteoblast differentiation include WNT10B, bone morphogenic protein 6 (BMP6), semaphorin 3A (SEMA3A), Cardiotrophin-1 (CT-1), Sphingosine 1 Phosphate (S1P), Collagen Triple Helix Repeat Containing 1 (CTHRC1) and Complement Component 3 (C3), whereas SEMA4D suppresses osteoblasts differentiation (**figure I7**) [70,71].

In addition, even though they are not expressed by osteoclasts, two additional pro-osteogenic factors should be mentioned, as they directly derive from the activity of these cells: Transforming Growth Factor β1 (TGF-β1) and Insulin-Like Growth Factor Type 1 (IGF-1). They are released by the bone matrix in response to osteoclastic bone resorption, and in this way, they are free to subsequently promote osteogenesis [70,85].

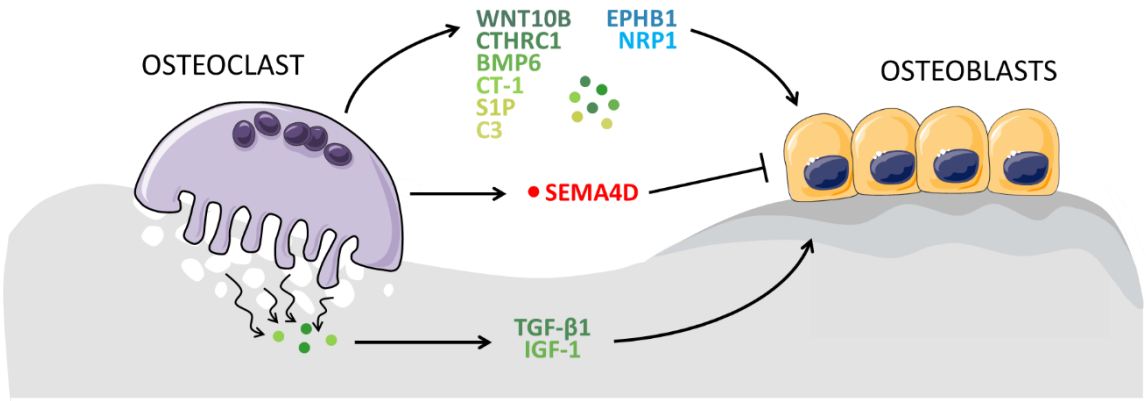


**Figure I7** | Osteoclasts-derived main factors expressed which influence the other bone cells (adapted from Han *et al*. [71]).

## 1.2.c Bone remodelling

Bones are continuously changing in an essential physiological process termed bone remodelling that renews the skeleton throughout lifespan. It maintains or improves bone strength by replacing primary, immature bone and old, micro-damaged or fractured bone, as well as maintaining calcium and phosphate homeostasis. The balance of bone resorption and deposition is essential to preserve the health of the tissue, avoiding pathological conditions [86,87].

All bone cells participate in the formation of the so-called basic multicellular units (BMU), which are responsible for bone remodelling. In these structures, bone cells interact both simultaneously and at various differentiation stages with their progenitors, other cells, and bone matrix constituents [88].

This process is regulated by proteins, local factors (such as cytokines and prostaglandins), or systemic factors (such as PTH, calcitonin, and estrogens). The main players regulating bone remodelling are the factors involved in osteoblasts-osteocytes-osteoclasts communications that have been already mentioned above. **Table I1** summarizes the main factors deriving from osteoclasts, osteoblasts, and osteocytes, as well as from a wide variety of other cell types (in particular from immune cells) that regulate bone remodelling. It is worth noting that several additional factors have been described as involved in this process; however, in some cases, their role still requires further elucidation, as inconsistent results have been obtained in different experimental settings [70,71,84,85,88–90].

| Osteogenic factors | | Anti-osteogenic factors | Osteoclastogenic factors | | Anti-osteoclastogenic factors | |
|---|---|---|---|---|---|---|
| WNT10B | IGF-1 | SEMA4D | RANKL | IL-6 | OPG | IL-13 |
| CTHRC1 | NO | SOST | M-CSF | IL-17 | WNT16 | IL-18 |
| BMP6 | ATP | DKK | TNF-α | IL-8 | FAS | IL-27 |
| CT-1 | FGF23 | NPY | HMGB1 | IL-11 | SEMA3A | IL-33 |
| S1P | BMP-2 | MEPE | SOST | IL-15 | EFNB2 | IL-35 |
| PGE2 | BMP-4 | | WNT5A | IL-23 | IL-3 | INF-α |
| WNTs | BMP-6 | | LAPA | IL-34 | IL-4 | IFN-β |
| EPHB1 | BMP-7 | | IL-1β | | IL-5 | INF-γ |
| NRP1 | BMP-9 | | | | IL-10 | |
| TGF-β1 | | | | | | |

**Table I1** | Main factors regulating osteogenesis and osteoclastogenesis.

# 1.3 ARTICULAR CARTILAGE

Cartilage is an avascular, aneural, alymphatic specialized connective tissue found in the synovial joints, spine, ribs, external ears, nose and airways, and the growth plates of children and adolescents. There are three main types of cartilage in the human body, with different structures and functions: hyaline cartilage, elastic cartilage, and fibrocartilage. This chapter focuses on the hyalin cartilage, which is found in the joints, the ribs, the nose, the larynx, and the trachea; it consists of an extracellular matrix (ECM) populated by a single cell type termed chondrocyte, which occupies 1-2% of the total volume of the tissue [91].

## 1.3.a Extracellular matrix (ECM)

The ECM consists of 70% of water and two major components: type II collagen (15-25%) and a large aggregating proteoglycan named aggrecan (10%): type II collagen forms fibrils which build up a systematically oriented network that entraps the negatively charged proteoglycan aggregates; moreover, several other collagens and non-collagenous proteins are present. Due to its peculiar structure, the articular ECM provides a high degree of resistance to deformation by compressive forces [92].

Articular cartilage is a very heterogeneous tissue, as four distinct regions can be observed (**figure I8**). Moving from the articular surface to the subchondral bone, the first three zones (superficial, middle, and deep) show a progressively decreasing type II collagen content, but increased fibrils thickness, concentration of aggrecan, and chondrocyte volume. In the first layer, fibers and chondrocytes are aligned parallel to the articular surface, and the latter are flattened and elongated. The middle zone is characterized by obliquely organized collagen fibrils and slightly larger chondrocytes at a relatively lower density. The deep zone presents perpendicularly organized fibrils and hypertrophic chondrocytes which tend to be grouped in a columnar organization. The fourth zone, known as calcified cartilage, is located just above the subchondral bone and is formed due to endochondral ossification, an essential process involved in bone formation in which cartilage becomes calcified and is subsequently replaced by bone during development. Even though this zone was initially thought to form a barrier to fluids, evidence indicates that active molecules can transit it, providing a mechanism by which products of chondrocytes or bone cells can influence the activity of the other cell types [93].

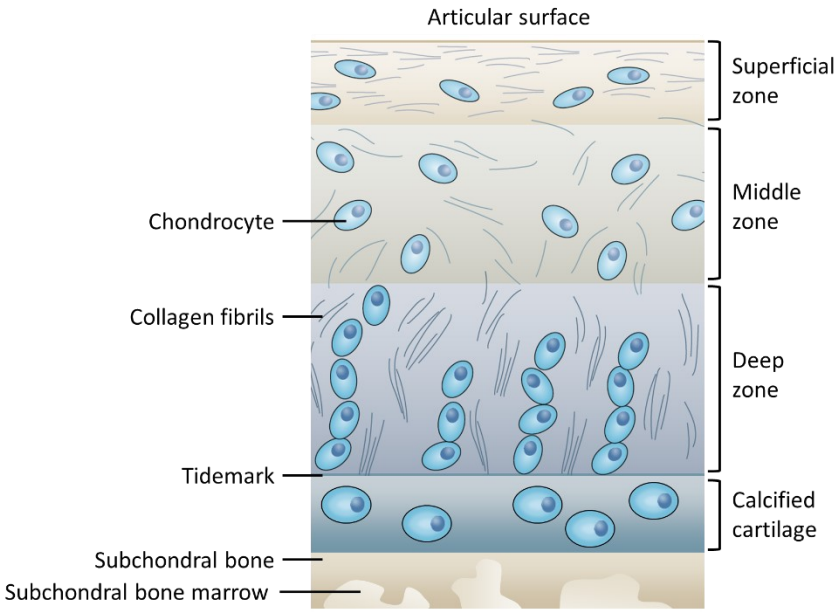


**Figure I8** | Structure of human adult articular cartilage (adapted form Martel-Pelletier *et al*. and Didomenico *et al*. [94,95]).

## 1.3.b Chondrocytes

As previously mentioned, chondrocytes differentiate from mesenchymal precursors under a peculiar signalling cascade involving FGF, hedgehog, BMP, TGF-β, and Wnt pathways. Moreover, the transcription factor Sry-type high-motility group box 9 (SOX9) is an early marker of the differentiating chondrocyte required for the onset of type II collagen expression, aggrecan, and other cartilage-specific matrix components. Wnt/β-catenin pathway is crucial in determining the MSCs differentiation to osteoblasts or chondrocytes as at low levels it promotes chondroprogenitor differentiation, whereas a high level is required for commitment to the osteoblastic lineage [96–98].

Differentiated chondrocytes may remain in a resting state eventually becoming the articular elements in articular joints or can proliferate differentiate to hypertrophic chondrocytes (characterized by type X collagen expression) and ultimately undergo apoptosis (**figure I9**). However, it has also been suggested that

hypertrophic chondrocytes may survive at the cartilage-bone junction and eventually de/transdifferentiate into bone marrow-associated skeletal stem and progenitor cells, osteoblasts, osteocytes, and adipocytes [99–104]. Therefore, whether cell death is the fate of hypertrophic chondrocytes or whether hypertrophy is a transient process that precedes osteogenesis remains known.

The hypertrophic differentiation of chondrocytes is mediated by several factors. Once again, the Wnt/β-catenin pathway plays a central role in the process, as after the chondrogenic commitment, enhanced levels of expression promote the chondrocyte differentiation into hypertrophic chondrocytes and the subsequent endochondral ossification. Moreover, RUNX2 acts as a positive regulator for chondrocyte maturation to hypertrophic phenotype and the subsequent osteogenesis. Finally, other factors are involved in this process, mainly acting on these two pathways [96,97].

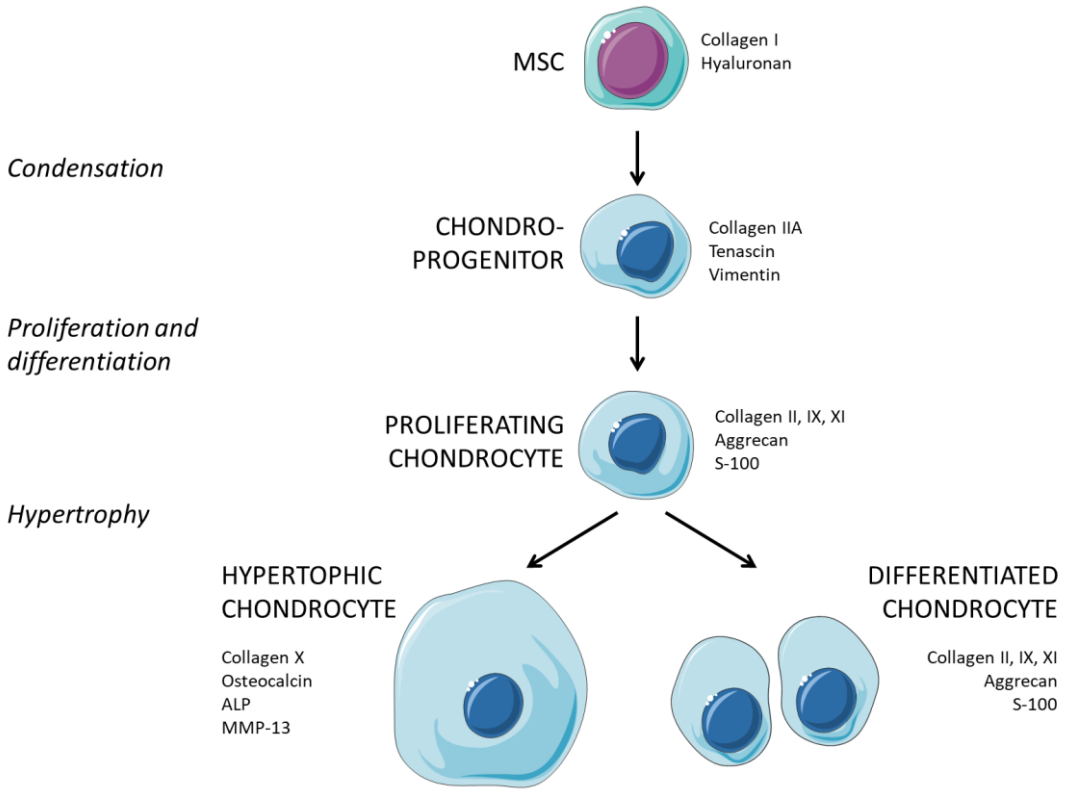


**Figure I9** | Chondrocyte differentiation from MSC and specific genes expressed at each step (adapted from Goldring *et al*. [97]).

## 1.4 SKELETAL MANIFESTATIONS OF GD

With an incidence in GD patients ranging from 80 to 94%, bone disease is one of the most prevalent aspects of GD type 1 and 3, whereas the far way less common type 2 patients do not show clinically relevant bone involvement, probably because the rapid neurological deterioration leads to death prior to the onset of bone pathology [105]. Considering that type 1 GD accounts for 90-95% of all GD patients, skeletal manifestations are the most predominant aspects of GD and represent the major cause of pain and disability, strongly reducing the quality of patients' life [106].

## 1.4.a Signs and symptoms of bone disease

Bone manifestations include structural changes, debilitating pain, and bone density abnormalities. Mikosch and Hughes [107] suggest a division of symptoms into primary, secondary, and tertiary bone changes (indicated in **figure I10**), triggered by infiltration of Gaucher cells in the bone marrow, resulting in impaired cytokines expression, alteration of vascularity, and increased local pressure.

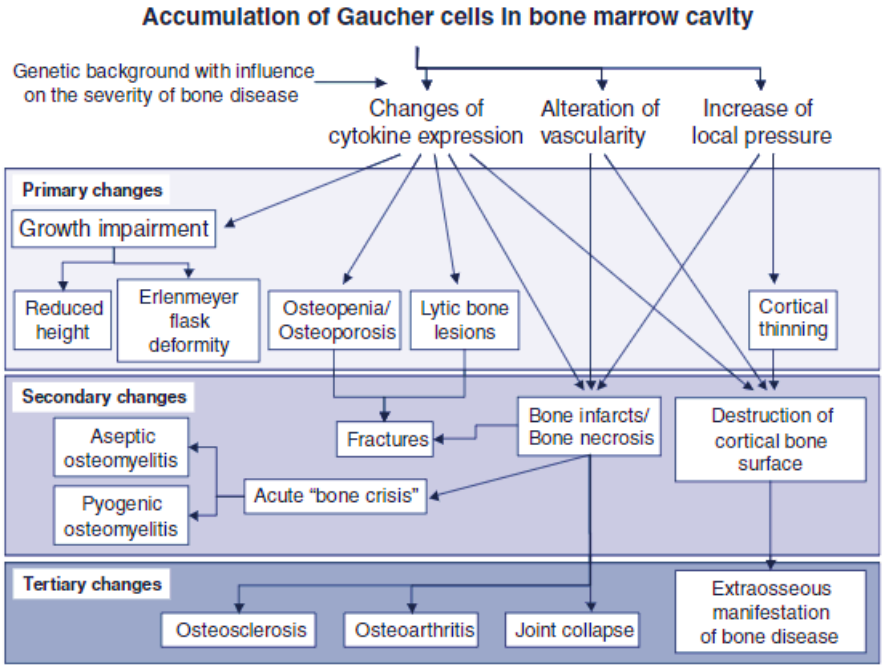


**Figure I10** | Overview of bone pathologies in GD seen as a sequence of events dividing them into primary, secondary, and tertiary bone changes [107].

Some of the primary acute changes can be at least partially reverted by ERT, which in some cases has also shown partial amelioration of bone crisis, pain, and infraction, but could not revert avascular osteonecrosis [5,106]. In addition, results from clinical trials for SRT show improvement in bone mass density, but overall, the efficacy on bone symptoms remains poorly evaluated [108,109]. As GD-approved treatment efficacy on bone symptoms remains poor, researchers introduced the idea of adjuvant therapies used in other pathologies, such as anti-resorptive or anabolic drugs [110].

## 1.4.b Molecular basis of bone involvement in GD

Despite the huge impact of bone symptoms on GD patients, the molecular basis of the process remains unclear. According to the mechanisms involved in bone remodelling, two main hypotheses have been proposed to explain the decrease in bone mineral density: increased bone resorption, and impaired bone formation [110]. Many approaches were exploited to study these aspects, including patients' biopsies, animal models, MSC- or induced pluripotent stem cells (iPS)- derived osteoblasts, wild-type (wt) peripheral blood mononuclear cells (PMBCs) or continuous monocytic cell line THP-1, both treated with an inhibitor of GCase (conduritol B epoxide, CBE – the so-called "chemical model"), sphingolipids, or conditioned media from wt and GD MSCs, osteoblasts, or osteocytes cell lines.

An impairment in the osteogenic process seems to be supported by both *in vivo* and *in vitro* observations (**figure I11**). In animal models, a reduction in proliferation and differentiation of MSCs to osteoblasts is noticed in GD mouse and zebrafish models, respectively [111,112]. *In vitro* systems display impaired differentiation from precursors, assessed as ALP activity, calcium, and collagen deposition and/or osteoblastic genes expression [113–117]. Interestingly, mature osteoblasts from a continuous cell line (SaOS) treated with CBE or GlcCer or GlcSph, do not display any difference in calcium deposition [114], suggesting an impairment in the differentiation process rather than in mature osteoblast activity. A possible explanation regards the capability of MSCs to differentiate into adipocytes or osteoblasts: MSCs preferentially perform adipogenesis when GlcCer is provided [118], and similarly, GD-derived MSCs showed a higher rate of adipogenesis than healthy controls-derived MSCs (**figure I11**) [116].

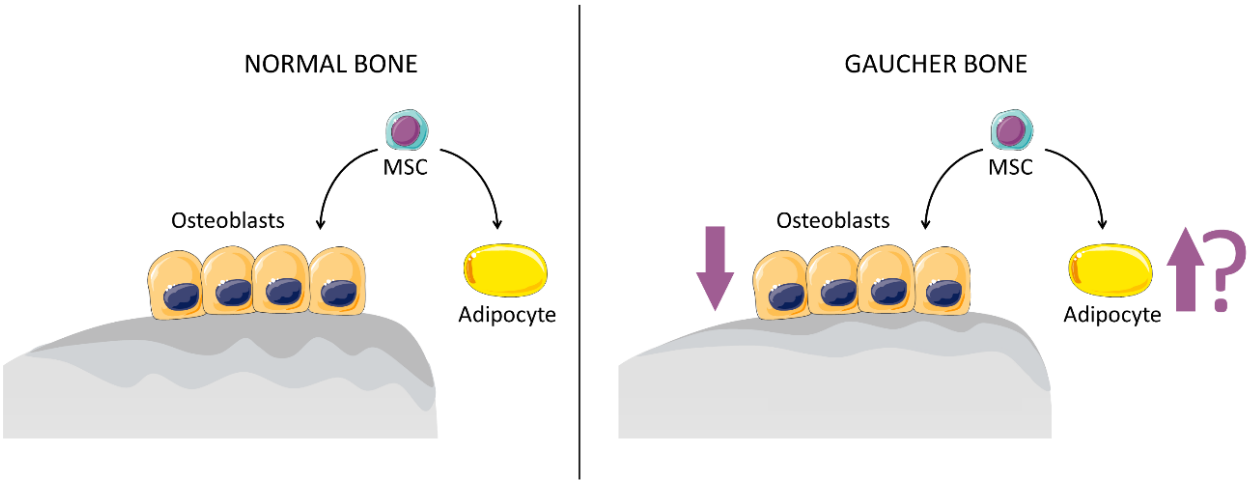


**Figure I11** | Impairment of bone deposition in GD.

On the contrary, the role of osteoclasts is debated, as evidences are inconsistent both *in vivo* and *in vitro*; in some *in vitro* systems, impairment in osteoclastogenesis and osteoclastic activity is documented, but it is still unclear whether either the microenvironment (i.e., pro-osteoclastogenic factor released by other cells) or the GCase substrates accumulation within osteoclasts/osteoclast precursors play the primary role in the process (**figure I12**). Evidence on bone resorption in some GD patients would suggest an increase in osteoclastogenesis and/or osteoclastic activity [119], but no differences in TRAP-positive osteoclasts formation are observed in GD mouse model [111]. Furthermore, even though evidence in *in vitro* systems including chemical and GD patient-derived cell models are inconsistent [113–116,120–126], increased osteoclastogenesis and bone resorption are observed in the wide majority of works in which conditioned media from GCase deficient osteocytes or MSCs are used to culture osteoclasts precursors [113,115,116,120,124–126], supporting the role of the microenvironment in the process. In addition, two independent chemical models of GD osteoclasts showed increased secretion of inflammatory cytokines which are known to trigger osteoclastogenesis [120,127], and TNF-α and IL-1β (which are known to be highly secreted in GD due to the inflammation process) were proved to play a role in the formation of mature osteoclasts [116,127]. On the other hand, as GlcCer was reported to cause increased osteoclastogenesis and osteoclasts activity, and as treatment with recombinant GCase was shown to reduce these two aspects in *in vitro* systems, it can be speculated that also glycosphingolipid accumulation plays a role in the impairment of bone resorption [114,122,123,126].

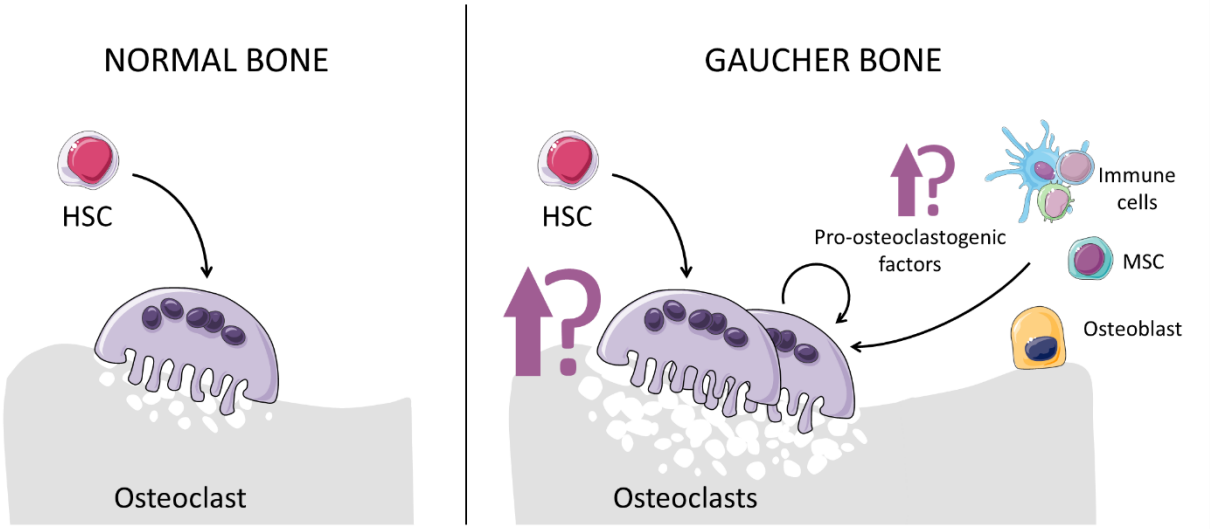


**Figure I12** | Impairment of bone resorption in GD.

## 1.4.c miRNAs and bone involvement in GD

Micro-RNAs (miRNAs) are single-stranded non-coding RNAs of 21-24 nucleotides with a key role in the post-transcriptional regulation of gene expression. They can be released outside the cells in complex with RNA-binding proteins or lipoproteins or loaded in microvesicles formed by plasma membrane blebbing, or in exosomes that are released in the extracellular space upon exocytic fusion of multivesicular bodies with the plasma membrane [128,129]. They play a role in pathogenic processes in many diseases, including the ones in which bone is affected [130–132].

Thus, it is not surprising that the exploration of the role of miRNAs in GD has emerged in the latest years, also with a particular focus on bone. In the first report on miRNAs and GD, the overexpression of miR-221-3p in GD zebrafish model was suggested to play a central role in reducing osteogenesis by affecting Wnt/β-catenin pathway [133]. Moreover, by performing miRNA profiling on 20 plasma samples from GD patients, Pawlinski and colleagues [134] identified miR-26b-5p as upregulated in GD samples in comparison to healthy controls. This miRNA is known to control two genes (*TRPS1* and *BMP-2*) involved in chondrocyte proliferation and differentiation, and osteoblasts proliferation, differentiation and apoptosis, respectively. Finally, during the last IWGGD symposium, a study on the miRNA expression profile of 60 GD naïve patients has been presented: authors identified a miRNA candidate whose level of expression correlates with the bone disease severity (Oral communication by Serrano-Gonzalo, entitled "Study of miRNA expression profiles in Gaucher patients and their relationship with the severity of bone involvement" at the IWGGD symposium in Leiden (NL), 8-11 May 2022).

# 2 AIM

Bone symptoms affect the vast majority of GD patients and severely limit their quality of life. Nevertheless, the molecular basis of bone disease is still unclear. Several lines of evidence point to an impairment of osteogenesis in terms of osteoblast proliferation and/or differentiation. On the other hand, the role of osteoclasts is still controversial, as evidence is conflicting both *in vivo* and *in vitro*. Even in those cases where increased osteoclast formation and osteoclast activity have been observed under GD or GD-imitating conditions, it is unclear whether the primary role is played by the microenvironment or by glycosphingolipid accumulation within the cells.

For these reasons, the general aim of this project was to explore the role of different cells in bone involvement in GD. Specifically, we aimed to (1) develop GD models of osteoclasts, osteoblasts, and chondrocytes (GBA KO cells) by using CRISPR/Cas9 editing technology to knock out (KO) the *GBA1* gene in continuous cell lines relevant to the study of bone pathophysiology, (2) characterize the different features and behaviour of GBA KO versus wild-type (wt) cells, and (3) examine cell-to-cell interactions.

# 3 MATERIAL AND METHODS

## 3.1 CELL CULTURE

Human monocytic cells deriving from an acute monocytic leukemia patient (THP-1) were cultured and maintained in RPMI 1640 medium (EuroClone, Pero, Italy) containing 10% fetal bovine serum (Gibco-Thermo Fisher Scientific, Waltham, MA, USA), 1% glutamine (Gibco-Thermo Fisher Scientific, Waltham, MA, USA), and 1% penicillin/streptomycin (Gibco-Thermo Fisher Scientific, Waltham, MA, USA), in a humidified atmosphere containing 5% $CO_2$ at 37 °C.

The osteosarcoma cell lines SaOS-2 (SaOS) and MG-63, the osteoblastic cells line Hobit, and primary osteoblasts were cultured and maintained in Dulbecco's modified Eagle's medium high glucose (EuroClone, Pero, Italy) containing 10% fetal bovine serum (Gibco-Thermo Fisher Scientific, Waltham, MA, USA) and 1% penicillin/streptomycin (Gibco-Thermo Fisher Scientific, Waltham, MA, USA), in a humidified atmosphere containing 5% $CO_2$ at 37 °C.

The human chondrocyte cell line C28I2 was cultured and maintained in Dulbecco's modified Eagle's medium/F12 (Cytiva, Marlborough, MA, USA) containing 10% fetal bovine serum (Gibco-Thermo Fisher Scientific, Waltham, MA, USA) and 1% penicillin/streptomycin (Gibco-Thermo Fisher Scientific, Waltham, MA, USA), in a humidified atmosphere containing 5% $CO_2$ at 37 °C.

## 3.2 CRISPR/Cas9 *GBA1* EDITING

*GBA1* editing was performed using Invitrogen TrueGuide Synthetic guide RNA (A35510 - CRISPR813153_SG) (sgRNA) and TrueCut™ Cas9 Protein v2, with Lipofectamine™ CRISPRMAX™ Cas9 transfection reagent (Invitrogen-Thermo Fisher Scientific, Waltham, MA, USA), according to the manufacturer's protocols. Briefly, cells were seeded one day before transfection in a 24-well plate (THP-1: $50 \times 10^3$ cells/well; SaOS and C28I2: $20 \times 10^3$ cells/well). Transfection was performed using 2000 ng of Cas9 protein, 12 pmols of sgRNA, 4 µL of Lipofectamine™ Cas9 plus reagent, and 1,5 µL of Lipofectamine™ CRISPRMAX™ reagent. After 48–72 h the edited pool was sorted by single-cell sorting in flow cytometry (BD FACSAria III, BD Biosciences, San Jose, CA, USA). Then, we analysed every single clone by Western blot (WB) to detect a lack or low levels of GCase: if so, we fully characterized the clone by measuring GCase activity, sequencing *GBA1* exon 3, and quantified Glucosylsphingosine (GlcSph).

## 3.3 DNA EXTRACTION, *GBA1* EXON 3 AMPLIFICATION, AND SEQUENCING

DNA was extracted from putative *GBA1* edited clones to perform sequence characterization using a DNeasy blood and tissue kit (Qiagen, Hilden, Germany) according to the manufacturer's protocols.

*GBA1* exon 3 and exon 3 flanking regions were PCR amplified using Platinum™ Taq DNA Polymerase high fidelity (Invitrogen-Thermo Fisher Scientific, Waltham, MA, USA) and primers 1F and 5R (**table 1**) to selectively amplify the gene and not the homologous pseudogene. Amplification was performed according to the following protocol: 94 °C 2 minutes; 10 cycles consisting of 94 °C 10 seconds, 57 °C 30 seconds, 68 °C 4 minutes; 20 cycles consisting of 94 °C 10 seconds, 57 °C 30 seconds, 68 °C 4 minutes, adding 20 seconds at each cycle; 68 °C 7 minutes. PCR products were purified from gel (1% agarose in TBE) using QIAquick gel extraction kit (Qiagen, Hilden, Germany) and cloned using a TOPO-TA cloning kit (Thermo Fisher Scientific, Waltham, MA, USA), according to the manufacturer's protocols. BigDye (Applied Biosystem-Thermo Fisher Scientific, Waltham, MA, USA) and primers 3F and 3R (**table 1**) were used in the sequencing reaction (26 cycles consisting of 95 °C 10 seconds, 50 °C 15 seconds, 62 °C 2 minutes). Sequences were purified in EtOH 70% and loaded in a 3500xL Genetic Analyzer (Applied Biosystems-Thermo Fisher Scientific, Waltham, MA,

USA). Sequencing analysis was performed using Chromas software (version 2.6.6, Technelysium Pty Ltd, South Brisbane, QLD, Australia). Accession numbers of RNA and protein sequences: NM_000157.3, NP_000148.2.

## 3.4. PROTEIN EXTRACTION AND WESTERN BLOT (WB)

To evaluate expression levels of GCase, cells were washed once with PBS and directly lysed in cell Lysis Buffer TNN (Tris-HCl 100 mM pH 8, NaCl 250 mM, NP40 0,5%), sonicated, and incubated on ice for 10 minutes. After centrifugation (10 minutes at 14'000 rpm at 4 °C), protein extracts were analysed for protein content using the Bradford assay, using the BioRad protein assay (BioRad, Hercules, CA, USA), following the manufacturer's instructions.

Protein extracts were resolved in sodium dodecyl sulfate-polyacrylamide gel electrophoresis (SDS-PAGE). Equal lysate amounts per lane were loaded on a 4%–20% gradient mini-protean TGX pre-cast gel (BioRad, Hercules, CA, USA) in running buffer (Tris 25 mM, Glycine 0,191 M, SDS 0,1% w/v). Fractionated proteins were transferred to nitrocellulose membrane (BioRad, Hercules, CA, USA) in transfer buffer (Tris 25 mM, Glycine 0,189 M, 40% MetOH); membranes were blocked in 5% blotting-grade blocker (BioRad, Hercules, CA, USA) in PBS-T (0,1% Tween 20 in PBS) for 1 hour. Then, membranes were incubated overnight at 4 °C with the appropriate primary antibody 1:1000 (GBA 2E2 (WH0002629M1, Sigma-Aldrich, St. Louis, MO, USA), actin (A2066, Sigma-Aldrich, St. Louis, MO, USA), then washed, incubated with the appropriate secondary antibody 1:1000 (Dako Agilent, Santa Clara, CA, USA) for 1 hour at RT and developed with SuperSignal West Dura/Pico reagents (Thermo Fisher Scientific, Waltham, MA, USA). The total expression of the protein of interest was normalized to actin levels. Blots were quantified by using a Uvitec Cambridge Imaging system (UVITEC, Cambridge, UK).

## 3.5 GCase, GBA2 AND GBA3 ENZYMATIC ACTIVITIES

GCase enzymatic activity was measured using the fluorogenic substrate 4-methylumbelliferyl-β-d-glucopyranoside (Sigma-Aldrich, St. Louis, MO, USA); the total amount of protein in cell lysates was determined using the Bradford assay, using the BioRad protein assay (BioRad, Hercules, CA, USA), following manufacturer's instructions. Briefly, 10 µL containing 10 µg of protein was incubated with 10 µL of substrate 5 mM in acetate buffer 0,1 M pH 4,2 at 37 °C for 3 h. The reaction was stopped with carbonate buffer 0,5 M pH 10,7 and the fluorescent product was quantified using a fluorimeter (SPECTRAmax Gemini XPS, Molecular Devices, San Jose, CA, USA) at an excitation wavelength of 365 nm and emission of 495 nm.

GBA2 and GBA3 potential activities were measured using the Activity-based probe (ABP) labelling β-glucosidases JJB367 Cy5 fluorescence [135]. Briefly, 25 µg proteins from cell lysates were incubated with 5 µl of 2,5 µM JJB367 and 15 µl of McIlvaine buffer (150 mM, pH 5,0) for 30 minutes at 37°C. 6,2 µl of Laemmli buffer were added to the samples which were then denatured for 5 minutes at 98°C and loaded into a 10% gel. Samples were resolved in sodium dodecyl sulfate-polyacrylamide gel electrophoresis (SDS-PAGE). Typhoon FLC 9500 (GE healthcare, Chicago, IL, USA) fluorescence scanning machine was used to acquire gel images. Coomassie staining was used as protein quantitation control.

## 3.6 LIPIDS MEASUREMENT

Glucosylsphingosine (GlcSph) in cell pellets was measured as previously described [54,136]. D5-glucosylsphingosine was used as an internal standard. Briefly, after cell lysis, protein precipitation, evaporation and reconstitution in mobile phase, reverse-phase liquid chromatography was performed using

a Shimadzu Nexera CL UHPLC (Shimadzu, Kyoto, Japan) and a Poroshell 120 EC-C8 column, 3,0 × 50,0 mm with 2,7 µm particle size (Agilent, Santa Clara, CA, USA). Mass spectrometry detection was carried out with AB Sciex 6500 QTrap tandem mass spectrometer (Sciex, Framingham, MA, USA) set in positive mode using an electrospray ionization (ESI). GlcSph levels were normalized for protein content, assessed using TPUC3 total protein urine/CSF (Roche, Basel, Switzerland) in Cobas 8000 (Roche, Basel, Switzerland) following the manufacturer's instructions.
Glucosylceramide (GlcCer), Ceramide (Cer), Sphingosine, Sphinganine, dihydroceramide (dh-Cer), and Glucosylcholesterol (GlcChol) were measured as previously described [137,138]: C17-dh-Ceramide was used as the internal standard for GlcCer, Cer, Sphinganine and dh-Cer, whereas 13C-Sphingosine and 13C-GlcChol were used as internal standards for Sphingosine and GlcChol, respectively. Lipids levels were normalized for protein content, assessed using BCA protein Assay kit (Thermo Fisher Scientific, Waltham, MA, USA) according to the manufacturer's protocol.

## 3.7 OSTEOCLASTOGENESIS

To differentiate monocytes into osteoclasts, $200 \times 10^3$ THP-1 were seeded in each well of a 24-multiwell plate on a glass coverslip. Cells were treated for 48 hours with 100 ng/ml Phorbol 12-myristate 13-acetate (PMA – Prepotech, London, UK), and then for 10 days with 50 ng/ml RANKL (Prepotech, London, UK) and 50 ng/ml M-CSF (Prepotech, London, UK), by replacing it every other day. Differentiated cells were either stained with Acid phosphatase, leukocyte (TRAP) kit (Sigma, St. Louis, MO, USA) following manufacturer's instructions or labelled with alpha-phalloidin (Sigma, St. Louis, MO, USA) and Hoechst. Cells were visualized at the microscope Leica DM600B (Leica, Wetzlar, Germany) and osteoclasts were identified as cells with 3 or more nuclei.
To assess the capability of SaOS and C28I2 conditioned media to induce osteoclastogenesis, we plated the same number of SaOS and C28I2 wt or GBA KO in RPMI, and after 48 hours we collected the conditioned media, counted the number of cells at that point and normalized the concentration of the medium by that number. Conditioned media were then diluted 1:1 with fresh medium. $200 \times 10^3$ THP-1 were seeded in each well of a 24-multiwell plate on a glass coverslip, and, after a 48 hours incubation with 100 ng/ml of PMA in fresh RPMI, the previously obtained conditioned media were supplemented with 50 ng/ml of M-CSF and provided to cells for 10 days, by replacing it every other day. Osteoclasts were labelled or stained and counted as described above.
To study the effects of Imiglucerase (Cerenzyme - Sanofi, Paris, France), Eliglustat (D,L-threo-PDMP – Matreya, State College, PA, USA) and PPS (bene pharmaChem, Geretsried, Germany) on osteoclastogenesis, these compounds were provided to THP-1 throughout the differentiation period in addition to M-CSF and RANKL at 1,6 µM, 20 µM, and 5 µg/ml, respectively. Osteoclasts were labelled or stained and counted as described above.

## 3.8 RNA EXTRACTION, REVERSE TRANSCRIPTION, AND QUANTITATIVE REAL-TIME PCR (qRT-PCR)

Total RNA was isolated using the QIAShredder and the RNeasy mini kit (Qiagen, Hilden, Germany). First strand cDNA synthesis was performed with 2 µg total RNA using Superscript IV Reverse Transcriptase (Invitrogen-Thermo Fisher Scientific, Waltham, MA, USA), according to manufacturer's instructions. Primers were designed from available human sequences using the primer analysis software Primer3 to specifically amplify *ALPL*, *COL1A1*, *RUNX2*, *COL2A1*, *COL10A1*, *SOX9*, *RANKL*, *OPG*, *GAPDH* (**table 1**). Quantitative Real-Time PCR (qRT-PCR) was performed using SYBR Green PCR master mix (Invitrogen-Thermo Fisher Scientific, Waltham,

MA, USA) in a QuantStudio 3 equipment (BioRad, Hercules, CA, USA), using the following protocol: hold stage 50° for 2 minutes, 95° for 7 minutes; PCR stage: 40 cycles of 95°C for 15 seconds, 63°C for 20 seconds; melting curve. *GAPDH* was used as an internal control. The comparative threshold (Ct) method was used for data analysis expressed as ΔΔCt.

## 3.9 ALKALINE PHOSPHATASE (ALP), ALIZARIN RED, AND SIRIUS RED STAININGS

ALP staining was performed in cultured SaOS, Hobit, and MG-63 cell lines by incubating cells with NBT/BCIP (Roche, Basel, Switzerland) for 15 minutes at 37°C. Cells were then visualized at the microscope Leica DMD108 (Leica, Wetzlar, Germany).

To assess the capability of SaOS of producing a mineralized matrix, Alizarin Red and Sirius Red stainings were used to visualize and quantify calcium and collagen deposition, respectively. $300 \times 10^3$ cells were plated in each well of a 12-multiwell plate and cultured for 14 days in the presence of 100 µM Dexamethasone (Sigma, St. Louis, MO, USA), 50 µg/ml L-Ascorbic acid 2-phosphate (Sigma, St. Louis, MO, USA), and 10 mM β-Glycerophosphate disodium salt hydrate (Sigma, St. Louis, USA), by replacing the medium every other day. To stain calcium deposits, cells were then washed twice with PBS (EuroClone, Pero, Italy), fixed for 15 minutes in PFA 4%, and incubated in 40 mM Alizarin Red (Sigma, St. Louis, MO, USA) for 30 minutes in gentle shaking. Cells were washed 5 times with $ddH_2O$ and images were captured at the Nikon eclipse TS100 microscope (Nikon, Minato, Tokyo, Japan). To extract the dye, 800 µl of 10% acetic acid was added to each well, and, after 30 minutes of gentle shaking, cells were collected using a scraper, and the cells in 10% acetic acid were transferred into a microcentrifuge tube. After vortexing for 30 seconds, samples were heated at 85°C for 10 minutes, incubated on ice for 5 minutes, and centrifugated at 14'000 g for 15 minutes. 500 µl of the supernatant were transferred to a new tube and diluted with 200 µl of 10% $NH_4OH$. The absorbance at 405 nm was read using nanodrop 2000c spectrophotometer (Thermo Scientific, Waltham, MA, USA).

To stain collagen, cells were washed three times with PBS, fixed in Bouin fluid for 1 hour at room temperature (RT), washed in acidified water (0,125 % v/v acetic acid glacial in water), and stained over-night (O/N) in gentle shaking at RT with Sirius Red Staining Solution (0,01% Sirius Red (Direct Red 80 – Sigma, St. Louis, MO, USA) in 1,3% picric acid solution). Cells were washed three times with 0,01 N HCl and images were captured. The dye was extracted by incubation with 400 µl of 0,1 N NaOH for 30 minutes at RT in gentle shaking and quantified by measuring the absorbance at 540 nm.

## 3.10 CYTOKINES RELEASE

To measure the release of the pro-inflammatory cytokines interleukin- 1, 6, 8, and TNF-α, SaOS, THP-1, and C28I2 were cultured for 48 hours, and their supernatants were collected. THP-1 cells were cultured in the presence of 100 ng/ml PMA to induce their differentiation into macrophages. The amount of cytokines in the conditioned media was measured by an immunoassay platform based on a microfluidic technology named ELLA (ProteinSimple, Bio-techne, Minneapolis, MN, USA), and normalized by the number of conditioning cells.

## 3.11 RANKL RELEASE

To measure the release of RANKL, SaOS wt and GBA KO A7 were cultured for 48 hours, their conditioned media were collected, and concentrated in 10 kDa Amicon Ultra-15 tubes (Merck Millipore, Burlington, MA, USA) for 10 minutes at 4000 g. The amount of RANKL was quantified using the Promokine Human sRANKL

ELISA Kit (PromoCell, Heidelberg, Germany) according to manufacturer's protocol. This kit allows the detection of soluble RANKL by distinguishing it from the OPG-bound RANKL.

## 3.12 miRNA PROFILE OF SaOS CELLS

To perform the miRNA profiling of SaOS wt and GBA KO A7, miRNAs were either extracted from the cells or exosomes. To isolate exosomes, cells were seeded in normal medium, which was replaced by FBS-free medium the following day. After 24 hours media were collected, filtered by passing through a 0,22 µm filter (Merck Millipore, Burlington, MA, USA), and concentrated in 100 kDa Amicon Ultra-15 tubes (Merck Millipore, Burlington, MA, USA) for 10 minutes at 4000 g. The conditioning cells were harvested and counted. The concentrated conditioned media were normalized for the number of conditioning cells and diluted to a final volume of 1 ml with FBS-free medium. 200 µl of ExoQuick (System Bioscience, Palo Alto, CA, USA) were added to each tube, and after an O/N incubation at 4°C, samples were centrifugated for 30 minutes at 1500 g at 4°C. Pellets were resuspended in 50 µl of PBS.
miRNAs extraction from either exosomes or harvested cells was performed using miRNeasy micro kit (Qiagen, Hilden, Germany), and miRNAs concentration in each sample was determined by Qubit Quant-iT microRNA Assay Kit (Thermo Fisher Scientific, Waltham, USA), according to manufacturer's protocols. QIAseq miRNA Library Kit (Qiagen, Hilden, Germany) was used to prepare the miRNA library; equal volumes of normalized libraries were sequenced on an Illumina MiSeq platform using an Illumina MiSeq Reagent kit v2 for 50 cycles (Illumina, San Diego, CA, USA).
Data were analysed using GeneGlobe software (Qiagen, Hilden, Germany) selecting geNorm as the normalization method.

## 3.13 miRNAs VALIDATION IN qRT-PCR

miRNA candidates identified and selected from the profiling were validated in qRT-PCR. To do that, miRNAs were extracted from either cells or exosomes and quantified as described before. 20 ng were retrotranscribed using the miRCURY LNA RT kit (Qiagen, Hilden, Germany) and amplified with miRCURY LNA SYBR Green PCR kit (Qiagen, Hilden, Germany) following manufacturer's instructions in QuantStudio™ 3 equipment (BioRad, Hercules, CA, USA). The list of selected miRNAs and their specific primer mixes (Qiagen, Hilden, Germany) are indicated in **table 2**. The comparative threshold (Ct) method was used for data analysis expressed as ΔΔCT.

## 3.14 CBE TREATMENT OF PRIMARY OSTEOBLASTS

To mimic GD in normal primary osteoblasts, $1 \times 10^6$ cells were seeded in a 100 mm plate. Cells were cultured for 3 or 6 days in the presence of 100 µM conduritol B epoxide (CBE – Calbiochem, San Diego, CA, USA), by replacing it every other day, and then characterized in terms of GCase activity and GlcSph accumulation.

## 3.15 miR-488-3p TRANSFECTION

To explore the role of miR-488-3p, $200 \times 10^3$ SaOS wt were seeded in wells of a 6-well plate. The following day, mirVana miR-488-3p Mimic or mirVana miRNA Mimic Negative Control #1 (Thermo Fisher Scientific, Waltham, MA, USA) were delivered to the cells (final concentration in the well: 50 nM) using Lipofectamine RNAiMAX (Thermo Fisher Scientific, Waltham, MA, USA), according to the manufacturer's protocol. After 48

hours, cells were collected and the expression of *ALPL*, *COL1A1*, and *RUNX2* was measured by qRT-PCR as described above.

## 3.16 NEUTROPHIL MIGRATION ASSAY

$80 \times 10^3$ C28I2 wt or GBA KO A1 were seeded in wells of a 24-multiwell plate and cultured for 48 hours. After that, some of the wells were used to collect the conditioned media, which were moved to clean wells. Cells from those wells were detached and their number was used to normalize the concentration of the conditioned media.

Neutrophils were isolated from healthy controls as previously described [139]. $4 \times 10^6$ neutrophils were loaded in each transwell insert (polycarbonate membrane with 8 µm pores – Falcon/Corning, Corning, NY, USA), which were then inserted into wells containing either cells and conditioned media or only the conditioned media. Plates were incubated for 2 hours, and neutrophils of the upper and lower chambers were labelled and quantified using BD multitest 6 color TBNK and Trucount Absolute Counting Tubes (BD, Franklin Lakes, NJ, USA) in flow cytometry (BD FACS Lyric, BD Biosciences, San Jose, CA, USA). The number of migrating and non-migrating cells was normalized by the number of conditioning cells.

## 3.17 STATISTICAL ANALYSIS

Statistical significance was determined by Student's t-test; $p < 0,05$ was considered statistically significant.

## 3.18 DISCLAIMER

Part of the figures was drawn using pictures from Servier Medical Art. ServierMedical Art by Servier is licensed under a Creative Commons Attribution 3.0 Unported License (https://creativecommons.org/licenses/by/3.0/).

**Table 1**: Primers sequences for PCR and qRT-PCR

| Primer | Sequence |
|---|---|
| 1F | 5’-CCTAAAGTTGTCACCCATAC-3’ |
| 5F | 5’-AGCAGACCTACCCTACAGTTT-3’ |
| 3F | 5’-GCAAGGCAGGTCTCAAACTC-3’ |
| 3R | 5’-CCCTCCAAATCCCTTCACTT-3’ |
| ALPL F | 5’-GTACAACACCAATGCCCAGG-3’ |
| ALPL R | 5’-CAGATTTCCCAGCGTCCTTG-3’ |
| COL1A1 F | 5’-GGCCAAGACGAAGACATCCC-3’ |
| COL1A1 R | 5’-GTTGTCGCAGACGCAGATCC-3’ |
| RUNX2 F | 5’-GACGAGGCAAGAGTTTCACC-3’ |
| RUNX2 R | 5’-GAGGCGGTCAGAGAACAAAC-3’ |
| COL2A1 F | 5’-GCCCAGTTGGGAGTAATG-3’ |
| COL2A1 R | 5’-CCAGGTTCACCAGGATTG-3’ |
| COL10A1 F | 5’-CGATACCAAATGCCCACAGG-3’ |
| COL10A1 R | 5’-GGACTTCCGTAGCCTGGTTT-3’ |
| SOX9 F | 5’-CAGGTGCTCAAAGGCTAC-3’ |
| SOX9 R | 5’-CGCTCTCGTTCAGAAGTC-3’ |
| RANKL F | 5’-CAAGGAGCTGTGCAAAAGGA-3’ |
| RANKL R | 5’-ATGGGATGTCGGTGGCATTA-3’ |
| OPG F | 5’-AGTGTCTTTGGTCTCCTGCT-3’ |
| OPG R | 5’-TCTGCGTTTACTTTGGTGCC-3’ |
| GAPDH F | 5’-TTTGTCAAGCTCATTTCCTGGTATG-3’ |
| GAPDH R | 5’-TCTCTTCCTCTTGTGCTCTTGCTG-3’ |

**Table 2**: qRT-PCR miRNAs validation

| miRNA | miRNA type | GeneGlobeID primer mix |
|---|---|---|
| has-miR-488-3p | Expressed and exosomal – candidate | YP00204469 |
| has-miR-93-3p | Expressed – candidate | YP00204470 |
| has-miR-195-5p | Expressed – candidate | YP00205869 |
| has-miR-490-5p | Exosomal – candidate | YP00206077 |
| has-miR-4784 | Exosomal – candidate | YP02107022 |
| has-miR-3679-5p | Exosomal – candidate | YP02109537 |
| has-miR-1233-5p | Exosomal – candidate | YP02105468 |
| has-miR-191-5p | Expressed – housekeeping | YP00204306 |
| has-miR-103a-3p | Expressed – housekeeping | YP00204063 |
| has-miR-16-5p | Expressed – housekeeping | YP00205702 |
| has-miR-106b-3p | Exosomal – housekeeping | YP00204020 |
| has-miR-23a-3p | Exosomal – housekeeping | YP00204772 |
| has-miR-7g-5p | Exosomal – housekeeping | YP00204565 |
| has-miR-7a-5p | Expressed and exosomal – housekeeping | YP00205727 |

# 4 RESULTS

# 4.1 *IN VITRO* MODELLING OF GD BONE AND CARTILAGE CELLS

As already mentioned, GD is an autosomal recessive lysosomal storage disorder caused by mutations in the GCase encoding gene (*GBA1*). With the aim of studying bone pathology, we decided to create *in vitro* models of the disease by CRISPR/Cas9 editing the *GBA1* gene on continuous cell lines.

## 4.1.a Modelling GD monocytes

We firstly developed and characterized a monocytic model of the disease, as monocytes can be differentiated into osteoclasts. Thus, we edited a human monocytic cell line deriving from an acute monocytic leukemia patient (THP-1) by targeting *GBA1* exon 3; we then performed a single cell sorting and screened each clonal population for GCase expression by western blot (WB) [140]. As shown in **figure R1A**, one out of 38 screened clones, named THP-1 GBA KO, expressed two proteins of lower molecular weight (MW) in comparison with GCase wild-type (wt). Sequencing analysis of the *GBA1* gene showed the presence of a large in-frame deletion causing the loss of the whole exon 3 [c.115+145_307+1del] in one allele, probably leading to the synthesis of a protein lacking 63 amino-acid residues, and a large deletion involving the final part of exon 3 and the first part of exon 4 (c.246_441del) in the other allele, probably leading to the exclusion of both exon 3 and 4 from the mature mRNA and the consequent synthesis of a GCase lacking 112 amino-acid residues (**figure R1B**). So, the presence of two faint bands with a lower MW compared to wt GCase (MW: 60 kDa) identified by WB, could be explained by the synthesis of two GCase forms arising from allele 1 p.(Ala40_Gly103del) with a predicted MW of 53 kDa, and from allele 2 p.(Ala40_Gly152del) with a predicted MW of 48 kDa, respectively. Indeed, this clone displayed an almost absent enzymatic activity (1% ± 0,04% of wt) (**figure R1C**) and, as expected, accumulated GlcSph (the deacylated metabolite of GlcCer) (**figure R1D**), recapitulating the hallmarks of the disease.

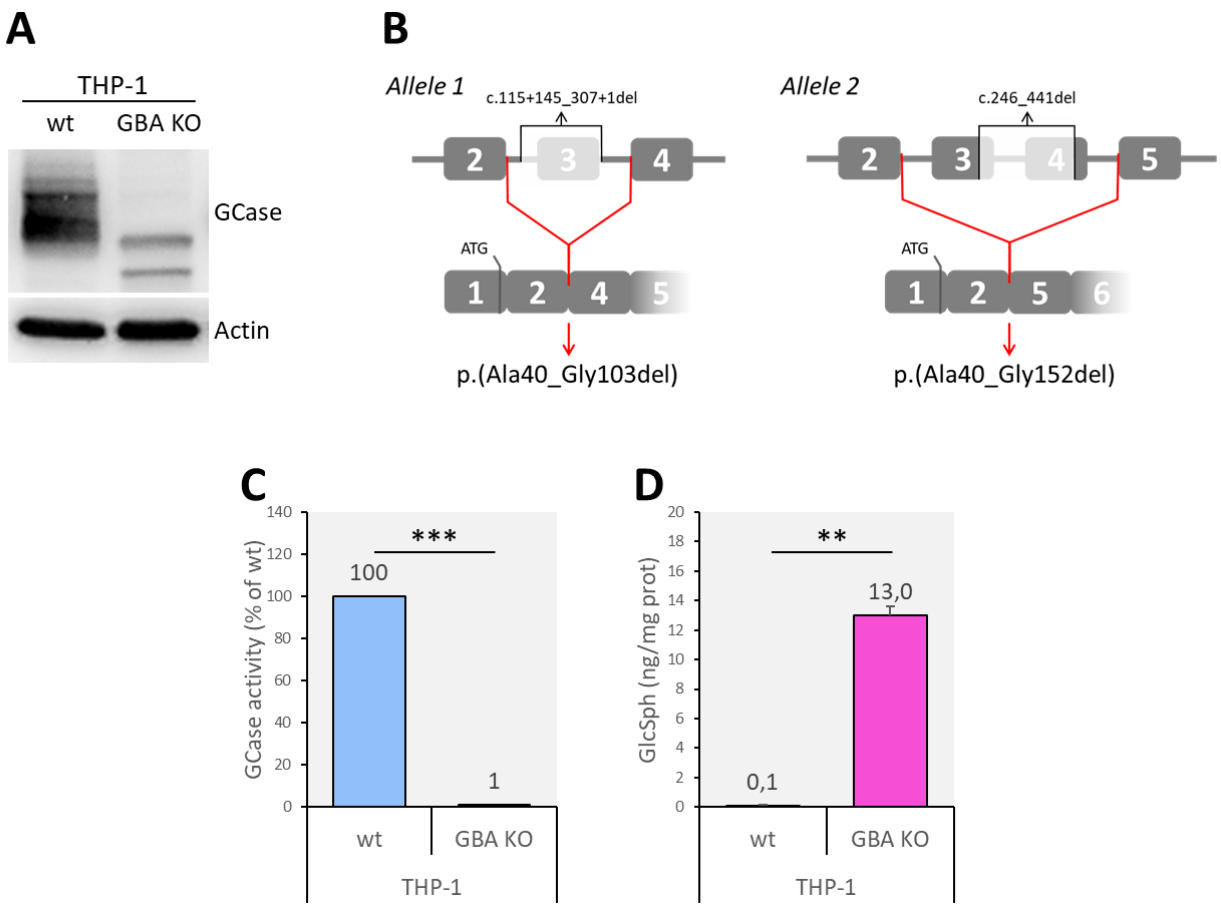


**Figure R1 | Modelling THP-1 monocytes**. A. GCase expression; B. Characterization of *GBA1* gene in THP-1 GBA KO and mRNA and protein prediction; C. GCase activity; D. GlcSph accumulation. *Results are expressed as mean ± SD of three independent experiments. **p-value < 0,01; ***p-value < 0,001.*

To further characterize the model, we studied the activity of other two non-lysosomal β-glucosidases and we analysed an extended lipid profile of these cells.

So, firstly, we measured the activity of the non-lysosomal glucosylceramidase (GBA2), which catalyses the hydrolysis of GlcCer at the cytosolic leaflet of membranes, and the cytosolic broad-specificity β-glucosidase (GBA3) which is thought to be involved in degrading xenobiotic β-glucosides in the cytosol [141–143]. As mentioned in the introduction, GBA2 may play a role in the pathogenesis of GD. GBA2 and GBA3 activities were measured by using a specific activity-based probe (ABP) which produces a fluorescent signal which is proportional to enzymatic activity; each β-glucosidase can be distinguished by its MW by analysing the product of the reaction by SDS-PAGE [135]. As reported in **figure R2A**, no differences in the activity of GBA2 and GBA3 were observed.

Secondly, we quantified the intracellular levels of several lipids of the GlcCer pathway (**figure R2B**). As expected, levels of glucosylceramide (GlcCer) were increased in GBA KO cells, resulting in a subsequent decrease in Ceramide (Cer) and its deacylated form Sphingosine (Sph). In addition, cells displayed increased levels of Sphinganine and its derivate Dihydroceramide (dh-Cer), probably as a compensatory mechanism triggered by the cell in an attempt to restore the Cer levels. Finally, we also noticed that GBA KO cells displayed an accumulation of Glucosylcholesterol (GlcChol), a transgycosylated product of the GlcCer (**figure R2C**).

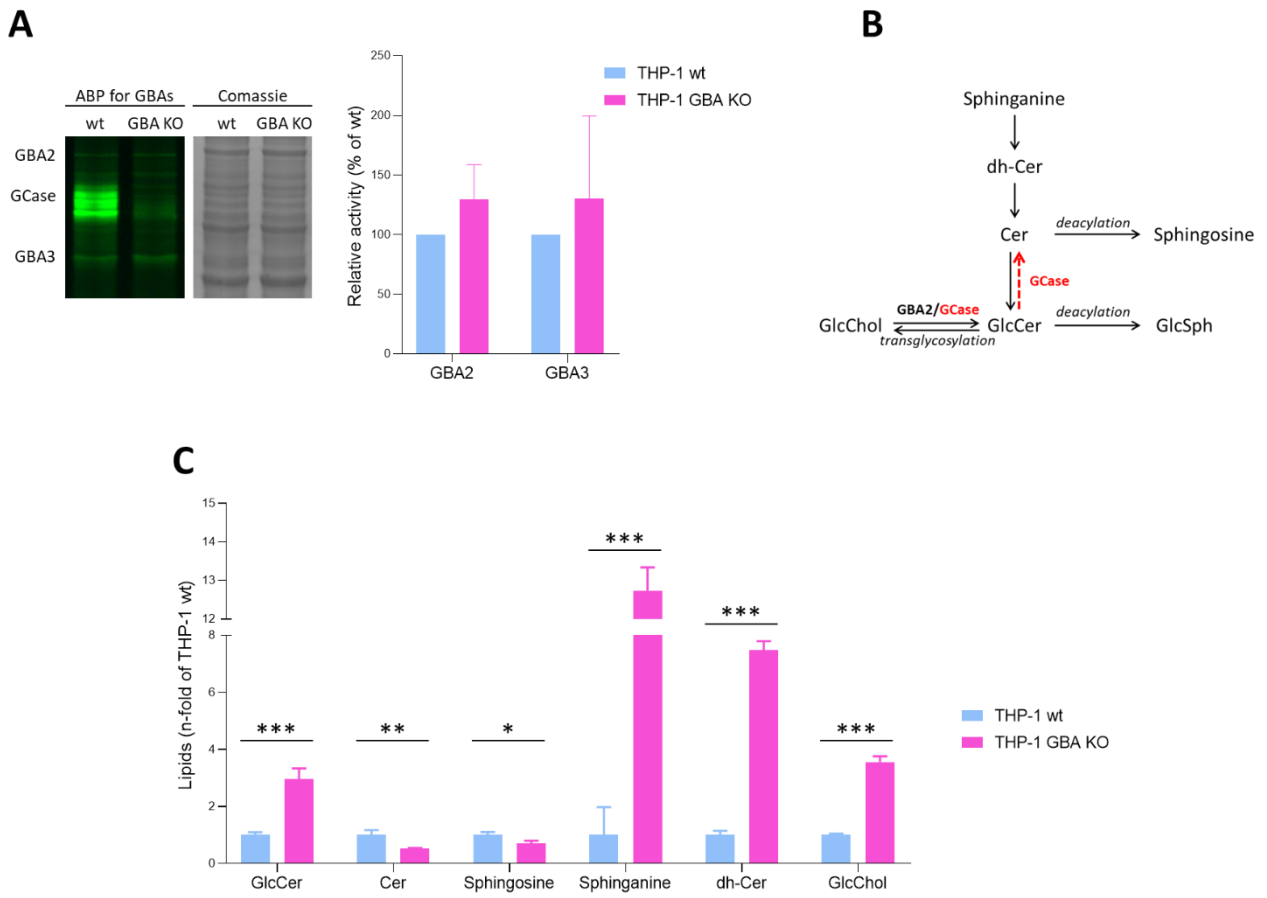


**Figure R2 | Characterization of THP-1 GBA KO cells**. A. GBA2 and GBA3 activity assessed by Activity Based Probe (ABP) and quantitation; B. Metabolic pathway involving GlcCer; C. Lipids levels. *Results are expressed as mean ± SD of three independent experiments. *p-value < 0,05; **p-value < 0,01; ***p-value < 0,001.*

These results indicate that the features of THP-1 GBA KO cells reflect the main characteristics of GD monocytic cells observed in affected patients.

## 4.1.b Modelling GD osteoblasts

To create a model of GD osteoblasts, we performed a preliminary study of a few osteoblasts-like cell lines available in our laboratory. Our attention was initially captured by Hobit cells, which are clonal normal immortalized adult human osteoblast-like cells, developed by Keeting and colleagues [144]. In addition, two human osteosarcoma cell lines, MG63 and SaOS-2 (SaOS) were available in our laboratory (a kind gift from Prof. Gianluca Tell, University of Udine, Udine, Italy). MG63 and SaOS are well-characterized osteoblast cell lines, widely exploited in research, that diverge in the differentiation status. Indeed, SaOS are commonly described as displaying a "mature" differentiated phenotype while MG63 represents an "immature" phenotype [145].

We characterized the three cell lines in terms of the activity of the osteoblastic marker Alkaline Phosphatase (ALP) and the capability of producing a mineralized matrix by culturing them in an osteoblastic differentiation medium for 14 days. In the case of Hobit and MG63 cells, the activity of ALP was very heterogeneous, with cells expressing high levels of the enzyme and others not expressing it at all, as displayed by ALP staining (**figure R3**). On the contrary, and as reported in the literature, SaOS homogeneously expressed high levels of ALP. As Hobit had the advantage of being normal cells rather than tumoral ones, we tried to obtain a homogeneous population with high ALP expression by isolating a single clone with elevated ALP activity. However, after amplification, the clonal population displayed once again a high rate of heterogenicity in ALP activity (**figure R3**). Moreover, among the tested cell lines, SaOS was the only one capable of producing a mineralized matrix, as assessed by Alizarin Red Staining to visualize calcium deposition. For these reasons, we selected SaOS to develop a GD model of osteoblasts.

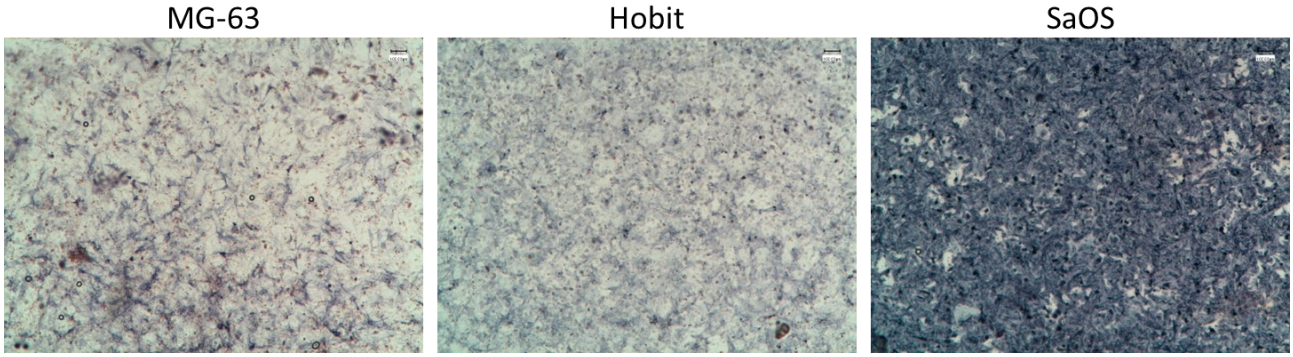


**Figure R3 | ALP activity in osteoblastic-like cell lines.** The amount of blue precipitate correlates with ALP activity.

Using the protocol developed to obtain THP-1 GBA KO cells, we CRISPR/Cas9 edited the *GBA1* gene and identified 2 out of 10 screened clones presenting low or absent GCase expression in WB (**figure R4A**). These clones were further characterized in terms of GCase activity: clone #1 (SaOS GBA KO #1) retained a 10% residual activity compared with non-edited cells, whereas clone A7 (SaOS GBA KO A7) displayed a 1% residual activity compared to non-edited cells (**figure R4B**). Consistently, one of the two alleles of SaOS GBA KO #1 presented a 3 bp deletion (c.249_251del), predicted to lead to the formation of a protein missing one amino-acid residue without any further change in the protein sequence [p.(Ser84del)]. This may explain the presence of a protein with a correct MW detected in WB and a relatively higher residual activity. As regards SaOS GBA KO A7, both alleles had missense mutations (allele 1: c.247_250del; allele 2: c.227_252del), leading to the formation of premature stop codons [predicted protein from allele 1: p.(Arg83Valfs*7); predicted protein from allele 2: p.(Phe76Trpfs*14)]. The presence of premature stop codons is likely to trigger the clearance of these aberrant mRNAs from the cell by nonsense-mediated mRNA decay: this can explain the lack of GCase protein expression observed by WB. In accordance with the residual GCase activity, even though also clone #1 accumulated GlcSph, we found a massive accumulation of this glycosphingolipid in clone A7 (**figure R4C**). For these reasons, only clone A7 was selected as the GD model for further experiments.

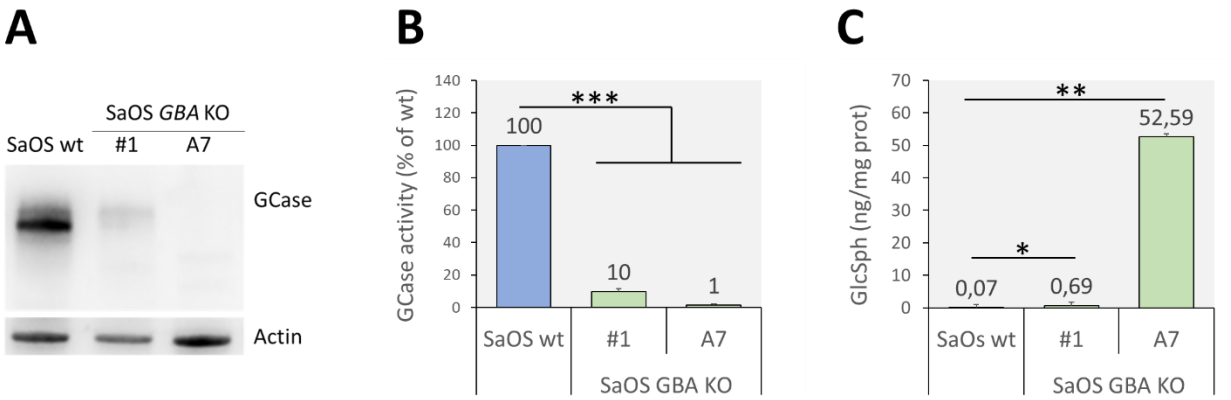


**Figure R4 | Modelling GD osteoblasts.** A. Gcase expression; B. Gcase activity; C. GlcSph accumulation. *Results are expressed as mean ± SD of three independent experiments. *p-value < 0,05 **p-value < 0,01; ***p-value < 0,001.*

## 4.1.c Modelling GD chondrocytes

Despite bone pain in GD is usually confined to one bone extremity or joint [41], no information regarding the status of chondrocytes in GD has been reported. Thus, we decided to model GD in a clonal cell line of immortalized normal chondrocytes named C28I2 [146]. Following the protocol already described above, we obtained four clones displaying absent or decreased GCase expression in WB and very low levels of GCase activity (clones A1, C4, D1, and C1) (**figure R5A** and **B**). We selected two of them (A1 and C1) for assessing GlcSph, as they displayed the lowest residual GCase activities. As clone A1 showed a massive accumulation of this biomarker (**figure R5C**), this clone was further characterized by *GBA1* sequencing: four alleles were detected, three of them carried a mutation leading to the formation of a premature stop codon, whereas one presented a large deletion involving exon 3 and the whole exon 4 of *GBA1* (Allele 1: c.249dupC → p.(Ser84Glnfs*15); Allele 2: c.247_250del → p.(Arg83Valfs*7); Allele 3: c.243_248delinsA → p.(Ser81Argfs*16); Allele 4: c.216_454+146del → p.?). The presence of premature stop codons is likely to trigger the clearance of these aberrant mRNAs from the cell by nonsense-mediated mRNA decay: this can explain the lack of GCase protein expression observed by WB. The presence of four alleles instead of the two expected can be explained by the genomic instability, which has been widely reported in immortalized cell lines [147]. However, as C28I2 represents an excellent chondrocyte model [148,149] and as all four alleles presented mutations, we decided to still consider GBA KO A1 chondrocytes a good model to study the cartilage implication of GD.

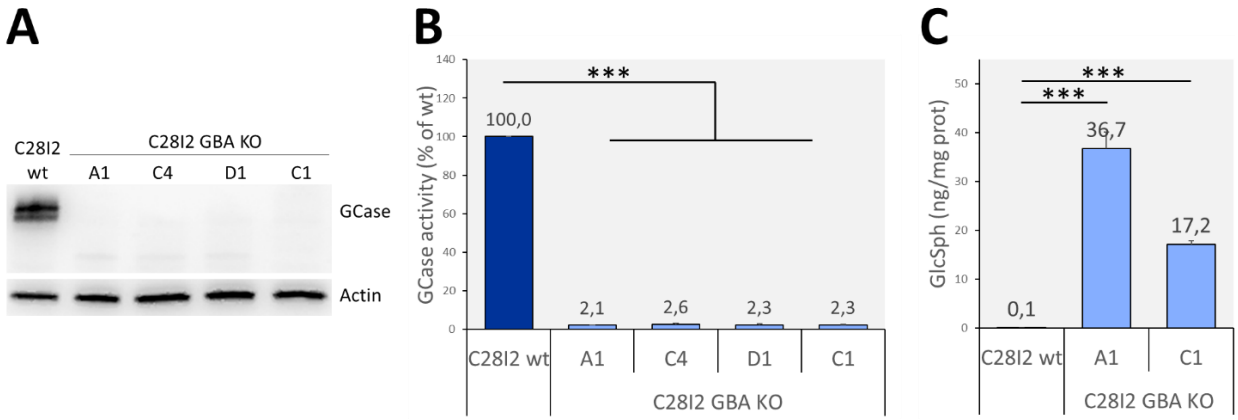


**Figure R5 | Modelling GD chondrocytes.** A. GCase expression; B. GCase activity; C. GlcSph accumulation. *GCase activity is expressed as mean ± SD of three independent experiments. ***p-value < 0,001.*

# 4.2 STUDYING GD BONE AND CARTILAGE CELLS

## 4.2.a Studying GD osteoclasts

As already mentioned, monocytes can be differentiated into osteoclasts by providing them with the appropriate stimuli. After two days of incubation with phorbol 12-myristate 13-acetate (PMA), THP-1 cells were cultured in presence of M-CSF and RANKL to induce osteoclastogenesis. After 10 days of treatment, we quantified the relative number of osteoclasts, identified as $TRAP^+$ cells with three or more nuclei. As all the cells displayed the typical brown colour indicative of $TRAP^+$ (**figure R6A**), to better observe the nuclei, osteoclasts count was repeated by labelling cells with phalloidin marking F-actin to clearly identify the cell, and Hoechst to label nuclei (**figure R6B**). In this way we could split the channels, improving the visualization of the nuclei. As reported in **figure R6C**, as expected, increased osteoclastogenesis was observed in GBA KO cells.

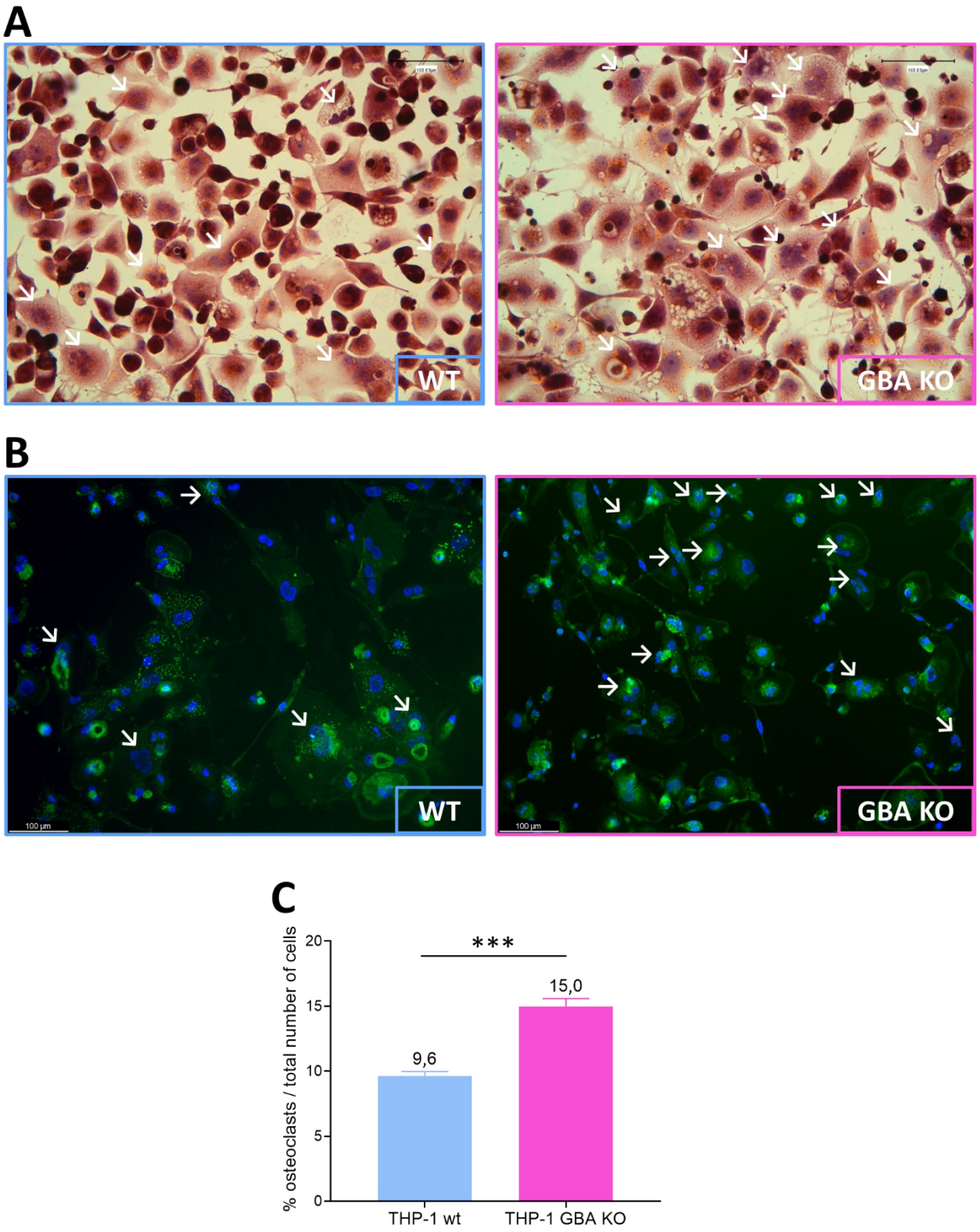


**Figure R6 | Studying osteoclastogenesis in THP-1 model.** A. TRAP (brown) and hematoxylin (purple) staining for osteoclasts and nuclei identification, respectively. White arrows indicate osteoclasts; B. immunofluorescence for F-actin (green) and nuclei (blue). White arrows indicate osteoclasts; C. Quantitation of osteoclastogenesis. *Results are expressed as mean ± SD of three independent experiments. ***p-value < 0,001.*

To further explore the possible mechanisms involved in the increased osteoclastogenic potential of GBA KO cells, during the differentiation cells were treated with the recombinant human GCase Imiglucerase, used as enzyme replacement therapy (ERT) or with Eliglustat, an inhibitor of the synthesis of GlcCer used in Substrate reduction therapy (SRT). As expected, both treatments reversed GlcSph accumulation in THP-1-derived macrophages (**figure R7A**) and were able to significantly decrease osteoclastogenesis in comparison with untreated GBA KO cells (**figure R7B**), suggesting a role of GlcSph accumulation in osteoclastogenesis. Furthermore, since we detected an increased production of IL-1β and TNF-α by THP-1 GBA KO- in comparison with THP-1 wt- derived macrophages (**figure R7C** and **D**)**,** we investigated whether inflammation may also play a role in the process. To this end, we exploited an anti-inflammatory compound known as Pentosan polysulfate sodium (PPS). Also in this case, a reduction in osteoclastogenesis was identified (**figure R7B**), even in the absence of changes in the GlcSph levels (**figure R7A**). It is worth underlining that not only PPS but also Imiglucerase (ERT) and Eliglustat (SRT) treatments resulted in decreased inflammation (**figures R7C** and **D**), which suggests that the reduction in glycosphingolipid accumulation may lead to a decreased osteoclastogenesis in an inflammation-dependent manner.

These data indicate that osteoclastogenesis is increased in GD and this process seems to be caused by glycosphingolipids accumulation and inflammation.

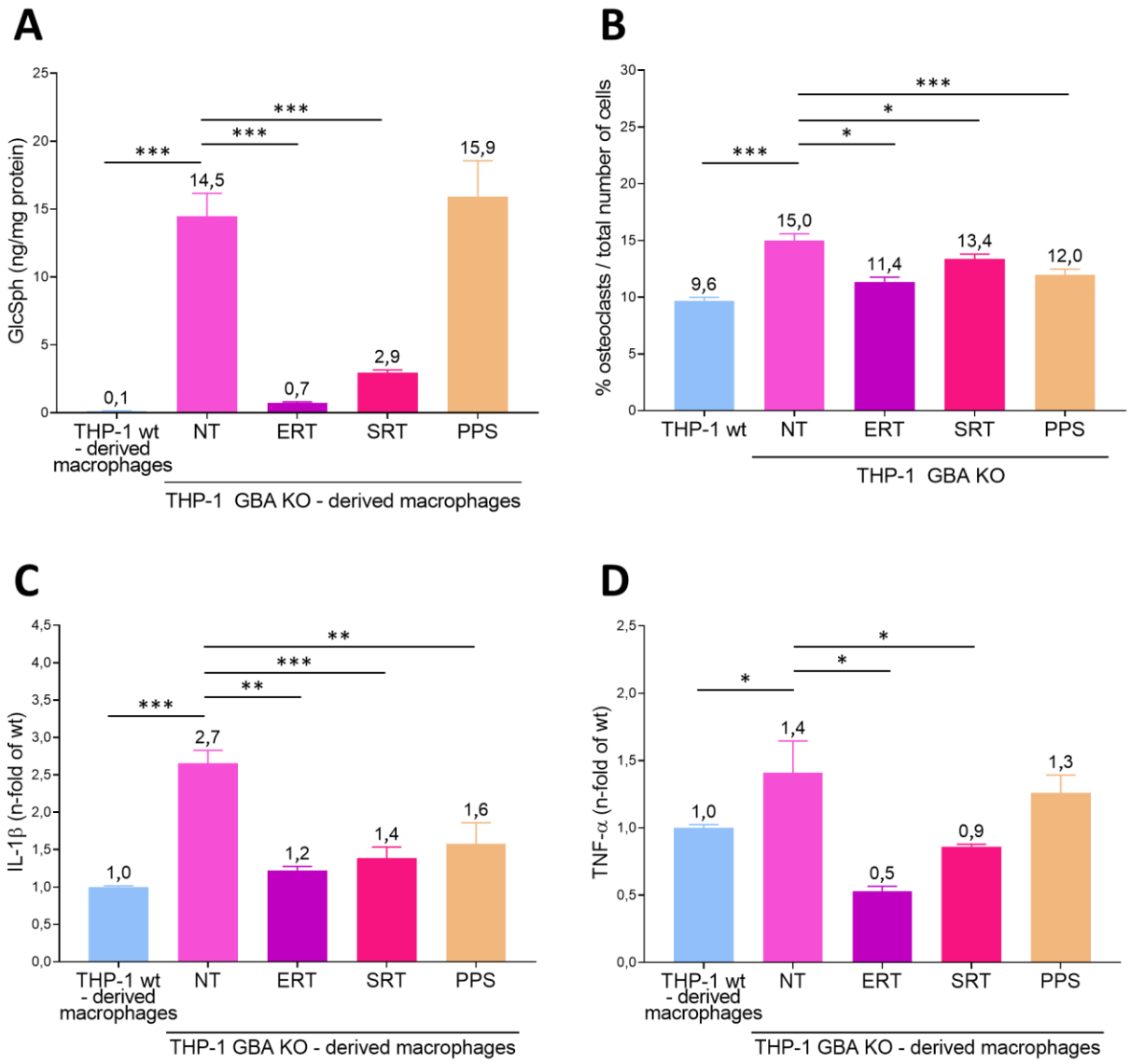


**Figure R7 | Exploring osteoclastogenesis under treatments.** A. GlcSph accumulation in THP-1 wt cells or in THP-1 GBA KO cell not treated (NT) or treated with recombinant human GCase (ERT), with Eliglustat (SRT) or PPS; B. Osteoclastogenesis in THP-1 wt cells or in THP-1 GBA KO cell not treated (NT) or treated with recombinant human GCase (ERT), with Eliglustat (SRT) or PPS; C. IL-1β release in THP-1 wt derived macrophages or in THP-1 GBA KO derived macrophages not treated (NT) or treated with recombinant human GCase (ERT), with Eliglustat (SRT) or PPS; D. TNF-α release in THP-1 wt derived macrophages or in THP-1 GBA KO derived macrophages not treated (NT) or treated with recombinant human GCase (ERT), with Eliglustat (SRT) or PPS. *Results are expressed as mean ± SD of three independent experiments. *p-value < 0,05; **p-value < 0,01; ***p-value < 0,001.*

## 4.2.b Studying GD osteoblasts

To characterize the selected model of GD osteoblasts (SaOS GBA KO clone A7 - see section 4.1.b) from the functional point of view, we firstly focused on two essential proteins involved in bone formation: ALP and type I collagen.

As already mentioned, ALP is an enzyme involved in the mineralization of bone, as it hydrolyses the phosphoric esters such as pyrophosphate (PPi) to generate inorganic orthophosphates (Pi), which together

with calcium form the hydroxyapatite crystals, representing the major components of the inorganic phase of the cellular matrix. Type I collagen is a triple helix protein consisting of two α1 chains and one α2 chain, and it is the most abundant component of the organic phase of the extracellular matrix and serves as a template upon which mineral is deposited (**figure R8A**) [150,151].

Thus, we measured the mRNA expression of the ALP encoding gene (*ALPL*) and the pro-α1 chain of collagen type I encoding gene (*COL1A1)*. We noticed a slight decrease in the mRNA expression of *ALPL* in the case of clone A7, which also displayed 50% of *COL1A1* mRNA expression (**figure R8B**).

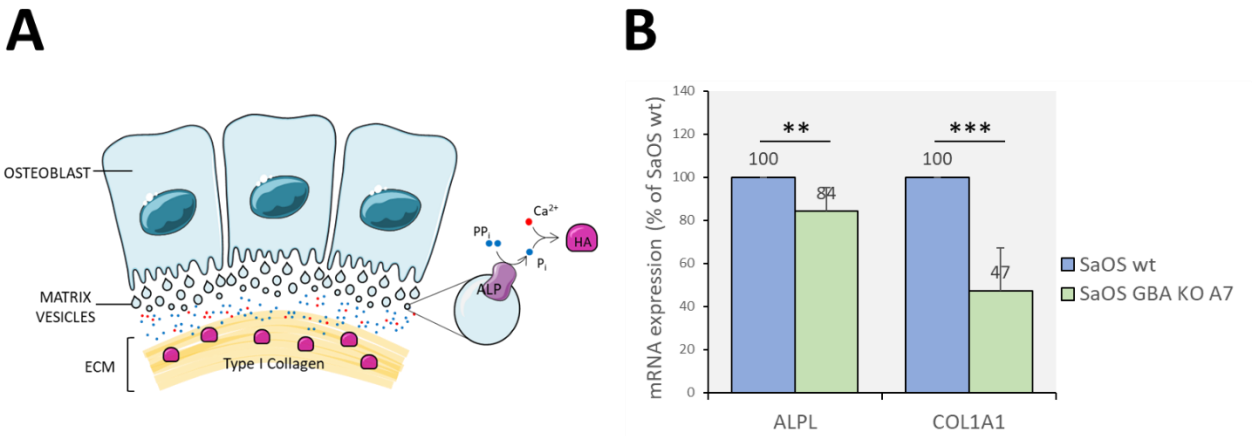


**Figure R8 | *ALPL* and *COL1A1* in SaOS osteoblast model.** A. overview of the roles of ALP and type I collagen in bone biology; B. mRNA expression of *ALPL* and *COL1A1*. *Results are expressed as mean ± SD of three independent experiments. **p-value < 0,01; ***p-value < 0,001.*

In light of these results, we assessed SaOS wt and clone A7 for ALP activity by performing ALP staining, in which the amount of blue precipitate depends on the activity of this enzyme. As reported in **figure R9A**, no clear difference could be observed. Then, we measured the amount of matrix deposition and mineralization by staining calcium deposits with Alizarin Red. Also in this case, no clear difference between the two cells could be observed (**figure R9B**), but when we performed the dye extraction and quantitation, we noticed a slight decrease in the case of GBA KO cells (**figure R9C**). Even though we reached statistical significance, we do not know whether this may actually have an impact from the biological point of view.

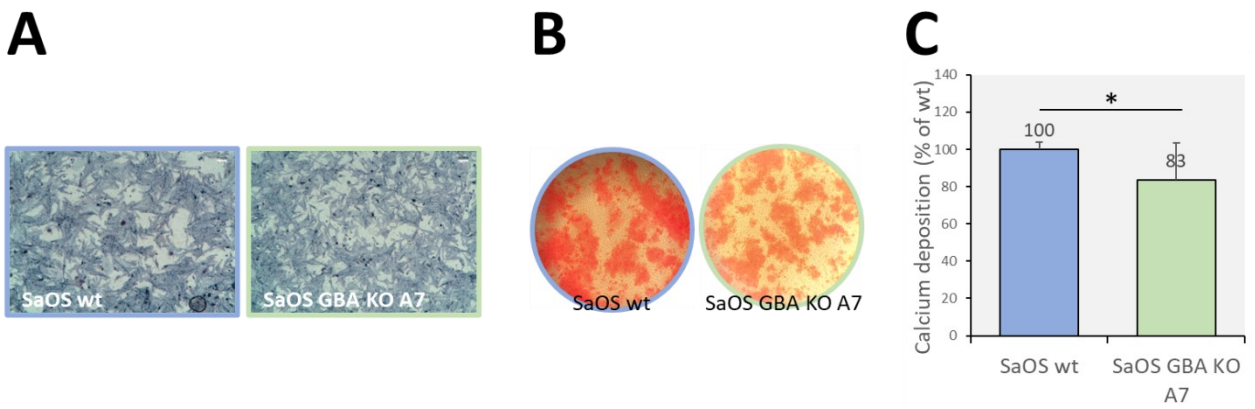


**Figure R9 | ALP and calcium deposition in SaOS osteoblast model.** A. ALP staining; B. Alizarin Red staining; C. Quantitation of Alizarin Red Staining. *Results are expressed as mean ± SD of three independent experiments. *p-value < 0,05.*

Secondly, we performed Sirius Red Staining to measure collagen deposition, which can be visualized as red deposits. In this case, a clear difference could be seen (**figure R10A**) and, indeed, when we performed the dye extraction and quantitation, SaOS GBA KO A7 cells displayed a significant reduction in collagen deposition (**figure R10B**).

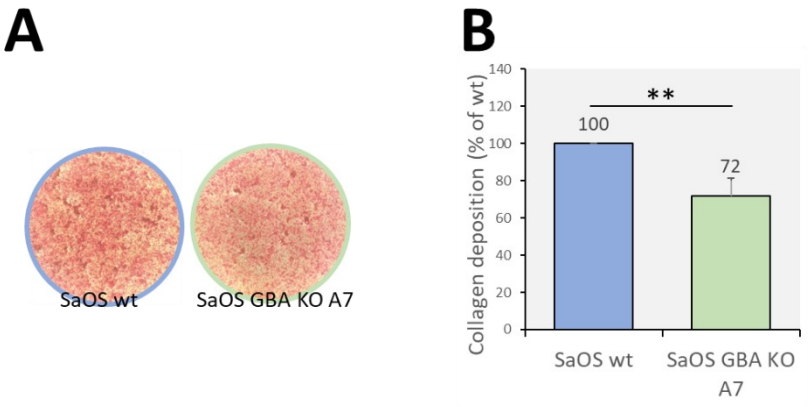


**Figure R10 | Collagen deposition in SaOS osteoblast model.** A. Sirius Red Staining for collagen deposition; B. Sirius Red Staining quantitation. *Results are expressed as mean ± SD of three independent experiments. **p-value < 0,01.*

These results suggest an impairment in the functioning of GD osteoblasts.

## *miRNA profiling of GD osteoblasts*

Micro-RNAs (miRNAs) play a role in pathogenic processes in many diseases, including several in which bone is affected [130–132]. Thus, intending to explore a possible role of miRNAs in bone pathology in GD, we decided to focus on the SaOS osteoblastic model, as these cells represent a homogeneous, mature, well-characterized population displaying features of GD. We performed a miRNA profiling of both expressed and exosomal miRNAs, exploiting next-generation sequencing techniques (NGS), and compared it with the profile of expressed and exosomal miRNAs detected in SaOS wt.

More than 700 miRNAs were identified. Among them, we focused on those differentially expressed in GBA KO versus wt SaOS cells, considering significant an increase or decrease > 2-fold and a p-value < 0,05. By applying these thresholds, we identified 7 up-regulated miRNAs (hsa-miR-548y, hsa-miR-208b-3p, hsa_piR_009294/gb/DQ582566/Homo, hsa-miR-466, hsa_piR_017814/gb/DQ594584/Homo, hsa-miR-597-5p, hsa-miR-488-3p) and only one downregulated miRNA (hsa-miR-195-5p) in SaOS GBA KO cells in comparison with SaOS wt (**figure 11A**).

Among the up-regulated miRNAs, we decided to further study miR-488-3p, as it displayed the highest differential expression, almost reaching a 5-fold increase in GBA KO cells in comparison to SaOS wt. Moreover, it was reported in the literature as a negative regulator of osteogenic differentiation of bone marrow stem cells [152]. All the other overexpressed miRNA identified with the criteria reported above were low expressed both in wt and GBA KO cells, thus they were excluded from the analysis. Finally, our attention was captured by miR-93-3p, whose level of expression in clone A7 was 1,83-fold of wt cells, and still statistically significant (p-value=0,043): this miRNA was described in the literature as a negative regulator of osteogenic differentiation [153] (**figure 11A**).

As the next step, we validated the data of miR-488-3p, miR-93-3p, and miR-195-5p by qRT-PCR. The only miRNA that showed the same trend observed by NGS was miR-488-3p, which displayed a 14-fold increase in GBA KO osteoblasts in comparison with wt (**figure 11B**).

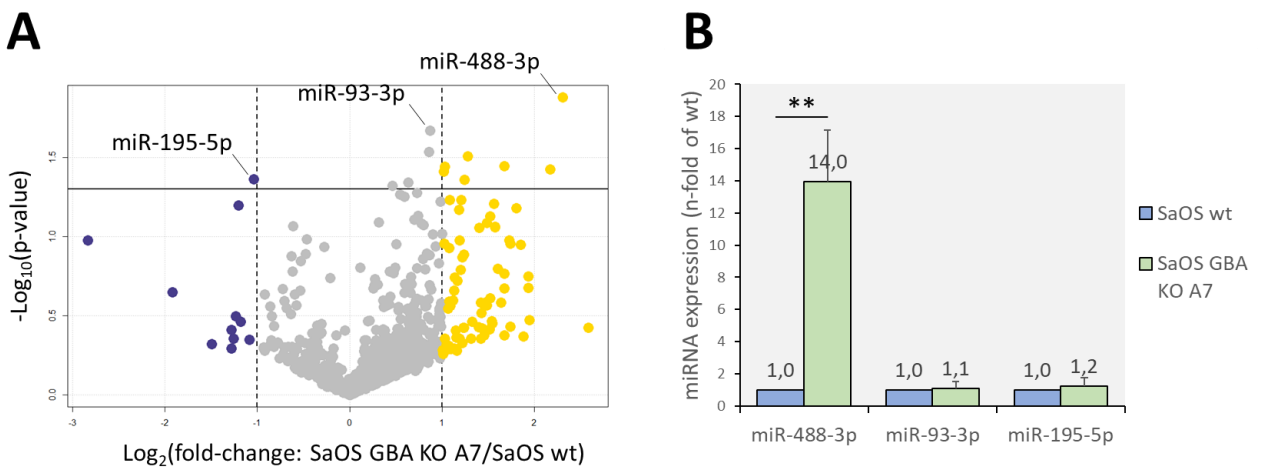


**Figure R11 | Expressed miRNA profile of SaOS osteoblast model.** A. Volcano plot of miRNA profile (the horizontal line indicates the p-value < 0,05 threshold, whereas the dotted lines indicate the 2-fold increase and decrease expression, compared to wt cells, on the right and left, respectively); B. qRT-PCR validation of miRNA expression of the most promising differentially expressed ones. *Results are expressed as mean ± SD of three independent experiments. **p-value < 0,01.*

In addition to the expressed miRNAs, we also analysed the exosomal miRNAs. Thus, we extracted miRNAs from exosomes isolated from the conditioned media of SaOS wt and GBA KO cells. We performed the miRNA profiling by NGS, and by applying the exclusion criteria reported above, we identified 5 upregulated miRNAs (hsa-miR-3679-5p, hsa-miR-3663-5p, hsa-miR-1233-5p, hsa-miR-6852-3p, hsa-miR-1178-3p) and 1 downregulated one (hsa-miR-490-5p) (**figure R12A**). Also in this case, all the upregulated miRNAs presented a very low expression both in SaOS wt and GBA KO, except for miR-1233-5p and miR-3679-5p which were further investigated. In addition, we noticed that miR-4784 was significantly upregulated, showing a 1,96-fold increase with a p-value of 0,026. Moreover, we noticed that miR-488-3p, which was overexpressed by SaOS GBA KO, was also increased in the exosomes from the same cells, even though the p-value was just above the significance threshold (p-value = 0,059). For these reasons, we performed the qRT-PCR validation of miR-1223-5p, miR-3679-5p, miR-4784, miR-488-3p and miR-490-5p.

As reported in **figure R12B**, we validated the overexpression of miR-488-3p, miR-1223-5p, and miR-4784, as well as the downregulation of miR-490-5p. No significant difference in the expression of miR-3679-5p was observed.

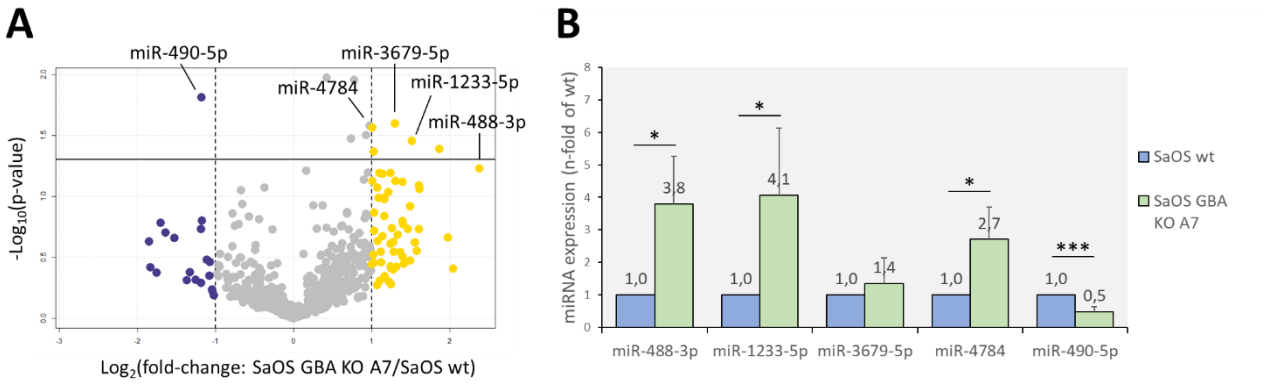


**Figure R12 | Exosomal miRNA profile of SaOS osteoblast model.** A. Volcano plot of miRNA profile (the horizontal line indicates the p-value < 0,05 threshold, whereas the dotted lines indicate the 2-fold increase and decrease expression, compared to wt cells, on the right and left, respectively); B. qRT-PCR validation of miRNA expression of the most promising differentially expressed ones. *Results are expressed as mean ± SD of three independent experiments. *p-value < 0,05, ***p-value < 0,001.*

As miR-488-3p resulted to be upregulated in both intracellular and exosomal preparations, we decided to further study the possible role of this miRNA in bone pathogenesis. To this end, we transfected SaOS wt with this miRNA (**figure R13A**), and we quantified the mRNA expression levels of *ALPL* and *COL1A1*. As reported in **figure R13B**, a slight decrease in *ALPL* expression and a marked decrease in *COL1A1* expression were observed. As miR-488-3p was described as a negative regulator of RUNX2 [152], we quantified the expression of this gene in transfected cells and we found a decrease in its expression. These results indicate a potential role of miR-488-3p in the downregulation of RUNX2, eventually causing a reduction in the expression of osteoblastic markers *ALPL* and *COL1A1*.

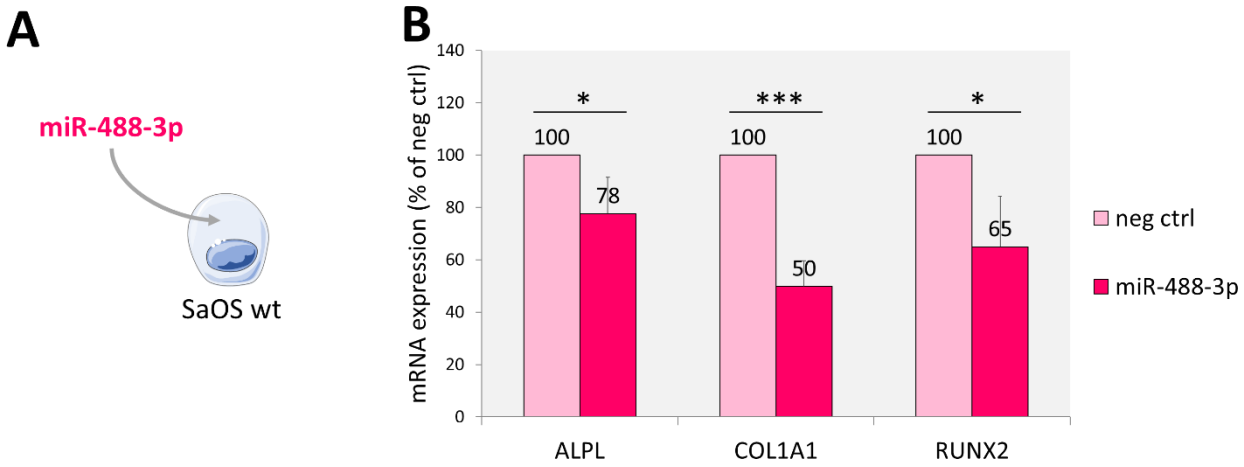


**Figure R13 | Role of miR-488-3p in the regulation of bone genes expression in wt SaOS osteoblasts.** A. Overview of the experiment; B. qRT-PCR on *ALPL*, *COL1A1*, and *RUNX2* on SaOS wt transfected with miR-488-3p or negative control (neg ctrl). *Results are expressed as mean ± SD of three independent experiments. *p-value < 0,05; ***p-value < 0,001.*

### *Validating miR-488-3p in primary osteoblasts*

Finally, we further validated the miR-488-3p results in human primary cultured osteoblasts. To mimic GD, we treated normal osteoblasts with conduritol B epoxide (CBE), an inhibitor of GCase. To understand whether the treatment induces the GD features in these cells, we measured the GCase activity and GlcSph accumulation after three and six days of treatment. As reported in **figure R14A**, a significant reduction in GCase activity was achieved under treatment (reaching a residual GCase activity of 2,8% of the activity found in untreated osteoblasts after 6 days), as well as a marked increase in GlcSph levels (**figure R14B**). As the treatment does not seem to affect the viability or the proliferation of osteoblasts, we selected 6 days as the appropriate timing to model GD in normal primary osteoblasts.

Thus, we treated osteoblasts with CBE, and after 6 days we performed the miRNAs extraction. We measured the levels of expression of miR-488-3p in qRT-PCR and we noticed a significant increase in its expression in CBE-treated osteoblasts (**figure R14C**).

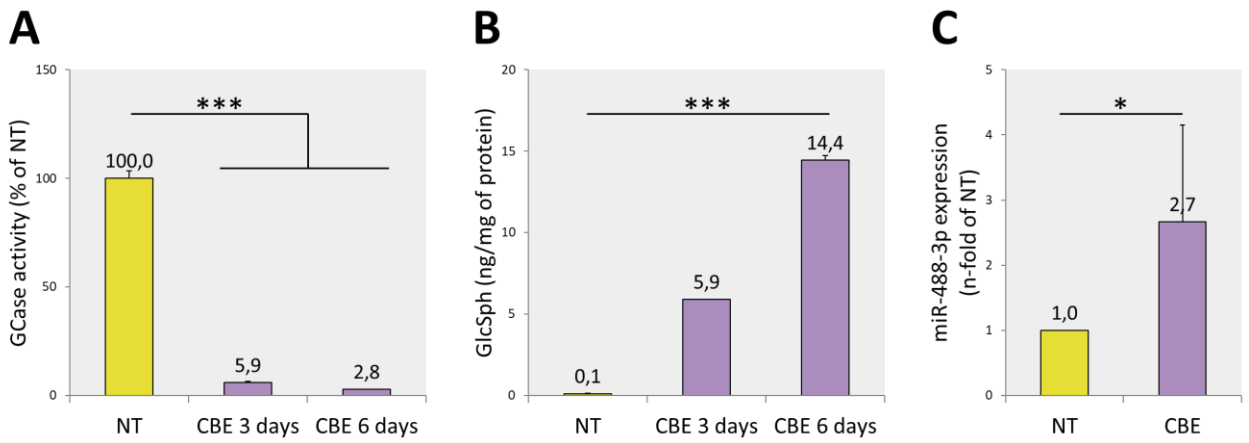


**Figure R14 | Modelling GD primary osteoblasts and analysis of miR-488-3p expression.** A. GCase activity of primary osteoblasts treated for three or six days with CBE or vehicle (NT); B. GlcSph accumulation in primary osteoblasts treated for three or six days with CBE or vehicle (NT); C. miR-488-3p expression in primary osteoblasts for six days with CBE or vehicle (NT). *Results are expressed as mean ± SD of three (GCase activity and GlcSph) or four (miR-488-3p expression) independent experiments. *p-value < 0,05; ***p-value < 0,001.*

These results suggest a possible role of miR-488-3p in the pathogenesis of bone involvement in GD.

## 4.2.c Studying GD chondrocytes

As previously mentioned, chondrocytes express several markers in accordance with their maturation status. Thus, we characterized the C28I2 chondrocyte model (C28I2 GBA KO clone A1 - see section 4.1.c) by measuring the mRNA expression of SOX9, the main transcription factor involved in chondrocyte maturation, the expression of type II collagen, which is expressed by differentiating chondrocytes, and the expression of type X collagen, representing the marker of hypertrophic chondrocytes [97].

As reported in **figure R15A**, no differences in *SOX9* mRNA expression were observed, whereas a reduction of collagen type II α1 chain (*COL2A1*) and an increase in collagen type X α1 chain (*COL10A1*) mRNA expression were recorded in C28I2 GBA KO A1 in comparison with C28I2 wt. These results indicate a possible impairment in the differentiation status of GD chondrocytes, which are likely to be committed to a hypertrophic fate.

We then decided to investigate whether GD chondrocytes may differ from the normal ones also in terms of their capability of bursting inflammation, which may somehow explain the pain experienced by some patients [41,154,155]. Thus, we measured the levels of inflammatory cytokines in the conditioned media from C28I2 wt or GBA KO A1. No differences in the secreted levels of IL-1β, TNF-α, and IL-6 were observed, whereas a massive amount of IL-8 was released by GBA KO cells in comparison to wt (**figure R15B**).

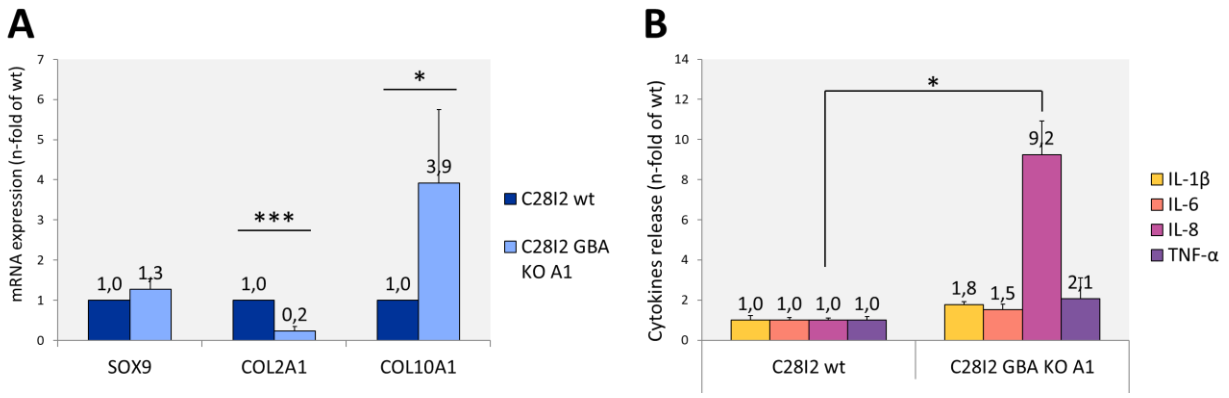


**Figure R15 | Studying C28I2 chondrocyte model.** A. mRNA expression of *SOX9*, *COL2A1*, *COL10A1*; B. Pro-inflammatory cytokines release. *Results are expressed as mean ± SD of three independent experiments. *p-value < 0,05; ***p-value < 0,001.*

As IL-8 is reported to act as a chemoattractant of neutrophils [156], we assessed the capability of GD or wt chondrocytes to attract neutrophils isolated from healthy donors. Therefore, we cultured C28I2 wt or GBA KO A1 for 48 hours to allow the cells to conditionate the medium. On day two, transwells were inserted in the wells containing the cultured chondrocyte cells and their conditioned medium, as well as in additional wells containing only the conditioned media (**figure R16A**). We isolated neutrophils from the peripheral blood of healthy controls, loaded them onto the transwells and after 2 hours we counted the number of neutrophils that migrated through the transwell, as well as the non-migrating ones. In the wells containing the chondrocyte cells and their conditioned medium, we noticed a higher rate of migration in wells containing GBA KO chondrocytes in comparison with wt, as assessed by flow cytometry (**figure R16B**). Surprisingly, no differences in the rate of migration were observed when only the supernatant of GBA KO chondrocytes was used to attract the neutrophils (**figure R16B**).

Moreover, as the number of conditioning C28I2 cells was used to normalize migration data, we detached cells from the bottom of the well and counted them. Interestingly, only in the counting chamber containing the detached C28I2 GBA KO cells, a massive number of cells much smaller than the C28I2 was observed (**figure R16C**). Even though a specific marker should be used to identify the neutrophils, this evidence may contribute to strengthening the observations reported above.

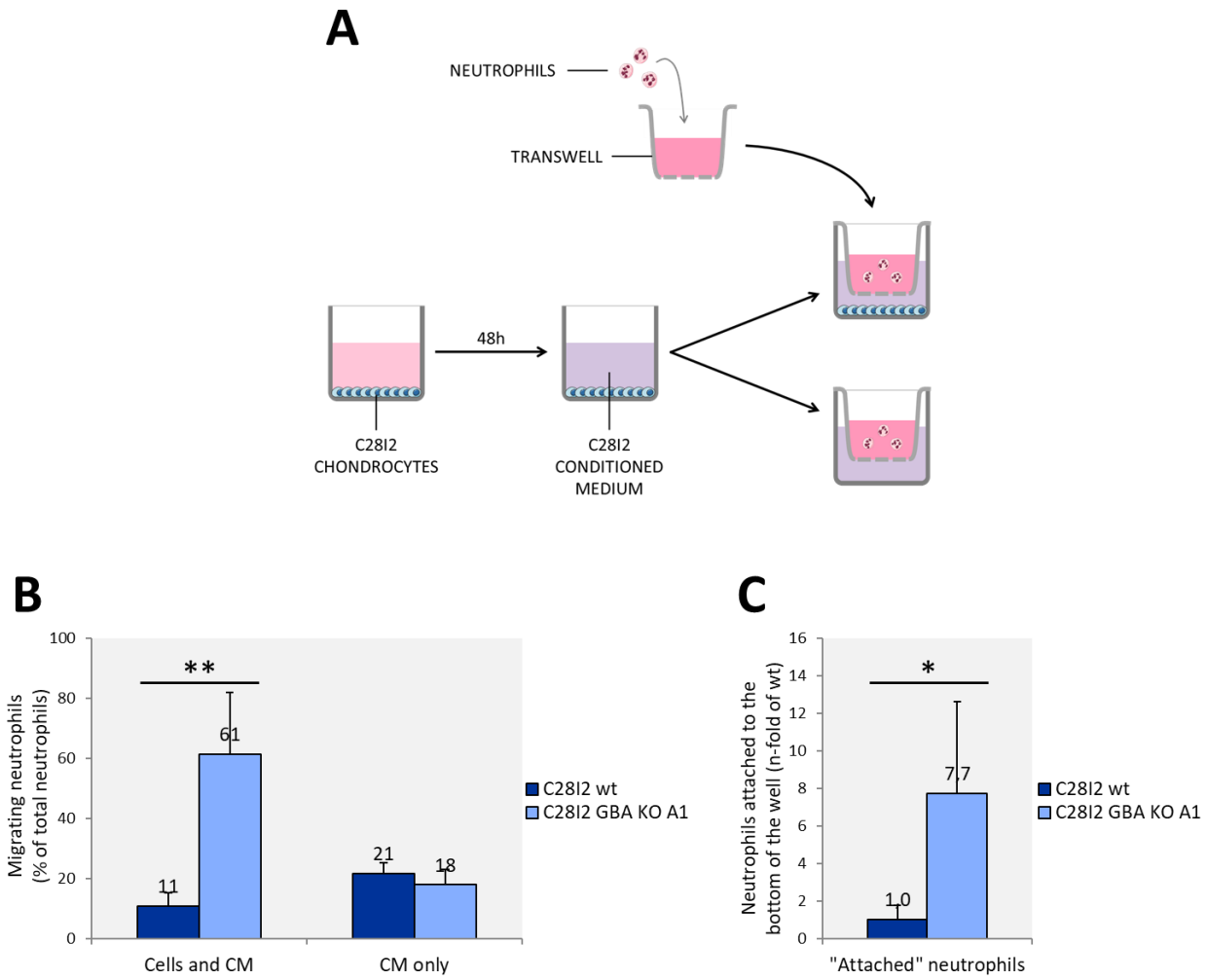


**Figure R16 | Exploring the role of C28I2 as neutrophils attractors.** A. Overview of the experiment; B. amount of neutrophils passing through the transwell analyzed by flowcytometry and expressed as (migrating neutrophils)/(migrating+non migrating neutrophils)*100, in the presence of either C28I2 and their conditioned media (CM) or the sole CM. B. Relative amount of neutrophils attached to the bottom of the well in which both the cells and their CM were present. *Results are expressed as mean ± SD of three independent experiments. *p-value < 0,05; **p-value < 0,01.*

These results indicate that GD chondrocytes may attract neutrophils at a higher rate in comparison to normal ones, but it seems unlikely that the soluble factor IL-8 is the sole responsible for this process, as no differences with the use of the solely conditioned medium were observed.

# 4.3 CELL TO CELL INTERACTIONS

## 4.3.a Osteoblasts and osteoclastogenesis

To study the possible interactions between different types of bone cells, we first decided to investigate osteoblasts-osteoclasts crosstalk. As already mentioned, osteoblasts produce the receptor activator of NF-KB ligand (RANKL), whose receptor RANK is located on the surface of osteoclasts. The binding RANKL/RANK induces osteoclastogenesis. However, osteoblasts also produce osteoprotegerin (OPG), which binds RANKL as well, avoiding its binding to RANK. Thus, RANKL and OPG have opposite effects on osteoclastogenesis [68]. For this reason, we measured the mRNA expression of *RANKL* and *OPG*: SaOS GBA KO A7 showed a 2-fold increase in *RANKL*/*OPG* ratio, indicating that the amount of RANKL free to bind RANK was higher (**figure R17A**). We tried to validate this observation by measuring the amount of the released free RANKL by performing an ELISA with the conditioned media of these cells, but we were not able to detect this protein with the commercial kit we used. To overcome this problem, we decided to differentiate THP-1 wt cells by culturing them with conditioned media from SaOS wt or GBA KO A7 with the addition of M-CSF (**figure R17B**). When we counted the number of osteoclasts as described above, THP-1 differentiated in the presence of conditioned medium from GBA KO cell showed a higher rate of osteoclastogenesis than THP-1 differentiated with medium conditioned by SaOS wt (**figure R17C**). This suggests that the impairment in osteoblastic function due to GD does influence the osteoclastogenic process, despite the "status" of the osteoclast precursor. To demonstrate that RANKL and/or OPG are the cause of this increased osteoclastogenesis, this latter experiment should be repeated by inhibiting RANKL and/or OPG synthesis.

As previously mentioned, many inflammatory cytokines are involved in osteoclastogenesis as regulatory factors. Thus, we measured the secretion of IL-1β, IL-6, TNF-α, and IL-8 by SaOS wt and GBA KO A7. No difference in the expression of these factors was observed (**figure R17D**). This may suggest that the increase in osteoclastogenesis detected in the presence of the conditioned medium from SaOS GBA KO A7 is unlikely to be due to a higher presence of well-established pro-osteoclastogenic inflammatory cytokines (i.e., IL-1β).

These data may suggest that the decrease in osteogenesis in GD is not only due to a decreased activity of osteoblasts but also to an increased activity of osteoclasts caused by the impairment of the normal osteoblasts-osteoclasts crosstalk.

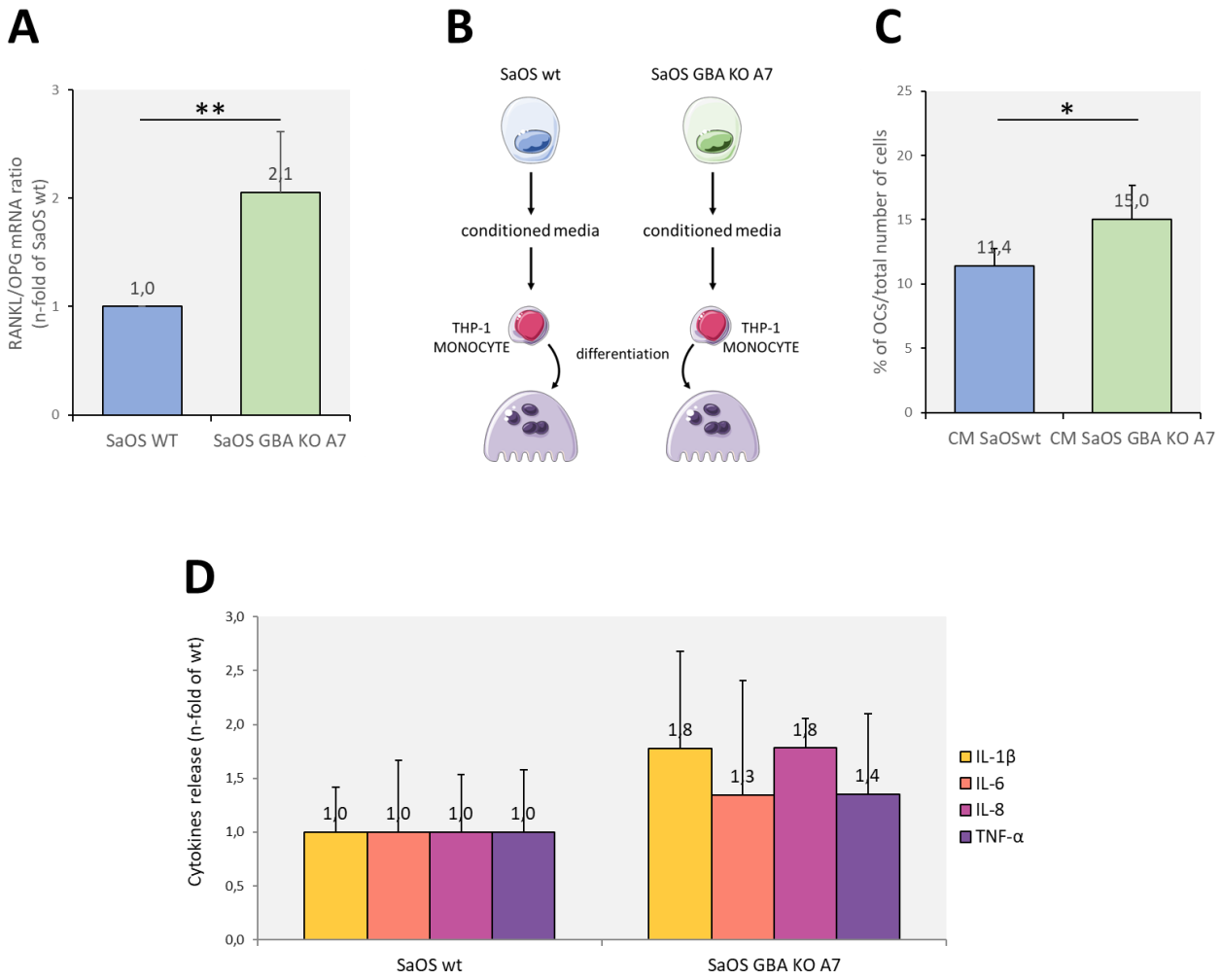


**Figure R17 | Exploring osteoblasts-osteoclasts crosstalk.** A. Overview of the experiment; B. *RANKL/OPG* mRNA expression ratio; C. osteoclastogenesis in the presence of conditioned medium (CM) from SaOS wt or SaOS GBA KO A7 expressed as the % of osteoclasts in the whole population; D. pro-inflammatory cytokines release in the supernatant by SaOS wt or SaOS GBA KO A7. *Results are expressed as mean ± SD of three independent experiments. *p-value < 0,05; **p-value < 0,01.*

## 4.3.b Chondrocytes and osteoclastogenesis

Finally, we wondered whether also C28I2 wt or GBA KO A1 may differentially influence osteoclastogenesis. As reported above, we noticed a marked increase in IL-8 release by GBA KO cells, and IL-8 was reported as a pro-osteoclastogenic factor. Thus, we performed a preliminary experiment similar to the one already described for osteoclastogenesis with conditioned media from SaOS cells: we cultured C28I2 wt and GBA KO A1, we collected their conditioned media, which we used to induce osteoclastogenesis of THP-1 monocytes in presence of M-CSF (**figure R18A**). Even though we did not reach the statistical significance (p-value=0,056) probably because the experiment was repeated only twice, we noticed an increase in the % of osteoclasts when the conditioned medium from C28I2 GBA KO A1 was used (**figure R18B**). To validate these observations, the experiment should be repeated; furthermore, inhibition of IL-8 should be performed to understand whether it can act as the key factor of the process. However, the percentage of osteoclasts in the whole

population was very low in comparison with the data reported for osteoclastogenesis in the presence of M-CSF and RANKL (**figure R6**) or in the presence of M-CSF and conditioned media from SaOS (**figure R17C**). For this reason, we will repeat this experiment by supplementing the conditioned media from C28I2 with M-CSF and RANKL. If an increase in the percentage of osteoclasts is confirmed, this will suggest that impairment in chondrocytes may also affect the osteoclastogenic process.

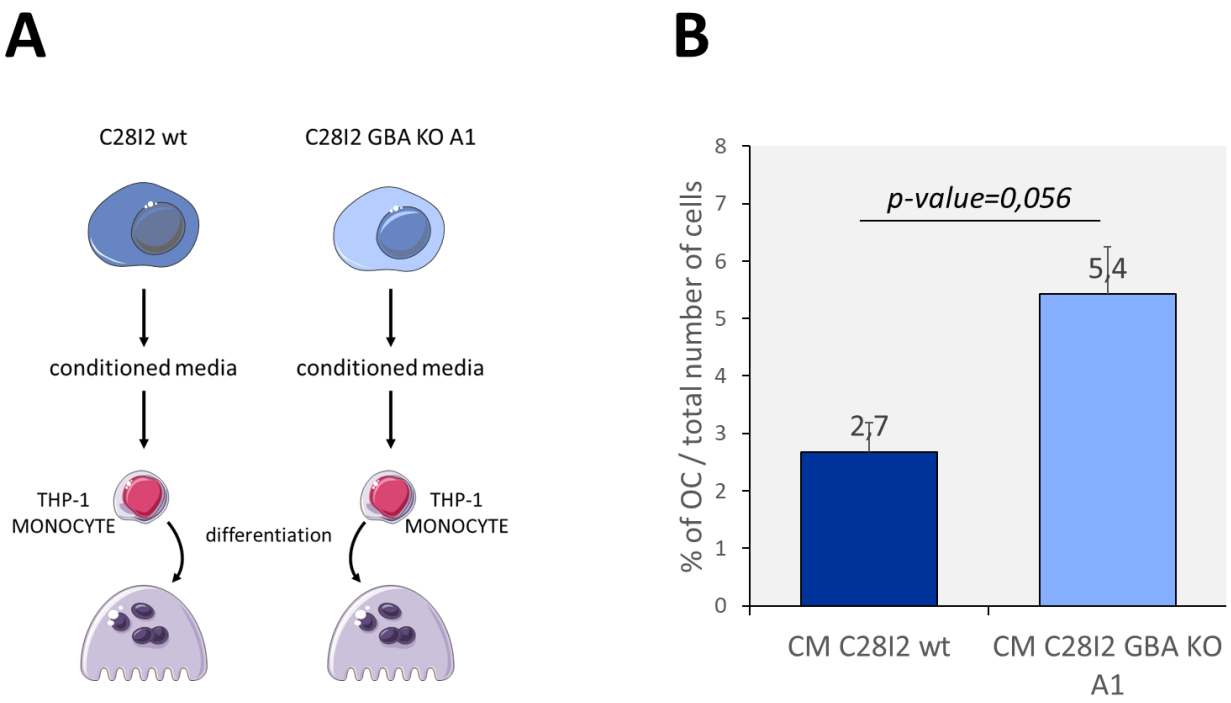


**Figure R18 | Exploring chondrocytes-osteoclasts crosstalk.** A. Overview of the experiment; B. osteoclastogenesis in the presence of conditioned medium (CM) from C28I2 wt or C28I2 GBA KO A1, expressed as the % of osteoclasts in the whole population; *Results are expressed as mean ± SD of two independent experiments.*

# 5 DISCUSSION

Mutations in the *GBA1* gene cause Gaucher Disease (GD), a multisystemic autosomal recessive lysosomal storage disorder characterized by a progressive accumulation of glycosphingolipids within the lysosomes [1,30]. Most GD patients report bone symptoms (including osteopenia, osteoporosis, osteonecrosis, and bone pain), which, along with neurological impairments that occur only in the most severe forms of the disease (approximately 5% of patients), represent the most debilitating aspect of the disease, severely reducing patients' quality of life [41].

The molecular basis of bone involvement in GD is not clear. However, several lines of evidence suggest that both osteoblasts and osteoclasts play a role in the pathogenic process, whereas almost no information is available about cartilage cells [110].

Researchers in the field of GD have been looking for effective cell models to pursue a better understanding of GD pathophysiology and to develop novel therapeutic approaches [157,158].

The development of genome editing technologies, and in particular the CRISPR/Cas9 platform, has provided researchers with a versatile tool that can be exploited for the generation of cellular models of diseases by introducing site-specific mutations within the gene of interest [159,160]. The application of this technology offers the possibility to generate isogenic cells, allowing the production of cellular models in which the only genetic difference between the wild-type (wt) and mutant cells is the disease-causative mutation. This type of model avoids the possibility of detecting non-disease-related phenotypes arising from differences in the genetic background of affected and control cells. In addition, the possible use of easily findable commercial cell lines allows the generation of disease models of different cell types relevant to disease pathology. Most of these cell lines are easy to grow in culture making them ideal tools for high-throughput experiments and drug screening [140].

Therefore, to study bone pathophysiology in GD, we created bone and cartilage cell models of the disease by CRISPR/Cas9 editing the *GBA1* gene in continuous cell lines.

## 5.1 IMPAIRED OSTEOCLASTOGENESIS IN THP-1 MONOCYTIC MODEL OF GD

We firstly developed and characterized a monocytic model of the disease (THP-1 GBA KO) which recapitulates the disease hallmarks: low GCase expression and residual activity, and accumulation of GlcSph [140]. We deepened the model by studying the activity of the other two β-glucosidases (GBA2 and GBA3), without noticing any difference in GBA KO cells in comparison with wt. An increase in GBA2 activity was expected, as this cytosol-faced retaining β-glucosidase is reported to be increased in GCase deficiency, acting as a transglycosylase and transferring glucose from GlcCer to cholesterol, generating glycosyl-β-cholesterol (GlcChol) [37]. Despite no difference in GBA2 activity, increased levels of GlcChol were observed in GBA KO cells (**figure D1**), which suggests that the lysosomal degradation of GlcChol by GCase is impaired when this enzyme is missing. As expected, levels of glucosylceramide (GlcCer) were increased in GBA KO cells, resulting in a subsequent decrease in Ceramide (Cer) and its deacylated form Sphingosine (Sph). In addition, we found an increase in the levels of Sphinganine and its derivate Dihydroceramide (dh-Cer), the source of Cer, probably as a compensatory mechanism triggered by the cell in an attempt to restore the Cer levels (**figure D1**).

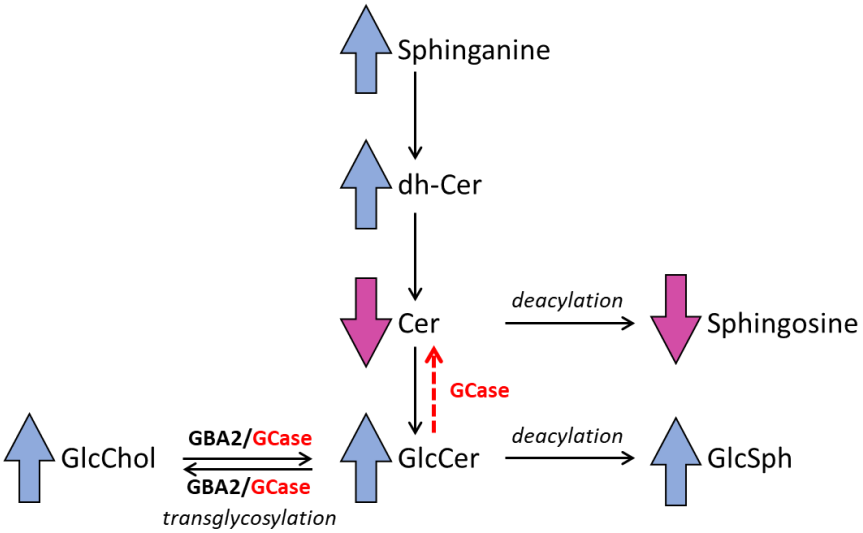


**Figure D1** | Changes in lipid profile in THP-1 GBA KO cells.

Next, we studied the ability of THP-1 monocytes to differentiate into osteoclasts, by providing them with the appropriate stimuli. We noticed an increase in osteoclastogenesis in THP-1 GBA KO cells in comparison with wt, which could be reverted by decreasing GlcSph accumulation by using either the recombinant human GCase (ERT) or Eliglustat to inhibit the synthesis of GlcCer (SRT). These data indicate that GBA KO monocytes present a higher osteoclastogenic potential than wt cells, leading to the generation of a higher number of osteoclasts, and that the accumulation of glycosphingolipids plays a crucial role in the process. Increased osteoclastogenesis in GD or GD miming conditions has been previously reported [114,122,123,126,161]. It is worth underling that the evidence of increased osteoclastogenesis in GD patients in comparison with healthy controls was obtained by comparing the rate of this process in peripheral blood mononuclear cells (PBMCs) [126] or monocytes isolated from the PBMCs pool [122,123]. However, in these models, the increased number of osteoclasts obtained after differentiation may reflect the higher number of pre-osteoclasts already present in the PBMCs population from GD patients when compared with healthy controls, probably due to the enhanced inflammatory environment in which these cells originate [126]. Moreover, monocytes isolated from PBMCs pool have already been interacting with other cells, including T and dendritic cells, which showed increased pro-inflammatory cytokines production in GD patients [126]. Thus, in those systems, the increased osteoclastogenesis cannot be explained only by the GCase deficiency and subsequent glycosphingolipid accumulation. On the contrary, our model consists of naïve cells, which have not been influenced by another microenvironment than the one consisting of the monocytic precursors they derive from.

In addition, the role of glycosphingolipids in osteoclastogenesis in GD has been suggested, as GlcCer was reported to cause increased osteoclastogenesis and osteoclasts activity, and as treatment with recombinant GCase was shown to reduce these two aspects [114,122,123,126]. Thus, our observations support the role of glycosphingolipid accumulation in inducing osteoclastogenesis.

On the other hand, also inflammation plays a role in this process, as decreased osteoclastogenesis has been observed using the anti-inflammatory compound PPS, which does not affect glycosphingolipid accumulation. The role of inflammation in enhancing osteoclastogenesis has been previously reported as well [115,127].

It should be noted that glycosphingolipid accumulation and inflammation are two related phenomena. Indeed, the increased osteoclastogenesis observed in THP-1 GBA KO may also be due to an enhanced release of pro-inflammatory cytokines by osteoclasts themselves or their precursors in a paracrine and/or autocrine manner. ERT and SRT treatments during osteoclast differentiation may reduce the inflammation in osteoclasts/osteoclasts precursors by decreasing glycosphingolipid accumulation and eventually cause decreased osteoclasts formation. In accordance with that, we demonstrate that THP-1 GBA KO-derived macrophages secreted higher levels of IL-1β and TNF-α, and that the levels of these pro-inflammatory cytokines are reduced under ERT or SRT. This may suggest that the increased osteoclastogenesis due to glycosphingolipid accumulation is mediated by inflammation.

**Figure D2** reports our findings on GD osteoclasts: we report a decreased osteoclastogenesis which could be due to inflammation, probably triggered by glycosphingolipid accumulation.

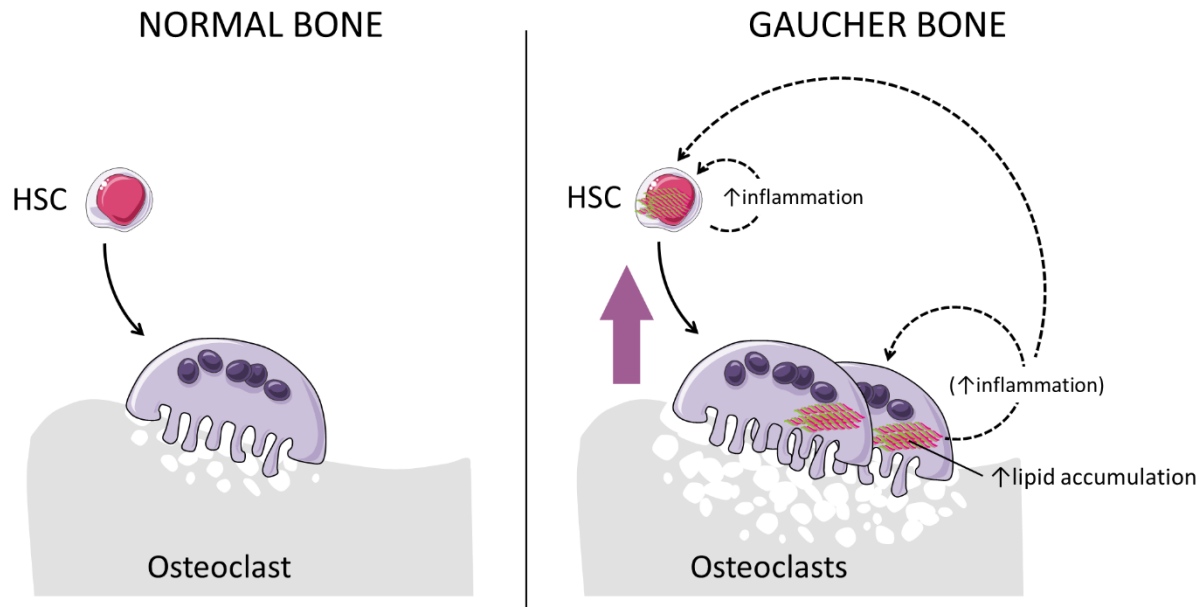


**Figure D2** | Overview of findings on osteoclastogenesis in our model of GD.

## 5.2 IMPAIRED OSTEOGENESIS IN SaOS OSTEOBLASTIC MODEL OF GD

We developed a model of GD osteoblasts by CRISPR/Cas9 editing the osteosarcoma cell line SaOS2, which displayed high levels of alkaline phosphatase (ALP) activity and could produce a mineralized matrix. We obtained a clone (SaOS GBA KO A7), which showed no GCase protein, low residual GCase activity, and a massive accumulation of GlcSph, and so we selected this clone as the model of GD osteoblast.

GBA KO A7 cells displayed a slight decrease in ALP gene (*ALPL*) expression and calcium deposition, and a marked decrease in collagen type I encoding gene (*COL1A1*) expression and collagen deposition. These data indicate an impairment in osteoblastic functioning and are in line with previously reported evidence. Indeed, decreased *ALPL* and *COL1A1* expression were observed in all reports in which these aspects have been studied [111,116,117], except for one in which an increase in *ALPL* was recorded [121]. With the exception

of one paper [121], a reduction in calcium and collagen deposition was recorded in all reports in which mesenchymal stem cells (MSCs) from GD patients were differentiated into osteoblasts [114,116,117]. These data indicate that GD MSCs present a lower tendency to differentiate into osteoblasts than normal MSCs. As previously mentioned, a possible explanation regards the capability of MSCs to differentiate into adipocytes or osteoblasts: MSCs preferentially perform adipogenesis when GlcCer is provided [118], and similarly, GD-derived MSCs showed a higher rate of adipogenesis than healthy controls-derived MSCs [116].

Impairment in osteogenesis is supported also by evidence obtained using animal models of the diseases, as decreased differentiation of osteoblasts was reported in GD mouse and zebrafish models. The suggested explanation for such observations includes a defective protein kinase C activation or increased oxidative stress and reduced Wnt/β-catenin signalling, respectively [111,112].

Only one group studied the function of mature osteoblasts by treating osteoblastic cell line SaOS2 with the GCase inhibitor conduritol B epoxide (CBE). Interestingly, the use of CBE on SaOS2 by Reed and colleagues did not affect osteogenesis, as treated and untreated cells did not diverge in terms of calcium deposition, and only a decrease in proliferation but not in calcium deposition was observed when GlcCer or GlcSph were provided to these cells [114]. Even though these data seem to exclude a role of mature osteoblasts in GD bone pathogenesis, our data do indicate a role of these cells in the process. The reason beyond the different observations may rely on the models themselves: by CRISPR/Cas9 knocking out of the *GBA1* gene, we created a chronic model of the disease that mimics what happens *in vivo*, whereas the GCase inhibition by CBE or providing sphingolipids to cells can be defined as a way of modelling an "acute version" of the disease. Data from Lecourt and colleagues support this hypothesis since these authors did not notice any difference in osteogenesis when normal MSCs were treated or not with CBE, but a reduction in many markers of osteoblasts was recorded when they compared normal MSCs to GD MSCs [113,120].

**Figure D3** reports our findings on GD and osteoblasts: we suggest that GD osteoblasts are depositing less collagen and probably less calcium, resulting in impaired osteogenesis.

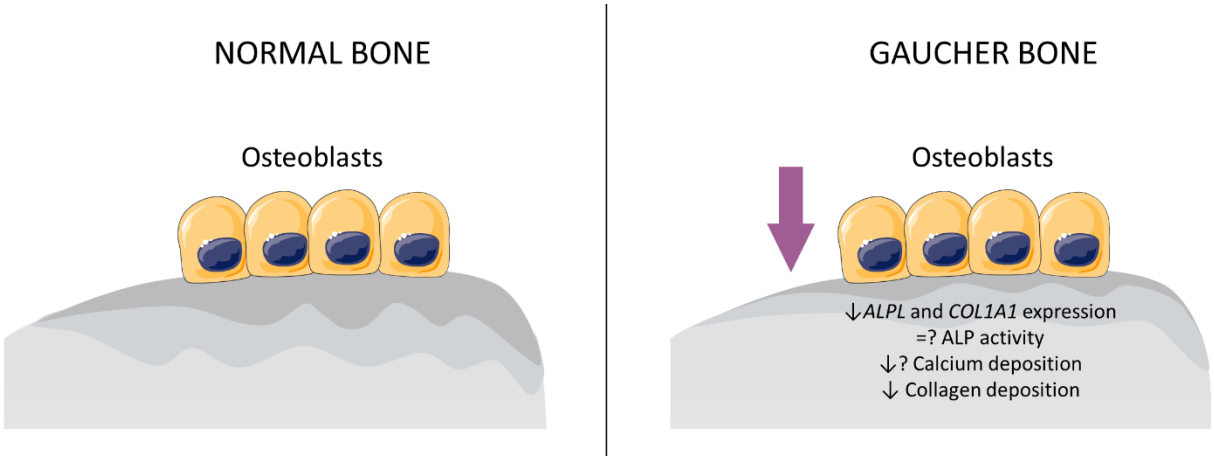


**Figure D3** | Overview of findings on osteogenesis in our model of GD.

## 5.3 THE POTENTIAL ROLE OF miR-488-3p IN IMPAIRING OSTEOGENESIS

The role of miRNAs in bone pathogenetic processes has been established: miRNAs regulate the development and function of MSCs, osteoclasts, and osteoblasts, playing a role in many pathological conditions in which bone is affected, including osteoporosis, osteonecrosis, rheumatoid arthritis, osteoarthritis, and osteosarcoma [130–132,162,163].

Intending to explore a possible role of miRNAs in GD bone disease, we performed the miRNA profiling of our osteoblast model, studying both expressed and secreted miRNAs. Even though we identified and validated several up- and down-regulated miRNAs, we focused on miR-488-3p, which was up-regulated in SaOS GBA KO cells in both expressed and exosomal miRNA pools.

To further validate this result, we tried to replicate the observations obtained using the SaOS GBA KO model in primary normal osteoblasts treated with the GCase inhibitor CBE. As expected, treatment with CBE resulted in a marked reduction of GCase expression and activity, as well as accumulation of GlcSph. Moreover, we confirmed the overexpression of miR-488-3p in this GD-miming condition compared with untreated cells. It is worth noting that the magnitude of the miR-488-3p increase was lower in comparison with the increase observed in SaOS GBA KO: once again, this discrepancy may be explained by the different type of model (acute with CBE versus chronic by *GBA1* KO) but may also depend on the magnitude of GCase activity reduction and/or GlcSph accumulation. Concerning the latter aspect, it could be extremely interesting to model GD on primary osteoblasts by using a recently developed GCase inhibitor, which was presented during the last IWGGD Symposium: this new compound displayed a stronger inhibitory capability and a higher selectivity for GCase than the commonly used CBE (Oral communication by Dr. Marta Artola, entitled "Selective nanomolar covalent GBA inhibitors for the generation of neuropathic Gaucher disease models" at the IWGGD symposium in Leiden (NL), 8-11 May 2022).

To analyse the possible contribution of miR-488-3p to the pathogenesis of bone disease, we transfected this miRNA into SaOS wt. We demonstrated that it downregulates the expression of *RUNX2*, *ALPL*, and *COL1A1*. The downregulation of *RUNX2* by miR-488-3p was previously demonstrated by luciferase assay [152]. It is possible to speculate that the reduction of mRNA expression of *ALPL* and *COL1A1* is a consequence of the downregulation of RUNX2, a transcription factor involved in the regulation of *ALPL* and *COL1A1* expression.

According to TargetScan prediction tool (https://www.targetscan.org/vert_80/; release 8.0), miR-488-3p may target several genes playing a role in bone or bone-related processes (**supplementary table 1** – page 71). To the best of our knowledge, no experimental data on miR-488-3p regulation of these genes have been reported; thus, exploring the effects of the potential targeting of these genes by miR-488-3p represents an interesting future perspective. Moreover, even though we focused on miR-488-3p, we would also like to study other candidates that have emerged from the miRNA profiling and that have been validated by qRT-PCR.

The role of miRNAs in bone involvement in GD has already been suggested by other authors: miR-26b-5p was found at a higher level in GD compared to healthy controls plasma samples [134], whereas the overexpression of miR-221-3p in GD zebrafish model was suggested to play a central role in reducing osteogenesis by affecting Wnt/β-catenin pathway [133]. However, no differences in these miRNAs were observed in our SaOS model of the disease.

**Figure D4** reports our findings on miR-488-3p and osteogenesis: we suggest that this miRNA can reduce the levels of osteogenesis by decreasing the expression of RUNX2, ALP, and type I collagen (*COL1A1*) encoding genes.

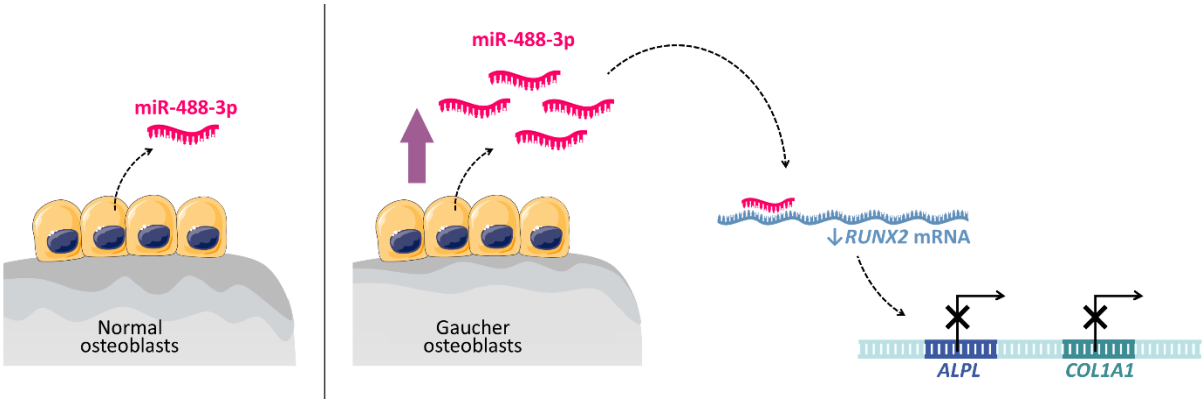


**Figure D4** | Overview of findings and potential way of action of miR-488-3p in osteoblasts.

## 5.4 IMPAIRED FEATURES AND BEHAVIOUR OF CHONDROCYTES IN THE C28I2 GD MODEL

As bone pain in GD is usually confined to one bone extremity or joint [41], we decided to model GD in a clonal cell line of immortalized normal chondrocytes named C28I2 [146], which has been extensively used to study chondrocyte function *in vitro* [148,149,164–169]. We selected a clone (C28I2 GBA KO A1) displaying no GCase protein, low residual GCase activity, and accumulating GlcSph.

In comparison with C28I2 wt, GBA KO A1 cells displayed lower levels of *COL2A1* and higher levels of *COL10A1* mRNA expression, suggesting a decreased production of type II collagen in favour of type X collagen. As previously mentioned, the expression of type X collagen is a marker of chondrocyte hypertrophy. The fate of these cells is unclear: apoptosis and de/transdifferentiation into bone marrow-associated skeletal stem and progenitor cells, osteoblasts, osteocytes, and adipocytes have been suggested [99–104]. As GD chondrocytes produce a lower amount of type II and higher amount of type X collagen than wt cells, it is possible to speculate an alteration of the cartilage matrix features: type II collagen is a fibril-forming collagen, whereas type X collagen is a network-forming collagens, as its short chains multimerize to form hexagonal lattices [170–172].

In addition, we found a massive release of IL-8 by GBA KO cells in comparison to wt. As this cytokine acts as a neutrophil chemoattractant [156], we assessed the ability of GD and wt chondrocytes to attract neutrophils isolated from a healthy donor, which may explain the pain experienced by some patients [41,154,155]. Interestingly, we did notice an increased neutrophil attraction by C28I2 GBA KO cells, but only in the presence of both the cells and the conditioned media, while no differences in neutrophil migration were observed when only the conditioned media containing the released IL-8 was used. This result suggests that IL-8 is not the only player in this process and it is likely that the presence of a receptor or changes in the plasma membrane of the chondrocyte cells are needed as well. To validate this observation, we plan to repeat the neutrophil migration assay by seeding C28I2 wt or GBA KO A1 and replacing the conditioned media with the fresh ones (not containing the IL-8 released by chondrocytes) before the loading of neutrophils in the transwell.

Neutrophil invasion and inflammation are the main aspects of the two major arthritic diseases, rheumatoid arthritis (RA) and osteoarthritis (OA), respectively. Even though their pathogenesis differs, in both cases inflammation eventually causes the production of factors such as matrix metalloproteinases (MMPs) which are responsible for the degradation not only of cartilage but also bone and tendons in joints [173–176]. Thus, it will not be surprising if also in GD chondrocytes or other infiltrating cells in joints may cause damage at the bone level.

To the best of our knowledge, only one group investigated cartilage tissue in GD, by exploiting zebrafish model [112]. Interestingly they noticed a decrease in *COL10A1* gene expression during the development, which suggests an impaired endochondral ossification process during skeletal development; however, no evident alterations of cartilage were observed in terms of mucopolysaccharides and type II collagen expression.

**Figure D5** reports our findings on GD and chondrocytes: we suggest that GD chondrocytes are different from the normal ones and probably committed to a hypertrophic fate. They seem to enhance inflammation by releasing high levels of IL-8 and attract neutrophils.

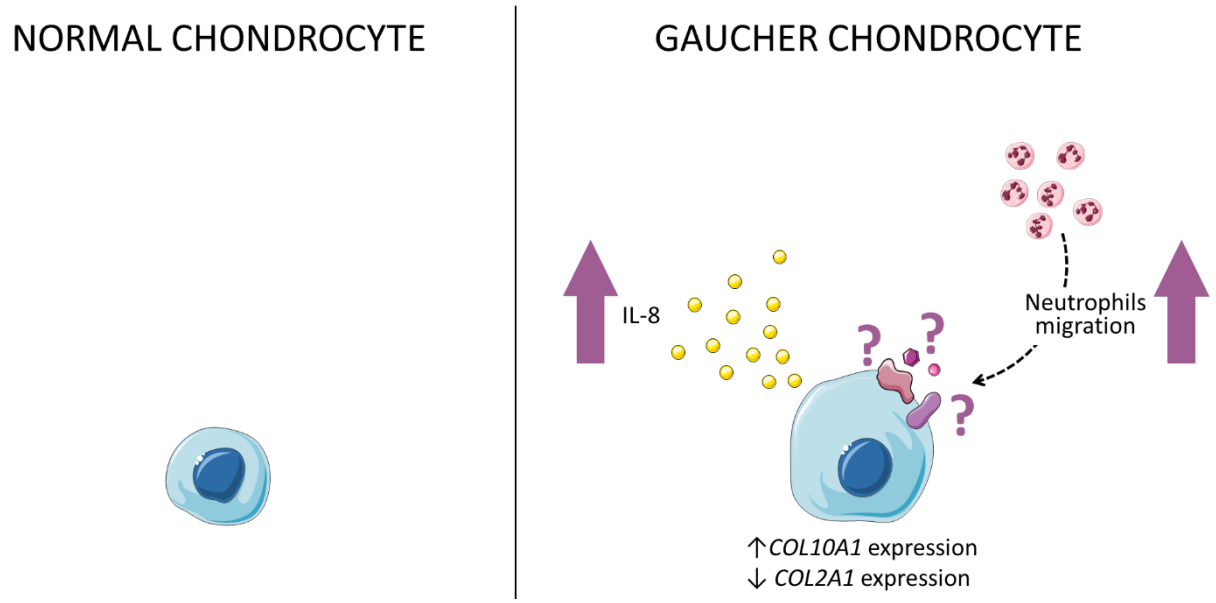


**Figure D5** | Overview of findings on chondrocytes in our model of GD.

## 5.5 IMPAIRED SIGNALLING FROM GD OSTEOBLASTS AND CHONDROCYTES MAY AFFECT OSTEOCLASTOGENESIS

To study the interactions between cells, we decided to investigate the effect of GD osteoblasts and chondrocytes on osteoclastogenesis. Although it would have been also interesting to study the effect of GD osteoclasts on osteoblasts and chondrocytes, our osteoclast model was not suitable to perform these experiments since while GD osteoblasts and chondrocytes represent homogeneous populations, GD osteoclasts are obtained by differentiating monocytes and therefore we obtained a heterogeneously differentiating population of macrophages, osteoclasts, and osteoclasts precursors.

We decided to investigate the role of osteoblasts in osteoclastogenesis as we found an increased *RANKL*/*OPG* expression ratio in SaOS GBA KO A7 in comparison with wt, which may suggest an increased release of free RANKL binding its receptor RANK on the surface of osteoclasts precursors inducing increased osteoclastogenesis and osteoclastic activity. Indeed, with the use of the conditioned medium from GBA KO cells on THP-1 wt, we noticed increased osteoclastogenesis in comparison to the use of the conditioned medium from SaOS wt. We did not find any difference in the release of IL-1β, TNF-α, IL-6, and IL-8 by SaOS GBA KO cells, thus we can exclude the role of these cytokines in enhancing osteoclastogenesis. To confirm that the increase in the release of RANKL by GD osteoblasts is the key player in the process, an inhibitor of this factor (i.e., OPG) should be used, or its synthesis should be decreased by silencing its gene, as we were not able to directly detect its presence in the supernatant of SaOS cells with the commercial kit we used.

Increased osteoclastogenesis and bone resorption have been observed in the wide majority of works in which conditioned media from GCase deficient osteocytes or MSCs are used to culture osteoclasts precursors [113,115,116,120,124–126], and three factors have been demonstrated to play a role in the process: RANKL, IL-1β, and TNF-α [115,116,124]. As the release of IL-1β and TNF-α is not increased in our osteoblast model, our data suggest that increased osteoclastogenesis in our setting might be mediated by RANKL as a pro-osteoclastogenic factor produced by osteoblasts and IL-1β and TNF-α as pro-osteoclastogenic factors produced by osteoclasts and/or osteoclasts precursors acting in an autocrine/paracrine fashion. However, many other factors than IL-1β, IL-6, TNF-α and IL-8 released by osteoblasts that have not been investigated in our SaOS model may mediate the process.

In a preliminary experiment, we evaluated the rate of osteoclastogenesis in the presence of conditioned media from C28I2 wt or GBA KO A1 supplemented with M-CSF, as increased levels of IL-8 were observed, and this factor has been reported as a positive regulator of osteoclastogenesis [177,178]. Even though we did not reach the statistical significance (p-value=0,056) probably because the experiment was repeated only twice, we noticed an increase in the percentage of osteoclasts when the conditioned medium from C28I2 GBA KO A1 was used. It is worth underlining that the percentage of osteoclasts obtained at the end of differentiation is lower in comparison with data from osteoclastogenesis induced by the conditioned media from SaOS, so it is possible to speculate that to clearly observe a difference in this process not only M-CSF but also RANKL should be provided to THP-1. In this way, the possible enhancing effect of IL-8 released from chondrocytes on osteoclastogenesis may emerge. If an increase in the percentage of osteoclasts in the presence of M-CSF and RANKL is confirmed, this will suggest that impairment in chondrocytes may also affect the osteoclastogenic process. To define IL-8 as the key player in the process, inhibition of this cytokine should be performed (i.e., using inhibitors of the IL-8 cognate receptors CXCR1 and CXCR2 or an IL-8 blocking antibody).

**Figure D6** reports our findings on osteoblasts and chondrocytes influence on osteoclastogenesis: we suggest that GD osteoblasts release high levels of free RANKL increasing osteoclastogenesis and that chondrocytes may do the same using IL-8 as the mediator in the process.

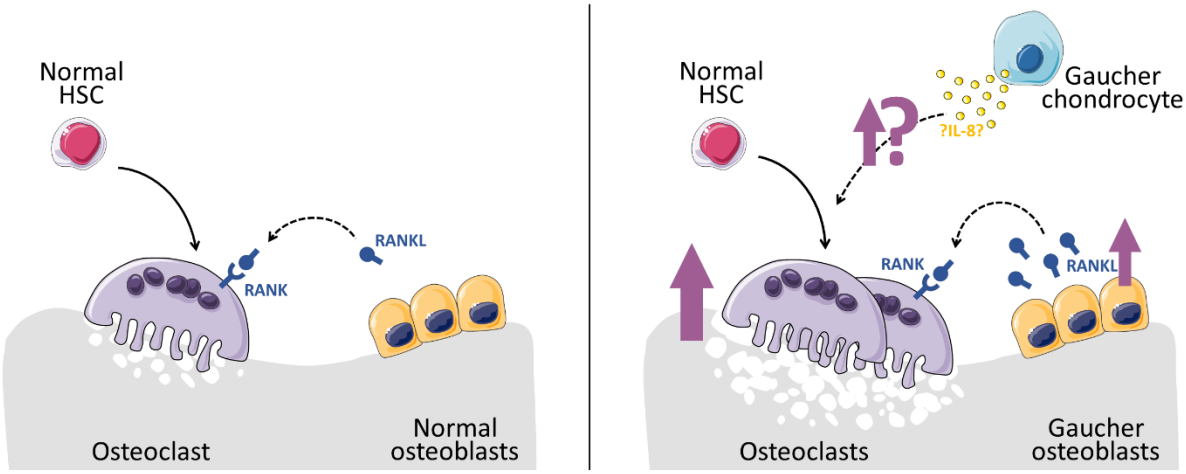


**Figure D6** | Overview of findings on GD osteoblasts and chondrocytes influence on osteoclastogenesis from normal monocytes.

# 6 CONCLUSIONS AND FUTURE PERSPECTIVES

The evidence on bone pathogenesis in GD is broad and sometimes contradictory; for this reason, in this work, we have tried to add a piece of knowledge to the overall picture. Our data suggest that both osteogenesis and osteoclastogenesis are affected by GCase deficiency. We demonstrated an impaired function of mature osteoblasts, suggesting that not only are fewer osteoblasts produced in GD patients as a consequence of impaired differentiation from MSCs, but they are also less active. By using naïve THP-1 cells, we supported the idea of a primary role of glycosphingolipid accumulation in impairing osteoclastogenesis, but also strengthened the role of pro-inflammatory factors in this process. We emphasized the importance of crosstalk between osteoblasts and osteoclasts, as we have shown that factors released by GD osteoblasts affect osteoclastogenesis. In addition, we added a new player in the process, as we detected alterations in GD chondrocytes that appear to induce neutrophil infiltration and may also influence osteoclastogenesis. Finally, we identified miR-488-3p as a potential player in bone disease.

Many of the experiments that may help explain or further clarify our data have already been mentioned throughout the discussion and will be performed in the near future. In particular, we would like to focus on the C28I2 chondrocyte model of GD to understand the potential role of these cells in neutrophil attraction and to deepen their role in osteoclastogenesis. In addition, we would like to investigate other aspects of chondrocyte function (such as matrix anabolism and catabolism) by providing specific stimuli and/or performing micromass culture, which has been shown to be an excellent method for culturing chondrocyte cell lines preserving their characteristic phenotype [179–181].

# ACKNOWLEDGMENTS

We would like to thank Prof. Hans Aerts and his collaborators Dr. Maria Ferraz and Qui Su of the Leiden Institute of Chemistry, Martina Fabris, Jessica Biasizzo, Antonella Paradiso, and Dania Ferino of the Institute of Clinical Pathology of the University Hospital of Udine, and Dr. Daniela Cesselli, Michela Bulfoni and Matteo Turetta of the Department of Medicine (DAME) of the University of Udine, who contributed to this work.

We would also like to thank Dr. Martin Jakab, Rosa Maria Borzì, and Prof. Gianluca Tell who kindly provided C28I2, SaOS2, MG-63, and Hobit cell lines used in this work.

# REFERENCES


[1] Brady RO, Kanfer JN, Shapiro D. Metabolism of glucocerebrosides II. Evidence of an enzymatic deficiency in Gaucher's disease. Biochem Biophys Res Commun 1965;18:221–5. https://doi.org/https://doi.org/10.1016/0006-291X(65)90743-6.

[2] Nilsson O, Svennerholm L. Accumulation of Glucosylceramide and Glucosylsphingosine (Psychosine) in Cerebrum and Cerebellum in Infantile and Juvenile Gaucher Disease. J Neurochem 1982;39:709–18. https://doi.org/10.1111/j.1471-4159.1982.tb07950.x.

[3] Andrade-Campos MM, de Frutos LL, Cebolla JJ, Serrano-Gonzalo I, Medrano-Engay B, Roca-Espiau M, et al. Identification of risk features for complication in Gaucher's disease patients: a machine learning analysis of the Spanish registry of Gaucher disease. Orphanet J Rare Dis 2020;15. https://doi.org/10.1186/S13023-020-01520-7.

[4] Roh J, Subramanian S, Weinreb NJ, Kartha R v. Gaucher disease - more than just a rare lipid storage disease. J Mol Med (Berl) 2022;100:499–518. https://doi.org/10.1007/S00109-021-02174-Z.

[5] Stirnemann J, Belmatoug N, Camou F, Serratrice C, Froissart R, Caillaud C, et al. A review of Gaucher Disease pathophysiology, clinical presentation and treatments. Int J Mol Sci 2017;18:441. https://doi.org/10.3390/ijms18020441.

[6] Dionisi-Vici C, Rizzo C, Burlina AB, Caruso U, Sabetta G, Uziel G, et al. Inborn errors of metabolism in the Italian pediatric population: A national retrospective survey. Journal of Pediatrics 2002;140:321–9. https://doi.org/10.1067/mpd.2002.122394.

[7] Burlina AB, Polo G, Rubert L, Gueraldi D, Cazzorla C, Duro G, et al. Implementation of Second-Tier Tests in Newborn Screening for Lysosomal Disorders in North Eastern Italy. Int J Neonatal Screen 2019;5. https://doi.org/10.3390/IJNS5020024.

[8] Sorge J, West C, Westwood B, Beutler E. Molecular cloning and nucleotide sequence of human glucocerebrosidase cDNA. Proc Natl Acad Sci U S A 1985;82:7289–93. https://doi.org/10.1073/PNAS.82.21.7289.

[9] Horowitz M, Wilder S, Horowitz Z, Reiner O, Gelbart T, Beutler E. The human glucocerebrosidase gene and pseudogene: structure and evolution. Genomics 1989;4:87–96. https://doi.org/10.1016/0888-7543(89)90319-4.

[10] Latham TE, Theophilus BDM, Grabowski GA, Smith FI. Heterogeneity of mutations in the acid beta-glucosidase gene of Gaucher disease patients. DNA Cell Biol 1991;10:15–21. https://doi.org/10.1089/DNA.1991.10.15.

[11] Hong CM, Ohashi T, yu XJ, Weiler S, Barranger JA. Sequence of two alleles responsible for Gaucher disease. DNA Cell Biol 1990;9:233–41. https://doi.org/10.1089/DNA.1990.9.233.

[12] Koprivica V, Stone DL, Park JK, Callahan M, Frisch A, Cohen IJ, et al. Analysis and classification of 304 mutant alleles in patients with type 1 and type 3 Gaucher disease. Am J Hum Genet 2000;66:1777–86. https://doi.org/10.1086/302925.

[13] Leonova T, Grabowski GA. Fate and sorting of acid beta-glucosidase in transgenic mammalian cells. Mol Genet Metab 2000;70:281–94. https://doi.org/10.1006/MGME.2000.3035.

[14] Berg-Fussman A, Grace ME, Ioannou Y, Grabowski GA. Human acid beta-glucosidase. N-glycosylation site occupancy and the effect of glycosylation on enzymatic activity. Journal of Biological Chemistry 1993;268:14861–6. https://doi.org/10.1016/S0021-9258(18)82412-7.

[15] Erickson AH, Ginns EI, Barranger JA. Biosynthesis of the lysosomal enzyme glucocerebrosidase. Journal of Biological Chemistry 1985;260:14319–24. https://doi.org/10.1016/S0021-9258(17)38720-3.

[16] Reczek D, Schwake M, Schröder J, Hughes H, Blanz J, Jin X, et al. LIMP-2 is a receptor for lysosomal mannose-6-phosphate-independent targeting of beta-glucocerebrosidase. Cell 2007;131:770–83. https://doi.org/10.1016/J.CELL.2007.10.018.

[17] Smith L, Mullin S, Schapira AHV. Insights into the structural biology of Gaucher disease. Exp Neurol 2017;298:180–90. https://doi.org/10.1016/J.EXPNEUROL.2017.09.010.

[18] Lieberman RL, Wustman BA, Huertas P, Powe AC, Pine CW, Khanna R, et al. Structure of acid β-glucosidase with pharmacological chaperone provides insight into Gaucher disease. Nature Chemical Biology 2007 3:2 2006;3:101–7. https://doi.org/10.1038/nchembio850.

[19] Grabowski GA, Gaft S, Horowitz M, Kolodny EH. Acid beta-glucosidase: enzymology and molecular biology of Gaucher disease. Crit Rev Biochem Mol Biol 1990;25:385–414. https://doi.org/10.3109/10409239009090616.

[20] Lieberman RL, Wustman BA, Huertas P, Powe AC, Pine CW, Khanna R, et al. Structure of acid beta-glucosidase with pharmacological chaperone provides insight into Gaucher disease. Nat Chem Biol 2007;3:101–7. https://doi.org/10.1038/NCHEMBIO850.

[21] HGMD Professional 2022.3 n.d. https://www.hgmd.cf.ac.uk/ (accessed December 13, 2022).

[22] Hruska KS, LaMarca ME, Scott CR, Sidransky E. Gaucher disease: mutation and polymorphism spectrum in the glucocerebrosidase gene (GBA). Hum Mutat 2008;29:567–83. https://doi.org/10.1002/HUMU.20676.

[23] Dardis A, Michelakakis H, Rozenfeld P, Fumic K, Wagner J, Pavan E, et al. Patient centered guidelines for the laboratory diagnosis of Gaucher disease type 1. Orphanet J Rare Dis 2022;17:442. https://doi.org/10.1186/S13023-022-02573-6.

[24] Vaccaro AM, Motta M, Tatti M, Scarpa S, Masuelli L, Bhat M, et al. Saposin C mutations in Gaucher disease patients resulting in lysosomal lipid accumulation, saposin C deficiency, but normal prosaposin processing and sorting. Hum Mol Genet 2010;19:2987–97. https://doi.org/10.1093/HMG/DDQ204.

[25] Tylki-Szymańska A, Czartoryska B, Vanier MT, Poorthuis BJMH, Groener JAE, Ługowska A, et al. Non-neuronopathic Gaucher disease due to saposin C deficiency. Clin Genet 2007;72:538–42. https://doi.org/10.1111/J.1399-0004.2007.00899.X.

[26] Kang L, Zhan X, Ye J, Han L, Qiu W, Gu X, et al. A rare form of Gaucher disease resulting from saposin C deficiency. Blood Cells Mol Dis 2018;68:60–5. https://doi.org/10.1016/J.BCMD.2017.04.001.

[27] Motta M, Camerini S, Tatti M, Casella M, Torreri P, Crescenzi M, et al. Gaucher disease due to saposin C deficiency is an inherited lysosomal disease caused by rapidly degraded mutant proteins. Hum Mol Genet 2014;23:5814–26. https://doi.org/10.1093/HMG/DDU299.

[28] Berkovic SF, Dibbens LM, Oshlack A, Silver JD, Katerelos M, Vears DF, et al. Array-based gene discovery with three unrelated subjects shows SCARB2/LIMP-2 deficiency causes myoclonus epilepsy and glomerulosclerosis. Am J Hum Genet 2008;82:673–84. https://doi.org/10.1016/J.AJHG.2007.12.019.

[29] Amrom D, Andermann F, Andermann E. Action Myoclonus – Renal Failure Syndrome. The Causes of Epilepsy: Common and Uncommon Causes in Adults and Children 2015:169–71. https://doi.org/10.1017/CBO9780511921001.024.

[30] Beutler E, Grabowski GA. Gaucher disease. In: Scriver CR, Beaudet AL, Valle D, Sly WS, editors. The Metabolic and Molecular Basis of Inherited Disease, New York, NY, USA: McGraw-Hill; 2001, p. 3635–68.

[31] Ferraz MJ, Kallemeijn WW, Mirzaian M, Herrera Moro D, Marques A, Wisse P, et al. Gaucher disease and Fabry disease: new markers and insights in pathophysiology for two distinct glycosphingolipidoses. Biochim Biophys Acta 2014;1841:811–25. https://doi.org/10.1016/J.BBALIP.2013.11.004.

[32] Boven LA, van Meurs M, Boot RG, Mehta A, Boon L, Aerts JM, et al. Gaucher cells demonstrate a distinct macrophage phenotype and resemble alternatively activated macrophages. Am J Clin Pathol 2004;122:359–69. https://doi.org/10.1309/BG5V-A8JR-DQH1-M7HN.

[33] Boot RG, Verhoek M, de Fost M, Hollak CEM, Maas M, Bleijlevens B, et al. Marked elevation of the chemokine CCL18/PARC in Gaucher disease: a novel surrogate marker for assessing therapeutic intervention. Blood 2004;103:33–9. https://doi.org/10.1182/BLOOD-2003-05-1612.

[34] Hollak CEM, van Weely S, van Oers MHJ, Aerts JMFG. Marked elevation of plasma chitotriosidase activity. A novel hallmark of Gaucher disease. J Clin Invest 1994;93:1288–92. https://doi.org/10.1172/JCI117084.

[35] Ferraz MJ, Marques ARA, Appelman MD, Verhoek M, Strijland A, Mirzaian M, et al. Lysosomal glycosphingolipid catabolism by acid ceramidase: Formation of glycosphingoid bases during deficiency of glycosidases. FEBS Lett 2016;590:716–25. https://doi.org/10.1002/1873-3468.12104.

[36] Rolfs A, Giese AK, Grittner U, Mascher D, Elstein D, Zimran A, et al. Glucosylsphingosine is a highly sensitive and specific biomarker for primary diagnostic and follow-up monitoring in Gaucher disease in a non-Jewish, Caucasian cohort of Gaucher disease patients. PLoS One 2013;8. https://doi.org/10.1371/JOURNAL.PONE.0079732.

[37] Aerts JMFG, Kuo CL, Lelieveld LT, Boer DEC, van der Lienden MJC, Overkleeft HS, et al. Glycosphingolipids and lysosomal storage disorders as illustrated by gaucher disease. Curr Opin Chem Biol 2019;53:204–15. https://doi.org/10.1016/J.CBPA.2019.10.006.

[38] Ghauharali-van der Vlugt K, Langeveld M, Poppema A, Kuiper S, Hollak CEM, Aerts JM, et al. Prominent increase in plasma ganglioside GM3 is associated with clinical manifestations of type I Gaucher disease. Clinica Chimica Acta 2008;389:109–13. https://doi.org/10.1016/J.CCA.2007.12.001.

[39] Marques ARA, Mirzaian M, Akiyama H, Wisse P, Ferraz MJ, Gaspar P, et al. Glucosylated cholesterol in mammalian cells and tissues: formation and degradation by multiple cellular β-glucosidases. J Lipid Res 2016;57:451–63. https://doi.org/10.1194/JLR.M064923.

[40] Linari S, Castaman G. Clinical manifestations and management of Gaucher disease. Clinical Cases in Mineral and Bone Metabolism 2015;12:157. https://doi.org/10.11138/CCMBM/2015.12.2.157.

[41] Pastores GM, Hughes DA. Gaucher Disease. GeneReviews® [Internet] 2018. https://www.ncbi.nlm.nih.gov/books/NBK1269/ (accessed November 16, 2022).

[42] Biegstraaten M, Mengel E, Maródi L, Petakov M, Niederau C, Giraldo P, et al. Peripheral neuropathy in adult type 1 Gaucher disease: a 2-year prospective observational study. Brain 2010;133:2909–19. https://doi.org/10.1093/BRAIN/AWQ198.

[43] Elstein D, Alcalay R, Zimran A. The emergence of Parkinson disease among patients with Gaucher disease. Best Pract Res Clin Endocrinol Metab 2015;29:249–59. https://doi.org/10.1016/J.BEEM.2014.08.007.

[44] Nascimbeni F, Dionisi Vici C, Vespasiani Gentilucci U, Angelico F, Nobili V, Petta S, et al. AISF update on the diagnosis and management of adult-onset lysosomal storage diseases with hepatic involvement. Dig Liver Dis 2020;52:359–67. https://doi.org/10.1016/J.DLD.2019.12.005.

[45] Dahl N, Wadelius C, Annerén G, Gustavson K-H. Mutation analysis for prenatal diagnosis and heterozygote detection of Gaucher disease type III (norrbottnian type). Prenat Diagn 1992;12:603–8. https://doi.org/10.1002/pd.1970120706.

[46] Dahl N, Hillborg PO, Olofsson A. Gaucher disease (Norrbottnian type III): probable founders identified by genealogical and molecular studies. Human Genetics 1993 92:5 1993;92:513–5. https://doi.org/10.1007/BF00216461.

[47] Dreborg S, Erikson A, Hagberg B. Gaucher disease--Norrbottnian type. I. General clinical description. Eur J Pediatr 1980;133:107–18. https://doi.org/10.1007/BF00441578.

[48] Machaczka M, Björkvall CK, Wieremiejczyk J, Arce MP, Myhr-Eriksson K, Klimkowska M, et al. Impact of imiglucerase supply shortage on clinical and laboratory parameters in Norrbottnian patients with Gaucher disease type 3. Arch Immunol Ther Exp (Warsz) 2015;63:65–71. https://doi.org/10.1007/S00005-014-0308-8.

[49] Revel-Vilk S, Szer J, Mehta A, Zimran A. How we manage Gaucher Disease in the era of choices. Br J Haematol 2018;182:467–80. https://doi.org/10.1111/BJH.15402.

[50] Kong W, Lu C, Ding Y, Meng Y. Update of treatment for Gaucher disease. Eur J Pharmacol 2022;926. https://doi.org/10.1016/J.EJPHAR.2022.175023.

[51] ClinicalTrials.gov n.d. https://clinicaltrials.gov/ct2/home (accessed January 16, 2023).

[52] Bendikov-Bar I, Horowitz M. Gaucher disease paradigm: from ERAD to comorbidity. Hum Mutat 2012;33:1398–407. https://doi.org/10.1002/HUMU.22124.

[53] Aries C, Lohmöller B, Tiede S, Täuber K, Hartmann G, Rudolph C, et al. Promising Effect of High Dose Ambroxol Treatment on Neurocognition and Motor Development in a Patient With Neuropathic Gaucher Disease 2. Front Neurol 2022;13. https://doi.org/10.3389/FNEUR.2022.907317.

[54] Ciana G, Dardis A, Pavan E, da Riol RM, Biasizzo J, Ferino D, et al. In vitro and in vivo effects of Ambroxol chaperone therapy in two Italian patients affected by neuronopathic Gaucher disease and epilepsy. Mol Genet Metab Rep 2020;25. https://doi.org/10.1016/j.ymgmr.2020.100678.

[55] Kim Y-M, Yum M-S, Heo SH, Kim T, Jin HK, Bae J-S, et al. Pharmacologic properties of high-dose ambroxol in four patients with Gaucher disease and myoclonic epilepsy. J Med Genet 2020;57:124–31. https://doi.org/10.1136/jmedgenet-2019-106132.

[56] Narita A, Shirai K, Itamura S, Matsuda A, Ishihara A, Matsushita K. Ambroxol chaperone therapy for neuronopathic Gaucher disease : A pilot study 2016:200–15. https://doi.org/10.1002/acn3.292.

[57] Pawlinski L, Malecki MT, Kiec-Wilk B. The additive effect on the antiepileptic treatment of ambroxol in type 3 Gaucher patient. The early observation. Blood Cells Mol Dis 2018;68:192–3. https://doi.org/10.1016/j.bcmd.2016.12.001.

[58] Ramadža DP, Zekušić M, Žigman T, Škaričić A, Bogdanić A, Mustać G, et al. Early initiation of ambroxol treatment diminishes neurological manifestations of type 3 Gaucher disease: A long-term outcome of two siblings. Eur J Paediatr Neurol 2021;32:66–72. https://doi.org/10.1016/J.EJPN.2021.03.013.

[59] Pantoom S, Hules L, Schöll C, Petrosyan A, Monticelli M, Pospech J, et al. Mechanistic Insight into the Mode of Action of Acid β-Glucosidase Enhancer Ambroxol. Int J Mol Sci 2022;23. https://doi.org/10.3390/IJMS23073536.

[60] Feng X. Chemical and Biochemical Basis of Cell-Bone Matrix Interaction in Health and Disease. Curr Chem Biol 2009;3:189. https://doi.org/10.2174/187231309788166398.

[61] Bassi A, Gough J, Zakikhani M, Downes S. Bone tissue regeneration. In: Bosworth LA, Downes S, editors. Electrospinning for Tissue Regeneration, Sawstone: Woodhead Publishing; 2011, p. 93–110. https://doi.org/10.1533/9780857092915.2.93.

[62] Florencio-Silva R, Sasso GRDS, Sasso-Cerri E, Simões MJ, Cerri PS. Biology of Bone Tissue: Structure, Function, and Factors That Influence Bone Cells. Biomed Res Int 2015;2015. https://doi.org/10.1155/2015/421746.

[63] Hu L, Yin C, Zhao F, Ali A, Ma J, Qian A. Mesenchymal Stem Cells: Cell Fate Decision to Osteoblast or Adipocyte and Application in Osteoporosis Treatment. Int J Mol Sci 2018;19:360. https://doi.org/10.3390/IJMS19020360.

[64] Long F. Building strong bones: molecular regulation of the osteoblast lineage. Nature Reviews Molecular Cell Biology 2011 13:1 2011;13:27–38. https://doi.org/10.1038/nrm3254.

[65] Plotkin LI, Bruzzaniti A. Molecular signaling in bone cells: regulation of cell differentiation and survival. Adv Protein Chem Struct Biol 2019;116:237. https://doi.org/10.1016/BS.APCSB.2019.01.002.

[66] Song L. Calcium and Bone Metabolism Indices. Adv Clin Chem 2017;82:1–46. https://doi.org/10.1016/BS.ACC.2017.06.005.

[67] Amarasekara DS, Kim S, Rho J. Regulation of Osteoblast Differentiation by Cytokine Networks. International Journal of Molecular Sciences 2021, Vol 22, Page 2851 2021;22:2851. https://doi.org/10.3390/IJMS22062851.

[68] Berardi S, Corrado A, Maruotti N, Cici D, Cantatore FP. Osteoblast role in the pathogenesis of rheumatoid arthritis. Mol Biol Rep 2021;48:2843. https://doi.org/10.1007/S11033-021-06288-Y.

[69] Maruotti N, Corrado A, Neve A, Cantatore FP. Bisphosphonates: effects on osteoblast. Eur J Clin Pharmacol 2012;68:1013–8. https://doi.org/10.1007/S00228-012-1216-7.

[70] Kim JM, Lin C, Stavre Z, Greenblatt MB, Shim JH. Osteoblast-Osteoclast Communication and Bone Homeostasis. Cells 2020, Vol 9, Page 2073 2020;9:2073. https://doi.org/10.3390/CELLS9092073.

[71] Han Y, You X, Xing W, Zhang Z, Zou W. Paracrine and endocrine actions of bone—the functions of secretory proteins from osteoblasts, osteocytes, and osteoclasts. Bone Research 2018 6:1 2018;6:1–11. https://doi.org/10.1038/s41413-018-0019-6.

[72] Choi JUA, Kijas AW, Lauko J, Rowan AE. The Mechanosensory Role of Osteocytes and Implications for Bone Health and Disease States. Front Cell Dev Biol 2021;9. https://doi.org/10.3389/FCELL.2021.770143.

[73] Robling AG, Bonewald LF. The Osteocyte: New Insights. Annu Rev Physiol 2020;82:485–506. https://doi.org/10.1146/ANNUREV-PHYSIOL-021119-034332.

[74] Qin L, Liu W, Cao H, Xiao G. Molecular mechanosensors in osteocytes. Bone Research 2020 8:1 2020;8:1–24. https://doi.org/10.1038/s41413-020-0099-y.

[75] Wang JS, Wein MN. Pathways Controlling Formation and Maintenance of the Osteocyte Dendrite Network. Curr Osteoporos Rep 2022. https://doi.org/10.1007/S11914-022-00753-8.

[76] Dallas SL, Prideaux M, Bonewald LF. The Osteocyte: An Endocrine Cell … and More. Endocr Rev 2013;34:658–90. https://doi.org/10.1210/ER.2012-1026.

[77] Karsenty G. Update on the Biology of Osteocalcin. Endocrine Practice 2017;23:1270–4. https://doi.org/10.4158/EP171966.RA.

[78] Elson A, Anuj A, Barnea-Zohar M, Reuven N. The origins and formation of bone-resorbing osteoclasts. Bone 2022;164. https://doi.org/10.1016/J.BONE.2022.116538.

[79] Qin A, Cheng TS, Pavlos NJ, Lin Z, Dai KR, Zheng MH. V-ATPases in osteoclasts: structure, function and potential inhibitors of bone resorption. Int J Biochem Cell Biol 2012;44:1422–35. https://doi.org/10.1016/J.BIOCEL.2012.05.014.

[80] Kartsogiannis V, Ng KW. Cell lines and primary cell cultures in the study of bone cell biology. Mol Cell Endocrinol 2004;228:79–102. https://doi.org/10.1016/J.MCE.2003.06.002.

[81] Schett G. Biology, Physiology, and Morphology of Bone. In: Firestein GS, Budd RC, Gabriel SE, McInnes IB, O'Dell JR, editors. Kelly's textbook of rheumatology. 9th edition, Philadelphia: Elsevier; 2013, p. 61–6.

[82] Feng X, Teitelbaum SL. Osteoclasts: New Insights. Bone Res 2013;1:11–26. https://doi.org/10.4248/BR201301003.

[83] Zhou P, Zheng T, Zhao B. Cytokine-mediated immunomodulation of osteoclastogenesis. Bone 2022;164. https://doi.org/10.1016/J.BONE.2022.116540.

[84] Kitaura H, Marahleh A, Ohori F, Noguchi T, Shen WR, Qi J, et al. Osteocyte-Related Cytokines Regulate Osteoclast Formation and Bone Resorption. Int J Mol Sci 2020;21. https://doi.org/10.3390/IJMS21145169.

[85] Chen X, Wang Z, Duan N, Zhu G, Schwarz EM, Xie C. Osteoblast-Osteoclast Interactions. Connect Tissue Res 2018;59:99. https://doi.org/10.1080/03008207.2017.1290085.

[86] Owen R, Reilly GC. In vitro Models of Bone Remodelling and Associated Disorders. Front Bioeng Biotechnol 2018;6:134. https://doi.org/10.3389/FBIOE.2018.00134.

[87] Rowe P, Koller A, Sharma S. Physiology, Bone Remodeling. StatPearls 2022.

[88] Bolamperti S, Villa I, Rubinacci A. Bone remodeling: an operational process ensuring survival and bone mechanical competence. Bone Research 2022 10:1 2022;10:1–19. https://doi.org/10.1038/s41413-022-00219-8.

[89] Jann J, Gascon S, Roux S, Faucheux N. Influence of the TGF-β Superfamily on Osteoclasts/Osteoblasts Balance in Physiological and Pathological Bone Conditions. Int J Mol Sci 2020;21:1–58. https://doi.org/10.3390/IJMS21207597.

[90] Yang N, Liu Y. The Role of the Immune Microenvironment in Bone Regeneration. Int J Med Sci 2021;18:3697–707. https://doi.org/10.7150/IJMS.61080.

[91] Krishnan Y, Grodzinsky AJ. Cartilage diseases. Matrix Biology 2018;71–72:51–69. https://doi.org/10.1016/J.MATBIO.2018.05.005.

[92] Lories RJ, Luyten FP. Overview of Joint and Cartilage Biology. In: Thakker R v., Whyte MP, Eisman JA, Igarashi T, editors. Genetics of Bone Biology and Skeletal Disease. 2nd edition, Cambridge, UK: Academic Press; 2018, p. 209–25. https://doi.org/10.1016/B978-0-12-804182-6.00013-7.

[93] Liu Y, Shah KM, Luo J. Strategies for Articular Cartilage Repair and Regeneration. Front Bioeng Biotechnol 2021;9. https://doi.org/10.3389/FBIOE.2021.770655.

[94] Martel-Pelletier J, Barr AJ, Cicuttini FM, Conaghan PG, Cooper C, Goldring MB, et al. Osteoarthritis. Nature Reviews Disease Primers 2016 2:1 2016;2:1–18. https://doi.org/10.1038/nrdp.2016.72.

[95] Didomenico CD, Lintz M, Bonassar LJ. Molecular transport in articular cartilage — what have we learned from the past 50 years? Nature Reviews Rheumatology 2018 14:7 2018;14:393–403. https://doi.org/10.1038/s41584-018-0033-5.

[96] Goldring MB. Chondrogenesis, chondrocyte differentiation, and articular cartilage metabolism in health and osteoarthritis. Ther Adv Musculoskelet Dis 2012;4:269–85. https://doi.org/10.1177/1759720X12448454/ASSET/IMAGES/LARGE/10.1177_1759720X12448454-FIG2.JPEG.

[97] Goldring MB, Culley KL, Wondimu E, Otero M. Cartilage and Chondrocytes. In: Firestein GS, Budd RC, Gabriel SE, McInnes IB, O'Dell JR, editors. Kelly's textbook of rheumatology. 9th edition, Philadelphia: Philadelphia; 2013, p. 34–59.

[98] Gadjanski I, Spiller K, Vunjak-Novakovic G. Time-dependent processes in stem cell-based tissue engineering of articular cartilage. Stem Cell Rev Rep 2012;8:863–81. https://doi.org/10.1007/S12015-011-9328-5.

[99] Goldring SR, Goldring MB. Biology of the normal Joint. In: Firestein GS, Budd RC, Gabriel SE, McInnes IB, O'Dell JR, editors. Kelly's textbook of rheumatology. 9th edition, Philadelphia: Elsevier; 2013, p. 1–19.

[100] Long JT, Leinroth A, Liao Y, Ren Y, Mirando AJ, Nguyen T, et al. Hypertrophic chondrocytes serve as a reservoir for marrow-associated skeletal stem and progenitor cells, osteoblasts, and adipocytes during skeletal development. Elife 2022;11:76932. https://doi.org/10.7554/ELIFE.76932.

[101] Zhou X, von der Mark K, Henry S, Norton W, Adams H, de Crombrugghe B. Chondrocytes transdifferentiate into osteoblasts in endochondral bone during development, postnatal growth and fracture healing in mice. PLoS Genet 2014;10. https://doi.org/10.1371/JOURNAL.PGEN.1004820.

[102] Yang L, Tsang KY, Tang HC, Chan D, Cheah KSE. Hypertrophic chondrocytes can become osteoblasts and osteocytes in endochondral bone formation. Proc Natl Acad Sci U S A 2014;111:12097–102. https://doi.org/10.1073/PNAS.1302703111/-/DCSUPPLEMENTAL/PNAS.201302703SI.PDF.

[103] Yang G, Zhu L, Hou N, Lan Y, Wu XM, Zhou B, et al. Osteogenic fate of hypertrophic chondrocytes. Cell Res 2014;24:1266–9. https://doi.org/10.1038/CR.2014.111.

[104] Park J, Gebhardt M, Golovchenko S, Perez-Branguli F, Hattori T, Hartmann C, et al. Dual pathways to endochondral osteoblasts: A novel chondrocytederived osteoprogenitor cell identified in hypertrophic cartilage. Biol Open 2015;4:608–21. https://doi.org/10.1242/BIO.201411031/-/DC1.

[105] Marcucci G, Zimran A, Bembi B, Kanis J, Reginster JY, Rizzoli R, et al. Gaucher disease and bone manifestations. Calcif Tissue Int 2014;95:477–94. https://doi.org/10.1007/S00223-014-9923-Y.

[106] Hughes D, Mikosch P, Belmatoug N, Carubbi F, Cox TM, Goker-Alpan O, et al. Gaucher Disease in Bone: From Pathophysiology to Practice. J Bone Miner Res 2019;34:996–1013. https://doi.org/10.1002/JBMR.3734.

[107] Mikosch P, Hughes D. An overview on bone manifestations in Gaucher disease. Wien Med Wochenschr 2010;160:609–24. https://doi.org/10.1007/S10354-010-0841-Y.

[108] Belmatoug N, di Rocco M, Fraga C, Giraldo P, Hughes D, Lukina E, et al. Management and monitoring recommendations for the use of eliglustat in adults with type 1 Gaucher disease in Europe. Eur J Intern Med 2017;37:25–32. https://doi.org/10.1016/J.EJIM.2016.07.011.

[109] Pastores GM, Elstein D, Hrebícek M, Zimran A. Effect of miglustat on bone disease in adults with type 1 Gaucher disease: a pooled analysis of three multinational, open-label studies. Clin Ther 2007;29:1645–54. https://doi.org/10.1016/J.CLINTHERA.2007.08.006.

[110] Rozenfeld PA, Crivaro AN, Ormazabal M, Mucci JM, Bondar C, Delpino M v. Unraveling the mystery of Gaucher bone density pathophysiology. Mol Genet Metab 2020:0–1. https://doi.org/10.1016/j.ymgme.2020.07.011.

[111] Mistry PK, Liua J, Yanga M, Nottolic T, McGratha J, Jaine D, et al. Glucocerebrosidase gene-deficient mouse recapitulates Gaucher disease displaying cellular and molecular dysregulation beyond the macrophage. Proc Natl Acad Sci U S A 2010;107:19473–8. https://doi.org/10.1073/PNAS.1003308107.

[112] Zancan I, Bellesso S, Costa R, Salvalaio M, Stroppiano M, Hammond C, et al. Glucocerebrosidase deficiency in zebrafish affects primary bone ossification through increased oxidative stress and reduced Wnt/β-catenin signaling. Hum Mol Genet 2015;24:1280–94. https://doi.org/10.1093/HMG/DDU538.

[113] Lecourt S, Mouly E, Freida D, Cras A, Ceccaldi R, Heraoui D, et al. A prospective study of bone marrow hematopoietic and mesenchymal stem cells in type 1 Gaucher disease patients. PLoS One 2013;8. https://doi.org/10.1371/JOURNAL.PONE.0069293.

[114] Reed MC, Schiffer C, Heales S, Mehta AB, Hughes DA. Impact of sphingolipids on osteoblast and osteoclast activity in Gaucher disease. Mol Genet Metab 2018;124:278–86. https://doi.org/10.1016/J.YMGME.2018.06.007.

[115] Mucci JM, Suqueli García F, de Francesco PN, Ceci R, di Genaro S, Fossati CA, et al. Uncoupling of osteoblast-osteoclast regulation in a chemical murine model of gaucher disease. Gene 2013;532:186–91. https://doi.org/10.1016/j.gene.2013.09.072.

[116] Crivaro A, Bondar C, Mucci JM, Ormazabal M, Feldman RA, Delpino M v, et al. Gaucher disease-associated alterations in mesenchymal stem cells reduce osteogenesis and favour adipogenesis processes with concomitant increased osteoclastogenesis. Mol Genet Metab 2020;130:274–82. https://doi.org/10.1016/j.ymgme.2020.06.003.

[117] Panicker LM, Srikanth MP, Castro-Gomes T, Miller D, Andrews NW, Feldman RA. Gaucher disease iPSC-derived osteoblasts have developmental and lysosomal defects that impair bone matrix deposition. Hum Mol Genet 2018;27:811–22. https://doi.org/10.1093/hmg/ddx442.

[118] Jang HJ, Lim S, Kim JM, Yoon S, Lee CY, Hwang HJ, et al. Glucosylceramide synthase regulates adipo-osteogenic differentiation through synergistic activation of PPARγ with GlcCer. FASEB J 2020;34:1270–87. https://doi.org/10.1096/FJ.201901437R.

[119] Ciana G, Martini C, Leopaldi A, Tamaro G, Katouzian F, Ronfani L, et al. Bone marker alterations in patients with type 1 Gaucher disease. Calcif Tissue Int 2003;72:185–9. https://doi.org/10.1007/S00223-001-2072-0/METRICS.

[120] Lecourt S, Vanneaux V, Cras A, Freida D, Heraoui D, Herbi L, et al. Bone marrow microenvironment in an in vitro model of gaucher disease: Consequences of glucocerebrosidase deficiency. Stem Cells Dev 2012;21:239–48. https://doi.org/10.1089/scd.2011.0365.

[121] Serra-Vinardell J, Roca-Ayats N, De-Ugarte L, Vilageliu L, Balcells S, Grinberg D. Bone development and remodeling in metabolic disorders. J Inherit Metab Dis 2020;43:133–44. https://doi.org/10.1002/JIMD.12097.

[122] Reed M, Baker RJ, Mehta AB, Hughes DA. Enhanced differentiation of osteoclasts from mononuclear precursors in patients with Gaucher disease. Blood Cells Mol Dis 2013;51:185–94. https://doi.org/10.1016/J.BCMD.2013.04.006.

[123] Reed MC, Bauernfreund Y, Cunningham N, Beaton B, Mehta AB, Hughes DA. Generation of osteoclasts from type 1 Gaucher patients and correlation with clinical and genetic features of disease. Gene 2018;678:196–206. https://doi.org/10.1016/J.GENE.2018.08.045.

[124] Bondar C, Ormazabal M, Crivaro A, Ferreyra-Compagnucci M, Delpino M, Rozenfeld PA, et al. Osteocyte Alterations Induce Osteoclastogenesis in an In Vitro Model of Gaucher Disease. Int J Mol Sci 2017;18. https://doi.org/10.3390/IJMS18010112.

[125] Crivaro AN, Mucci JM, Bondar CM, Ormazabal ME, Ceci R, Simonaro C, et al. Efficacy of pentosan polysulfate in in vitro models of lysosomal storage disorders: Fabry and Gaucher Disease. PLoS One 2019;14. https://doi.org/10.1371/JOURNAL.PONE.0217780.

[126] Mucci JM, Cuello MF, Kisinovsky I, Larroude M, Delpino M v., Rozenfeld PA. Proinflammatory and proosteoclastogenic potential of peripheral blood mononuclear cells from Gaucher patients: Implication for bone pathology. Blood Cells Mol Dis 2015;55:134–43. https://doi.org/10.1016/J.BCMD.2015.05.009.

[127] Mucci JM, Scian R, de Francesco PN, García FS, Ceci R, Fossati CA, et al. Induction of osteoclastogenesis in an in vitro model of Gaucher disease is mediated by T cells via TNF-α. Gene 2012;509:51–9. https://doi.org/10.1016/J.GENE.2012.07.071.

[128] Guay C, Regazzi R. Circulating microRNAs as novel biomarkers for diabetes mellitus. Nature Reviews Endocrinology 2013 9:9 2013;9:513–21. https://doi.org/10.1038/nrendo.2013.86.

[129] Gebert LFR, MacRae IJ. Regulation of microRNA function in animals. Nature Reviews Molecular Cell Biology 2018 20:1 2018;20:21–37. https://doi.org/10.1038/s41580-018-0045-7.

[130] Moore BT, Xiao P. MiRNAs in bone diseases. Microrna 2013;2:20–31. https://doi.org/10.2174/2211536611302010004.

[131] Bravo Vázquez LA, Moreno Becerril MY, Mora Hernández EO, León Carmona GG de, Aguirre Padilla ME, Chakraborty S, et al. The Emerging Role of MicroRNAs in Bone Diseases and Their Therapeutic Potential. Molecules 2022;27. https://doi.org/10.3390/MOLECULES27010211.

[132] Gao Y, Patil S, Qian A. The Role of MicroRNAs in Bone Metabolism and Disease. International Journal of Molecular Sciences 2020, Vol 21, Page 6081 2020;21:6081. https://doi.org/10.3390/IJMS21176081.

[133] Costa R, Bellesso S, Lualdi S, Manzoli R, Pistorio V, Filocamo M, et al. A transcriptional and post-transcriptional dysregulation of Dishevelled 1 and 2 underlies the Wnt signaling impairment in type I Gaucher disease experimental models. Hum Mol Genet 2020;29:274–85. https://doi.org/10.1093/HMG/DDZ293.

[134] Pawliński Ł, Polus A, Tobór E, Sordyl M, Kopka M, Solnica B, et al. MiRNA Expression in Patients with Gaucher Disease Treated with Enzyme Replacement Therapy. Life 2021;11:1–24. https://doi.org/10.3390/LIFE11010002.

[135] Schröder SP, van de Sande JW, Kallemeijn WW, Kuo CL, Artola M, van Rooden EJ, et al. Towards broad spectrum activity-based glycosidase probes: synthesis and evaluation of deoxygenated cyclophellitol aziridines. Chemical Communications 2017;53:12528–31. https://doi.org/10.1039/C7CC07730K.

[136] Polo G, Burlina AP, Kolamunnage TB, Zampieri M, Dionisi-Vici C, Strisciuglio P, et al. Diagnosis of sphingolipidoses: a new simultaneous measurement of lysosphingolipids by LC-MS/MS. Clinical Chemistry and Laboratory Medicine (CCLM) 2017;55:403–14. https://doi.org/10.1515/CCLM-2016-0340.

[137] Boer DEC, Mirzaian M, Ferraz MJ, Nadaban A, Schreuder A, Hovnanian A, et al. Glucosylated cholesterol in skin: Synthetic role of extracellular glucocerebrosidase. Clinica Chimica Acta 2020;510:707–10. https://doi.org/10.1016/J.CCA.2020.09.017.

[138] Katzy RE, Ferraz MJ, Hazeu M, Overkleeft HS, Aerts JMFG. In situ glucosylceramide synthesis and its pharmacological inhibition analysed in cells by 13 C5 -sphingosine precursor feeding and mass spectrometry. FEBS Lett 2022;596:2400–8. https://doi.org/10.1002/1873-3468.14448.

[139] Cui C, Schoenfelt KQ, Becker KM, Becker L. Isolation of polymorphonuclear neutrophils and monocytes from a single sample of human peripheral blood. STAR Protoc 2021;2. https://doi.org/10.1016/J.XPRO.2021.100845.

[140] Pavan E, Ormazabal M, Peruzzo P, Vaena E, Rozenfeld P, Dardis A. Crispr/cas9 editing for gaucher disease modelling. Int J Mol Sci 2020;21. https://doi.org/10.3390/ijms21093268.

[141] Yahata K, Mori K, Arai H, Koide S, Ogawa Y, Mukoyama M, et al. Molecular cloning and expression of a novel klotho-related protein. J Mol Med (Berl) 2000;78:389–94. https://doi.org/10.1007/S001090000131.

[142] Boot RG, Verhoek M, Donker-Koopman W, Strijland A, van Marle J, Overkleeft HS, et al. Identification of the non-lysosomal glucosylceramidase as beta-glucosidase 2. J Biol Chem 2007;282:1305–12. https://doi.org/10.1074/JBC.M610544200.

[143] van Weely S, Brandsma M, Strijland A, Tager JM, Aerts JMFG. Demonstration of the existence of a second, non-lysosomal glucocerebrosidase that is not deficient in Gaucher disease. Biochim Biophys Acta 1993;1181:55–62. https://doi.org/10.1016/0925-4439(93)90090-N.

[144] Keeting PE, Scott RE, Colvard DS, Anderson MA, Oursler MJ, Spelsberg TC, et al. Development and characterization of a rapidly proliferating, well-differentiated cell line derived from normal adult human osteoblast-like cells transfected with SV40 large T antigen. Journal of Bone and Mineral Research 1992;7:127–36. https://doi.org/10.1002/jbmr.5650070203.

[145] Czekanska EM, Stoddart MJ, Richards RG, Hayes JS. In search of an osteoblast cell model for in vitro research. Eur Cell Mater 2012;24:1–17. https://doi.org/10.22203/ECM.V024A01.

[146] Goldring MB, Birkhead JR, Suen LF, Yamin R, Mizuno S, Glowacki J, et al. Interleukin-1 beta-modulated gene expression in immortalized human chondrocytes. J Clin Invest 1994;94:2307–16. https://doi.org/10.1172/JCI117595.

[147] Ouellette MM, McDaniel LD, Wright WE, Shay JW, Schultz RA. The establishment of telomerase-immortalized cell lines representing human chromosome instability syndromes. Hum Mol Genet 2000;9:403–11. https://doi.org/10.1093/HMG/9.3.403.

[148] Finger F, Schörle C, Zien A, Gebhard P, Goldring MB, Aigner T. Molecular phenotyping of human chondrocyte cell lines T/C-28a2, T/C-28a4, and C-28/I2. Arthritis Rheum 2003;48:3395–403. https://doi.org/10.1002/ART.11341.

[149] Claassen H, Schicht M, Brandt J, Reuse K, Schädlich R, Goldring MB, et al. C-28/I2 and T/C-28a2 chondrocytes as well as human primary articular chondrocytes express sex hormone and insulin receptors--Useful cells in study of cartilage metabolism. Ann Anat 2011;193:23–9. https://doi.org/10.1016/J.AANAT.2010.09.005.

[150] Naomi R, Ridzuan PM, Bahari H. Current Insights into Collagen Type I. Polymers (Basel) 2021;13. https://doi.org/10.3390/POLYM13162642.

[151] Michigami T, Ozono K. Roles of phosphate in skeleton. Front Endocrinol (Lausanne) 2019;10:180. https://doi.org/10.3389/FENDO.2019.00180/BIBTEX.

[152] Huang Y, Hou Q, Su H, Chen D, Luo Y, Jiang T. miR-488 negatively regulates osteogenic differentiation of bone marrow mesenchymal stem cells induced by psoralen by targeting Runx2. Mol Med Rep 2019;20:3746–54. https://doi.org/10.3892/MMR.2019.10613.

[153] Peng W, Zhu SX, Wang J, Chen LL, Weng JQ, Chen SL. Lnc-NTF3-5 promotes osteogenic differentiation of maxillary sinus membrane stem cells via sponging miR-93-3p. Clin Implant Dent Relat Res 2018;20:110. https://doi.org/10.1111/CID.12553.

[154] Gigis I, Pitsilos C, Samoladas E, Pavlopoulos C, Hytiroglou P, Ditsios K, et al. Gaucher Disease: An Unusual Cause of Knee Pain. J Am Acad Orthop Surg Glob Res Rev 2022;6. https://doi.org/10.5435/JAAOSGLOBAL-D-21-00243.

[155] Kattoor AJ, Bauer TW, Berkowitz M, Polster JM, Lichtin AE. Ankle pain in a young woman with Gaucher disease. Cleve Clin J Med 2015;82:607–13. https://doi.org/10.3949/CCJM.82A.14108.

[156] Matsushima K, Yang D, Oppenheim JJ. Interleukin-8: An evolving chemokine. Cytokine 2022;153:155828. https://doi.org/10.1016/J.CYTO.2022.155828.

[157] Borger DK, Aflaki E, Sidransky E. Applications of iPSC-derived models of Gaucher disease. Ann Transl Med 2015;3:295. https://doi.org/10.3978/j.issn.2305-5839.2015.10.41.

[158] Borger DK, Sidransky E, Aflaki E. New macrophage models of Gaucher disease offer new tools for drug development. Macrophage (Houst) 2015;2:e712–e712.

[159] Santos R, Amaral O. Advances in Sphingolipidoses: CRISPR-Cas9 Editing as an Option for Modelling and Therapy. Int J Mol Sci 2019;20:5897. https://doi.org/10.3390/ijms20235897.

[160] Aflaki E, Westbroek W, Sidransky E. The Complicated Relationship between Gaucher Disease and Parkinsonism: Insights from a Rare Disease. Neuron 2017;93:737–46. https://doi.org/10.1016/J.NEURON.2017.01.018.

[161] van Dussen L, Lips P, Everts VE, Bravenboer N, Jansen IDC, Groener JEM, et al. Markers of bone turnover in Gaucher disease: modeling the evolution of bone disease. J Clin Endocrinol Metab 2011;96:2194–205. https://doi.org/10.1210/JC.2011-0162.

[162] Iaquinta MR, Lanzillotti C, Mazziotta C, Bononi I, Frontini F, Mazzoni E, et al. The role of microRNAs in the osteogenic and chondrogenic differentiation of mesenchymal stem cells and bone pathologies. Theranostics 2021;11:6573–91. https://doi.org/10.7150/THNO.55664.

[163] Kim KM, Lim SK. Role of miRNAs in bone and their potential as therapeutic targets. Curr Opin Pharmacol 2014;16:133–41. https://doi.org/10.1016/J.COPH.2014.05.001.

[164] Quintiens J, de Roover A, Cornelis FMF, Escribano-Núñez A, Sermon A, Pazmino S, et al. Hypoxia and Wnt signaling inversely regulate expression of chondroprotective molecule ANP32A in articular cartilage. Osteoarthritis Cartilage 2022. https://doi.org/10.1016/J.JOCA.2022.10.019.

[165] Campos Y, Fuentes G, Almirall A, Que I, Schomann T, Chung CK, et al. The Incorporation of Etanercept into a Porous Tri-Layer Scaffold for Restoring and Repairing Cartilage Tissue. Pharmaceutics 2022;14. https://doi.org/10.3390/PHARMACEUTICS14020282.

[166] Kittl M, Winklmayr M, Helm K, Lettner J, Gaisberger M, Ritter M, et al. Acid- and Volume-Sensitive Chloride Currents in Human Chondrocytes. Front Cell Dev Biol 2020;8. https://doi.org/10.3389/FCELL.2020.583131/FULL.

[167] Zada S, Pham TM, Hwang JS, Ahmed M, Lai TH, Elashkar O, et al. Chlorogenic acid protects human chondrocyte C28/I2 cells from oxidative stress-induced cell death through activation of autophagy. Life Sci 2021;285:119968. https://doi.org/10.1016/J.LFS.2021.119968.

[168] García-Couce J, Schomann T, Chung CK, Que I, Jorquera-Cordero C, Fuentes G, et al. Thermosensitive Injectable Hydrogels for Intra-Articular Delivery of Etanercept for the Treatment of Osteoarthritis. Gels 2022;8. https://doi.org/10.3390/GELS8080488.

[169] Thorpe JR, Wilson RA, Mesiano S, Malemud CJ. Tofacitinib Inhibits STAT Phosphorylation and Matrix Metalloproteinase-3, -9 and -13 Production by C28/I2 Human Juvenile Chondrocytes. Open Access Rheumatol 2022;14:195. https://doi.org/10.2147/OARRR.S363736.

[170] Gudmann NS, Karsdal MA. Type X Collagen. In: Karsdal MA, editor. Biochemistry of Collagens, Laminins and Elastin: Structure, Function and Biomarkers, Cambridge, USA: Academic Press; 2016, p. 73–6. https://doi.org/10.1016/B978-0-12-809847-9.00010-6.

[171] Gudmann NS, Karsdal MA. Type II Collagen. In: Karsdal MA, editor. Biochemistry of Collagens, Laminins and Elastin: Structure, Function and Biomarkers, Cambridge, USA: Academic Press; 2016, p. 13–20. https://doi.org/10.1016/B978-0-12-809847-9.00002-7.

[172] Kaur J, Reinhardt DP. Extracellular Matrix (ECM) Molecules. In: Vishwakarma A, Sharpe P, Shi S, Ramalingam M, editors. Stem Cell Biology and Tissue Engineering in Dental Sciences, Cambridge, USA: Academic Press; 2015, p. 25–45. https://doi.org/10.1016/B978-0-12-397157-9.00003-5.

[173] Burrage PS, Mix KS, Brinckerhoff CE. Matrix metalloproteinases: role in arthritis. Front Biosci 2006;11:529–43. https://doi.org/10.2741/1817.

[174] Goldring MB, Otero M. Inflammation in osteoarthritis. Curr Opin Rheumatol 2011;23:471. https://doi.org/10.1097/BOR.0B013E328349C2B1.

[175] Tseng CC, Chen YJ, Chang WA, Tsai WC, Ou TT, Wu CC, et al. Dual Role of Chondrocytes in Rheumatoid Arthritis: The Chicken and the Egg. Int J Mol Sci 2020;21. https://doi.org/10.3390/IJMS21031071.

[176] Otero M, Goldring MB. Cells of the synovium in rheumatoid arthritis. Chondrocytes. Arthritis Res Ther 2007;9:1–13. https://doi.org/10.1186/AR2292/FIGURES/1.

[177] Herrero AB, García-Gómez A, Garayoa M, Corchete LA, Hernández JM, San Miguel J, et al. Effects of IL-8 Up-Regulation on Cell Survival and Osteoclastogenesis in Multiple Myeloma. Am J Pathol 2016;186:2171–82. https://doi.org/10.1016/J.AJPATH.2016.04.003.

[178] Bendre MS, Montague DC, Peery T, Akel NS, Gaddy D, Suva LJ. Interleukin-8 stimulation of osteoclastogenesis and bone resorption is a mechanism for the increased osteolysis of metastatic bone disease. Bone 2003;33:28–37. https://doi.org/10.1016/S8756-3282(03)00086-3.

[179] Greco K v., Nalesso G, Kaneva MK, Sherwood J, Iqbal AJ, Moradi-Bidhendi N, et al. Analyses on the mechanisms that underlie the chondroprotective properties of calcitonin. Biochem Pharmacol 2014;91:348–58. https://doi.org/10.1016/J.BCP.2014.07.034.

[180] Kaneva MK, Greco K v., Headland SE, Montero-Melendez T, Mori P, Greenslade K, et al. Identification of Novel Chondroprotective Mediators in Resolving Inflammatory Exudates. J Immunol 2017;198:2876–85. https://doi.org/10.4049/JIMMUNOL.1601111.

[181] Greco K V., Iqbal AJ, Rattazzi L, Nalesso G, Moradi-Bidhendi N, Moore AR, et al. High density micromass cultures of a human chondrocyte cell line: a reliable assay system to reveal the modulatory functions of pharmacological agents. Biochem Pharmacol 2011;82:1919–29. https://doi.org/10.1016/J.BCP.2011.09.009.

# SUPPLEMENTARY

**Supplementary Table 1 | Predicted miR-488-3p target genes and their roles in bone and bone-related processes.** miR-488-3p targets were predicted by TargetScan (https://www.targetscan.org/vert_80/; release 8.0); genes were clustered by David software (https://david.ncifcrf.gov/; version 2021) using Functional annotation chart and filtered according to terms related to bone or bone-related processes.

| GENE | | ROLE IN BONE / BONE RELATED PROCESSES |
|---|---|---|
| BMP2 | bone morphogenetic protein 2 | chondrocyte differentiation<br>osteoclast differentiation<br>skeletal system development<br>bone mineralization |
| FGFR3 | fibroblast growth factor receptor 3 | endochondral bone growth<br>chondrocyte differentiation<br>chondrocyte proliferation<br>skeletal system development<br>bone mineralization |
| EXT1 | exostosin glycosyltransferase 1 | endochondral bone growth<br>chondrocyte proliferation<br>skeletal system development |
| HIF1A | hypoxia inducible factor 1 subunit alpha | chondrocyte differentiation<br>bone mineralization |
| MMP16 | matrix metallopeptidase 16 | chondrocyte proliferation<br>skeletal system development |
| NRP3 | natriuretic peptide receptor 3 | skeletal system development<br>osteoclast proliferation |
| RANKL | receptor activator of NF-kB ligand | osteoclast differentiation<br>osteoclast proliferation |
| BMPR1A | bone morphogenetic protein receptor type 1A | chondrocyte differentiation<br>bone mineralization |
| ACVR2B | activin A receptor type 2B | bone mineralization |
| ATP2B1 | ATPase plasma membrane Ca2+ transporting 1 | bone mineralization |
| BNC2 | basonuclin 2 | endochondral bone growth |
| CREB1 | cAMP responsive element binding protein 1 | osteoclast differentiation |
| IGF1 | insulin like growth factor 1 | skeletal system development |
| LOX | lysyl oxidase | bone mineralization |
| NFIB | nuclear factor I B | chondrocyte differentiation |
| PIK3R1 | phosphoinositide-3-kinase regulatory subunit 1 | osteoclast differentiation |
| RXRB | retinoid X receptor beta | bone mineralization |
| RPS6KA3 | ribosomal protein S6 kinase A3 | skeletal system development |
| SLC8A1 | solute carrier family 8 member A1 | bone mineralization |

*Al termine di questo percorso desidero ringraziare tutte le persone che mi hanno accompagnata sin dall'inizio e quelle con cui ho avuto il piacere di condividere un pezzo di cammino.*

*Grazie Andrea per credere in me e per avermi dato un sacco di possibilità, che mi hanno fatta cambiare e crescere come persona e professionalmente: mi sento molto fortunata. Grazie amigo Maxi perché con te al mio fianco ogni esperimento è realizzabile e nessun problema è irrisolvibile…e le giornate sono più leggere. Grazie Paolo, se non avessi avuto te come prima guida in questo posto dubito fortemente che mi troverei a questo punto: ti ringrazio soprattutto per avermi insegnato come lavorare con metodo ("il mio quaderno di dottorato era grosso così!"). Grazie Stefi, i perché già li sai, mi manchi. Grazie Silvia per essere sempre una disponibile confidente (e garantire l'ordine in laboratorio). Grazie Nat per trasmettere serenità…ce n'è sempre bisogno. Grazie Marti per le risate e per viziarmi con cioccolata di ogni tipo. Grazie Consu, la quantità di tempo che si risparmia quando è tutto ben rifornito, pulito ed ordinato è immensa…sei eccezionale!*

*Grazie di cuore a chi ha contributo ai bei risultati di questa tesi: Dania per i lipidi – ma forse dovrei ringraziarti soprattutto per le proteine, Daniela e Michela per la citofluorimetria e i preziosi consigli. Ovviamente, Matteo, per le infinite mattinate passate a sortare …ma anche per i pomeriggi torridi a guardare foglie non verdi.*

*Ci tengo a ringraziare anche tutti coloro i quali mi hanno accolta per un periodo più o meno lungo nei loro laboratori. Martín, Fátima, Franco e Gastón, a Buenos Aires ho iniziato a lavorare "da sola", anche se sola non mi sono proprio mai sentita, ed è stata l'esperienza che mi ha fatta rendere definitivamente conto di quanto mi piaccia questo lavoro. Grazie Hans, Maria e Qin, è stato un privilegio lavorare nel vostro laboratorio ed avere la possibilità di discutere di scienza con voi. Gracias Paula, mi segunda jefa, algún día quisiera llegar a ser una mujer fuerte como vos! Hasta el próximo meeting.*

*Grazie, infine, Amici, per la spensieratezza che mi donate, mamma e papà, per esserci sempre e Umbi per ricordarmi che valgo. Vi voglio bene. Last but not least, Giorgio…ogni mio traguardo è anche tuo, Siuuuuum!*